THE EFFECT OF ENVIRONMENT ON THE FRACTURE OF BRITTLE SOLIDS

by

R. F. G. MacMILLAN

B.Sc. University of Natal, South Africa
B.Sc. (HONS) University of Natal, South Africa
M.Sc. University of Natal, South Africa

A thesis submitted in partial fulfilment
of the requirements for the degree of

DOCTOR OF PHILOSOPHY

in the Department of
Mineral Engineering

We accept this thesis as conforming to
the required standard

THE UNIVERSITY OF BRITISH COLUMBIA
February, 1968

In presenting this thesis in partial fulfilment of the requirements for an advanced degree at the University of British Columbia, I agree that the Library shall make it freely available for reference and study. I further agree that permission for extensive copying of this thesis for scholarly purposes may be granted by the Head of my Department or by his representatives. It is understood that copying or publication of this thesis for financial gain shall not be allowed without my written permission.

Department of Mineral Engineering

The University of British Columbia
Vancouver 8, Canada

Date 20/2/68

ABSTRACT

The effect of specific active environment on the fracture strength of glass and polymethyl methacrylate was investigated using an indirect tensile testing technique.

The strength of glass was not affected by exposure to dry gaseous N_2 and CO_2. At low water vapour coverages, (<1/3 monolayer), the tensile strength of glass was reduced by approximately 50%. Further increase in water vapour pressure did not weaken the solid to a much greater extent. The existence of surface microcracks governs the absolute tensile fracture strength, and any process which varies the flaw geometry acts to vary the tensile fracture strength. Soaking in the liquid has the same effect as adsorption from the vapour phase near saturation. All vapour adsorbates caused a weakening, the magnitude of the decrease increasing with increasing ability of the adsorbate to screen the surface Si^{++++} cores. Moisture was the most active environment encountered.

Polymethyl methacrylate did not weaken in the vapour phase despite multilayer adsorption, but stressing in

wetting liquids did cause drastic failure, with a 57% decrease in tensile strength. Non-wetting liquids do not affect the strength of the acrylic plastics.

Fracture experiments on a quartzitic rock in aqueous solutions of surfactant, (quartenary ammonium salts), show that the weakening due to surfactant adsorption is negligible, since water itself causes the maximum strength reduction. The adsorption of surfactant is only a secondary effect.

A mechanism has been proposed for the stress-environmental failure of brittle solids. This mechanism recognizes the existence of micro-cracks, regards the stable crack propagation stage of the fracture process to be environment sensitive, and involves the strain-activated adsorption resulting in a decrease in cohesion at the flaw apex. The magnitude of the weakening is critically dependent on the nature of the bonding in the solid surface.

A literature review of stress-sorption cracking, with an emphasis on non-metallic systems, is included.

J. Leja,
Professor,
Supervisor.

ACKNOWLEDGEMENTS

The guidance and friendship of my research supervisor, Dr. J. Leja, throughout the course of this study are gratefully acknowledged.

I wish to thank the various members of the Department of Mineral Engineering and my colleagues for many helpful discussions.

The construction of the vacuum cell by Mr. P. Sunderland is greatly appreciated, as is the typing of this thesis by Mrs. C. Guarnaschelli.

A special vote of thanks to my wife Lynne, for her patience and support over the years leading to this dissertation.

The following scholarships are gratefully acknowledged,

Giant Yellowknife Mines Limited (1965-66)

Shell Canada Scholarship for Research (1966-67)

National Research Council Studentship (1967-68).

TABLE OF CONTENTS

LIST OF FIGURES

LIST OF FIGURES (Continued)

LIST OF FIGURES (Continued)

LIST OF TABLES

LIST OF TABLES (Continued)

CHAPTER ONE

INTRODUCTION

1:1 General

The use of an active chemical environment to promote cracking would be extremely beneficial in any application where the fracture of a solid is required (e.g. crushing and grinding). Much effort has been expended in devising methods to prevent stress accelerated failure, particularly in metallic systems, but little thought has been applied to its constructive use. Recent aspects of lunar drilling[1] have led to the realization that stress environmental cracking is being subconsciously applied in most fracture operations, although little is known of the mechanism.

1:2 Statement of the Problem

Stress environmental cracking is a study of fundamental, as well as practical interest, since it involves a unique interplay of surface chemistry, electrochemistry and solid state. The phenomenon may be defined as a process whereby failure of a solid occurs as a result of an accelerated mechano-chemical reaction in a stressed region, in an

active environment. Failure occurs at a strength level well below that which would be experienced in the absence of the environment.

None of the investigations of stress cracking occurring in both metallic and non-metallic systems, have led to a theory or mechanism which adequately explains the peculiar selectivity of the solid/environment system. Non-metallic systems, in particular, have received very little attention. As early as 1864, Dupre'[2] conceived that the fracture strength of solids might be related to the energy of the newly formed surfaces. Many theories have been forthcoming involving the reduction of surface free energy resulting from specific adsorption, thereby leading to a strength reduction of the solid; especially since Griffith[3] rephrased the Dupre' concept and formulated it. However, deviations[4][5][6] are more the rule than the exception, demonstrating the need for a more complete mechanistic treatment.

Therefore, the purpose of this dissertation is to investigate possible stress-environmental cracking systems on non-metallic brittle materials, with a view to explaining the action of the environment and the selectivity of the solid/environment system.

1:3 The Scope and Approach of the Study

The investigation was carried out on four brittle materials. Silica is ideally suited for studying the chemistry of surfaces due to its isotropic nature and high chemical reactivity, therefore two inorganic glasses were selected. Firstly, a highly porous Vycor glass for adsorption and fracture studies and, secondly, a borosilicate glass to counter effects which might result from the porous nature of the Vycor glass.

By way of comparison, a brittle acrylic plastic was chosen, because the fracture pattern at room temperature appears similar to glass. The covalent bonding of the plastic and its low energy surface, might be expected to yield vastly differing environmental effects from the ionic silicas.

Experiments on a quartzitic rock were designed to sort out some of the confusion occurring in reported effects in the literature, whilst also briefly considering the possibilities of a practical application.

The utilization of tensile stresses is not to artificially restrict the problem, but arises from the fact that stress accelerated failure only occurs in tension. The indirect tensile test affords a rapid comparative method for measuring tensile fracture strength.

The project has been conducted in four phases, as follows: (1) Historical review of the problem (2) Prelimi-

nary exploration of the cracking techniques. (3) Controlled experimentation. (4) Theoretical evaluation and the postulation of a fracture mechanism.

Experimentally the investigation is comprised of two main sections.

(1) Adsorption Studies

The determination of adsorption isotherms led to calculated surface free energy changes and surface coverage values.

(2) Fracture Studies

(a) Fracture of the solids in controlled vapour and liquid environment.

(b) Examination of the fracture surfaces by optical microscopy and transmission electron microscopy using a replica technique.

The results of these experiments, together with the various accepted fracture theories, were used to interpret the fracture mechanism in the various systems. In particular, a mechanism based on the bonding of the solid surface is suggested as an explanation for the stress environmental cracking in brittle materials.

1:4 Historical Review

Preliminary investigations by Rehbinder et al[7] in 1944, showed that the addition of small amounts of surface active agents to the surrounding liquid medium, resulting in adsorption on the solid surfaces, is capable of reducing the resistance of the solid to stress.

This phenomenon termed the "Rehbinder Effect" may be used to facilitate the boring of hard rocks, disintegration of solids in milling, and in abrasion. Rehbinder added electrolytes, (.01-.1%), to the flushing water for rotary drills and found an increase in drilling speed of as much as 20-60%.

> "The mechanism is associated with the penetration of the surface active species into the strained solid along the surface of the microcracks, which develop in the course of deformation. Due to the reciprocating nature of the bit the stress imparted to the solid is periodic. When the stress ceases to act, the 'embryo-microcracks' tend to heal. The cohesive forces are however, bound to the adsorbed layer, coating the surfaces of the minute cracks and the crack is prevented from 'healing'"[7].

These investigations on the change in mechanical properties of a material, which accompanies the adsorption of surface active agent, opened the door to a very obscure and controversial field.

In 1949 Von Szantho[8] published the first detailed investigation on the effect of additives in wet grinding. His results showed that the addition of a flotation collector considerably lowered the amount of energy required for grind-

ing of quartz.

Using cement bricks in a dry grinding circuit Gotte and Ziegler[9] showed an increase of 20-100%, in grinding capacity (i.e. reduction in energy), when non-polar surface active gases and vapours were admitted to the system.

W. von Engelhardt[10] (1943) found that certain polar liquids had a softening effect on quartz being ground with a widia tipped wheel. He showed that small additions of surface active agents such as fatty acids, produce higher hardness values for quartz, but with increased concentrations the hardness fell appreciably. An 80% sulphite lye increases the amount of quartz ground in standard time by 43 per cent, as compared to values in water. Engelhardt's results indicated that certain organic liquids such as hexane and benzol increased quartz hardness; whilst others such as acetic acid, pentanols and cetyl alcohol had a softening effect. It appeared that non-polar liquids produced an increase in hardness, whilst polar/non-polar liquids reduced the hardness, the effect increasing with molecular chain length.

Moorthy and Tooley[11] determined the effects of certain organic liquids on the strength properties of glass. In all cases, except nitrobenzene, breaking strengths were higher under the organics than in water, ranging from a 36% to 19% increase for alcohols to values of 90% for heptane, benzene and toluene. The strength of all specimens was lower in water than in air.

In Japan a theoretical treatment of the effect of environment was carried out by M. Sato[12]. He developed an equation for the surface tension of a solid γ_s,

$$\gamma_s = -\gamma_\ell / (\Delta f / f)$$

where γ_ℓ = Surface Tension of the wetting liquid

f = Breaking Stress in the dry state

Δf = Change in f due to adsorption.

His experiments showed that the tensile strength decreases in a bending test with the presence of wetting liquid, regardless of the type of material. The decrease was dependent on γ_ℓ. The greater the wettability (the difference between γ_s and γ_ℓ), the lower the decrease in strength, i.e. a linear relationship exists between $\Delta f/f$ and γ_ℓ.

Frangiskos and Smith[13], (1957), studied the action of electrolytes, NaCl and Na_2CO_3, and surface active agents such as silicones, on quartz, using a laboratory stamp mill to duplicate the reciprocating nature of a percussion drill. In all cases the efficiency of the grind, in the presence of the additive, increased. The efficiency is measured by the surface area of the product as measured by air permeability tests. The effect was concentration dependent.

An attempt was made by Ghosh, Harris and Jowett[14], at Leeds University in 1960, to repeat the work of Frangiskos and Smith. The results, based on the new surface area pro-

duced, showed that whenever an additive is used, there is an overall increase in the surface area on grinding.

In 1963 Hammond and Ravitz[15], measuring the fracture strength of fused silica rods found the decrease in the fracture strength and the corresponding decrease in the surface free energy to be consistent with the Griffith theory of brittle fracture. The fracture strength decreases as the environmental vapours become more polar.

A patent by Siebel and Zeisel[16] claimed the use of various additives in grinding and gave some figures for the grinding of a siliceous lead-zinc ore in a laboratory rod mill. For a feed size of 0-7 mm the grinding efficiency was reported as the percentage material greater than a given size from 1 mm to .1 mm, for various grinding times. Calgon was one of the additives used, the improvement in the fineness of the grind being generally of the order of 30% at concentrations of .01-.04%.

In 1954 Alberti[17] was granted a patent on the use of dispersing agents as additives in grinding but no numerical results were listed.

Gilbert and Hughes[18] experimented on the use of additives for improving the efficiency of wet grinding. Initially, tests on the grinding of quartz in a three-inch diameter ring ball mill using a silicone, showed no substantial improvement in the grinding performance. However for quartzite a lesser quantity of fines was produced.

Using a five-inch diameter ball mill at two mill speeds and a silicone additive, very slight improvements in the grind were experienced, but these were well below those quoted by previous workers using similar additives in a stamp mill. On using a cationic wetting agent at varying concentrations and pH's, slight decreases in the grinding efficiency resulted. Addition of electrolytes, sodium carbonate, sodium silicate and sodium hexametaphosphate in a six-inch diameter rod mill gave negative results. Only the latter had any effect on the fineness of the grind, producing a coarser product. The authors conclude that in conventional rod and ball mills, the use of inorganic additives results only in a decrease in grinding efficiency, or has no effect at all.

A number of references have been made as to the influence of moisture on the compressive strength of rocks, showing in general that as the moisture content increases, the compression strength decreases.

Price[19] and, Colback and Wiid[20], in a series of tests on rocks, conclude that the reduction in strength from the "dry" to the saturated condition is dependent on the reduction of the surface free energy of the specimen by the presence of a surface active liquid. The latter also show a linear decrease of the strength with the surface tension of the immersing liquid, as calculated by M. Sato[12].

In a study on the causes of rock deterioration Dr. T.R. Dunn[21] at the Rensselaer Polytechnic Institute,

concluded that breakdown of the rock could be caused by "ordering" of polar molecules in adsorption surfaces, in a warming and cooling environment.

Using the method of Hertz for the cone fracture of glass, Roesler[22] has shown that the presence of chemical environment at the crack tip caused crack propagation at very much smaller levels of load, than in air.

Rehbinder and Aslanova[23] report that in the presence of water vapour, or of surface active species adsorbed from aqueous solutions, glass fibres show an elastic effect, which increases as the stress approaches the rupture stress. Chemical etching of the surface layer to remove surface fissures increased the fiber strength.

A similar effect, called liquostriction has been reported by Benedicks[24], the phenomenon being the expansion of solid due to adsorption. Benedicks and Harden[25] in a paper on the "wetting effect", (the change in the solid tensile strength resulting from the wetting liquid), showed both positive and negative effects i.e. weakening and strengthening of the solid. Glass wetted with H_2O gave a decrease of about 40% whereas tar oil gave an increase of 30% for the same material. They conclude that the effect is a function of the liquid surface tension, the magnitude of the effect being very different for different solids. For increasing solids hardness, the relative decrease in the tensile strength diminishes.

In metallic systems N.J. Petch[122] has explained the fracture of steels containing hydrogen by the surface diffusion of hydrogen to the crack apex where it adsorbs, reducing surface energy of metal atoms subject to a tensile force. Uhlig coined the phrase "stress-sorption cracking" to apply to this failure mechanism[123]. It was proposed that selective adsorption along the crack walls lowers the surface free energy, operating conjointly with electrochemical action along paths where defects predominate and where compositional gradients exist. The cracking of mild steel in boiling nitrate solutions[124] was discussed in terms of the stress-sorption mechanism by adsorption of OH^- and NO_3^- ions along cracking paths under tensional stresses.

A series of experiments on the swelling of compacts of chalk, kaolin and coal[26][27], enhance the idea that adsorption causes a reduction in strength only if accompanied by appreciable swelling, but not otherwise. A particular coal[26] showed marked swelling on adsorption of vapours of benzene, acetone and methanol, but only slight swelling in water vapour. The strength was correspondingly reduced in the organic solvents but not in water, whilst the reduction in surface free energy as calculated by the Gibbs equation was appreciable in all three cases.

Flood and his[28] collaborators in a thermodynamic treatment, have presented an expression which correlates the

elastic properties and the adsorption properties. Their theoretical treatment allows the reproduction of experimental volume changes due to adsorption to be made with reasonable accuracy.

Conclusion

There is ample evidence of a strength reducing mechanism of non-metallic materials in a variety of environments. However, no satisfactory explanations have been given for the effects, whilst the theories of brittle fracture fail to explain the selectivity of the phenomenon. There is also a great deal of controversial data arising from experiments on silicious material, as to the direction and magnitude of the effect. A development of the theoretical foundations involved in a fracture system may serve to elucidate the problem.

CHAPTER TWO

EXPERIMENTAL

2:1 Materials

(i) Vycor Glass

The Vycor glass was supplied by Corning Glass in the form of cylinders of height .5 inches and diameter .5 inches. Designated Corning No. 7930, this glass approximates fused silica in many of its properties. It is prepared by a process in which the relatively high fluxing oxide is melted and formed to the desired shape, but somewhat oversize. The fluxes are then removed by acid leaching. The leached material is then fired at high temperatures to consolidate the remaining porous silica structure, which causes it to shrink to its final size.

Composition of Vycor No. 7930

SiO2	96%
B_2O_2	3%
Na_2O	0.4%
$Al_2O_3 \pm ZrO_2$	1%

(ii) Kimble Glass

Specimens of the borosilicate glass were prepared from a .5 inch diameter glass rod by cutting on a diamond saw. The ends were then polished on a grinding wheel using carborundum paste. Although cutting and polishing do influence the tensile fracture strength, specimens prepared in this manner showed less scatter in strength values than the Vycor glass.

Composition of Kimble Glass

SiO_2	75%	B_2O_3	10%
Na_2O	7%	Al_2O_3	5%
BaO	2%	CaO	1%

(iii) Polymethyl Methacrylate

The plastic was obtained in the form of .5 inch diameter caste rods. Specimens were prepared by machining on a lathe.

(iv) Chemicals

All gases were purified by passing through a drying train consisting of silica gel, ascarite (CO_2 removal), a heated copper foil in a glass tube for oxygen removal, and anhydrous calcium sulphate, (Drierite). The water was double distilled with an equivalent conductance of 0.9×10^{-6} mhos. Technical grade mercury was used in all manometers and cut-off valves. The organic solvents were reagent grade. Solvents were double distilled in an all glass still, the head and

tail fractions being rejected. Further drying was effected by storage over a suitable drying agent. To eliminate the H_2O contamination of the hygroscopic solvents, adsorption was carried out by evaporating the solvent from the frozen liquid.

(v) Rock Specimens

Any rock specimens were used in the "as is" condition. To eliminate the moisture and grease contaminants the specimens were washed with carbon tetrachloride, then methanol, oven dried at 60°C and stored in a dessicator.

2:2 Specimen Preparation

(i) Vycor Glass

Activation of the Vycor specimens was achieved by careful drying. The glass was oven dried at 60°C for one hour to prevent breakage from thermal shock. The specimens were then baked in a vacuum of 8×10^{-7} mm Hg in the specially designed vacuum cell, Fig. 6, for a period of 48 hours at approximately 100°C. The initial pump-down must be extremely slow, since rapid evaporation of the water causes cracking due to thermal changes.

Fig. 1 shows the effect of baking temperature on the absorptive capacity at a given vapour pressure. Thus for devices to be used at room temperature, 180°C is the most effective activating temperature. Due to the size of the cell a temperature of only 100°C could be obtained with external heating.

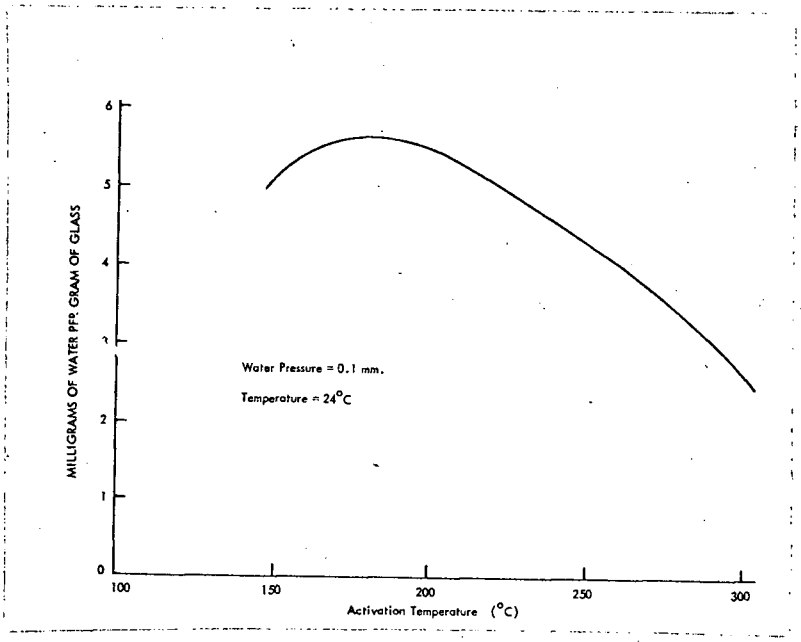

(a) Effect of Activation Temperature on Adsorptive Capacity at room temperature and a water vapour pressure of 0.1 mm

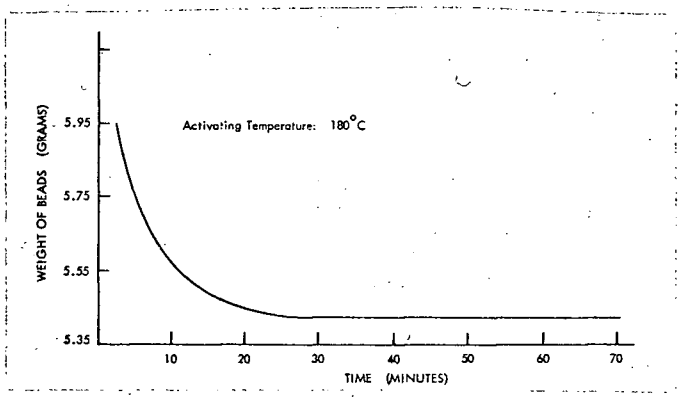

(b) Weight Loss vs. Time at an Activation Temperature of 180°C

FIGURE 1. ACTIVATION OF VYCOR GLASS
(Corning Glass Works, Corning N.Y.)

(ii) Other Specimens

Specimens of borosilicate glass and rock were evacuated at 8×10^{-7} mm Hg for 48 hours at 100°C prior to the experiment, whilst with polymethyl methacrylate no external heating was used due to changes in physical properties at low temperatures.

2:3 Fracture Measuring Techniques

A variety of techniques have been employed in the study of fracture of brittle solids. Impact tests on a notched bar utilize the conventional Charpy and Izod testing machines. In both systems the specimen is struck by a swinging pendulum and the energy required to cause fracture is measured by the loss in energy of the pendulum[29].

Most comminution studies determine grindability by measuring the surface area produced in a particular grinding test. The energy input to the mill is then compared to the surface area produced[13]. Other techniques[16] involve free crushing conditions, yielding a similar result of load versus particle size distribution produced; or the propagating of existing cracks or notches in cleavage tests[30].

Compression tests on rocks[31], glass[32] and more generally concrete[33] have been carried out to yield compressive strength, but since environmental effects occur only in tension this type of test was not applicable. Tensile tests as applied to metals are frequently utilized, but the problem

of manufacturing specimens from brittle non-metallic materials precludes this simple technique. Experiments have been attempted by pulling machined specimens, but specimen variations, especially surface variations, make the results suspect.

Fracture velocities may be measured with ultrasonic techniques or by high speed-photography[34]. Roesler[35] applied the technique of Hertz for controlled crack propagation experiments. The technique involves the use of a cylindrical indenter to which a load is applied. The spherical crack propagates in a conical fashion so that the crack area is increasing continuously. Thus the crack will stop propagating until the load is increased further. The technique affords a useful means of studying environmental effects since the chemical can be applied at the indenter tip. However, for opaque solids the method is limited.

Bending tests[36] have been applied by many workers and prove to be simple and easily adaptable to vacuum systems. With glass specimens however the scatter is fairly high ($\pm$ 29%) making results difficult to analyse.

The Brazilian Test

As early as 1883, Hertz[37] proposed a theory for the state of stress developed when a cylinder is compressed across its diameter. The theoretical basis has been dealt with by Timoshenko[38], Frocht[39] and others. A Brazilian,

Caniero[40], proposed a method whereby the tensile strength of cylindrical specimens could be determined. During recent years the method, which is both rapid and simple, has been used to establish a comparative tensile strength for rocks.

Theory

The Brazilian test is based upon the state of stress developed when a cylindrical specimen is compressed diametrically between platens as illustrated in Fig. 2.

Assuming plane stress and considering the disk, with concentrated load in the diameter the following three general equations can be used to express the stress conditions at all points within the disk,

$$\sigma_x = \frac{2P}{\pi t}\left[\frac{(R-y)x^2}{r_1^4} + \frac{(R+y)x^2}{r_2^4} - \frac{1}{D}\right]$$

$$\sigma_y = \frac{2P}{\pi t}\left[\frac{(R-y)^3}{r_1^4} + \frac{(R+y)^3}{r_2^4} - \frac{1}{D}\right]$$

$$\sigma_{xy} = \frac{2P}{\pi t}\left[\frac{(R-y)^2x}{r_1^4} - \frac{(R+y)^2x}{r_2^4}\right]$$

where

$$r_1^2 = x^2+(R-y)^2$$

$$r_2^2 = x^2+(R+y)^2$$

Of primary interest is the maximum tensile stress

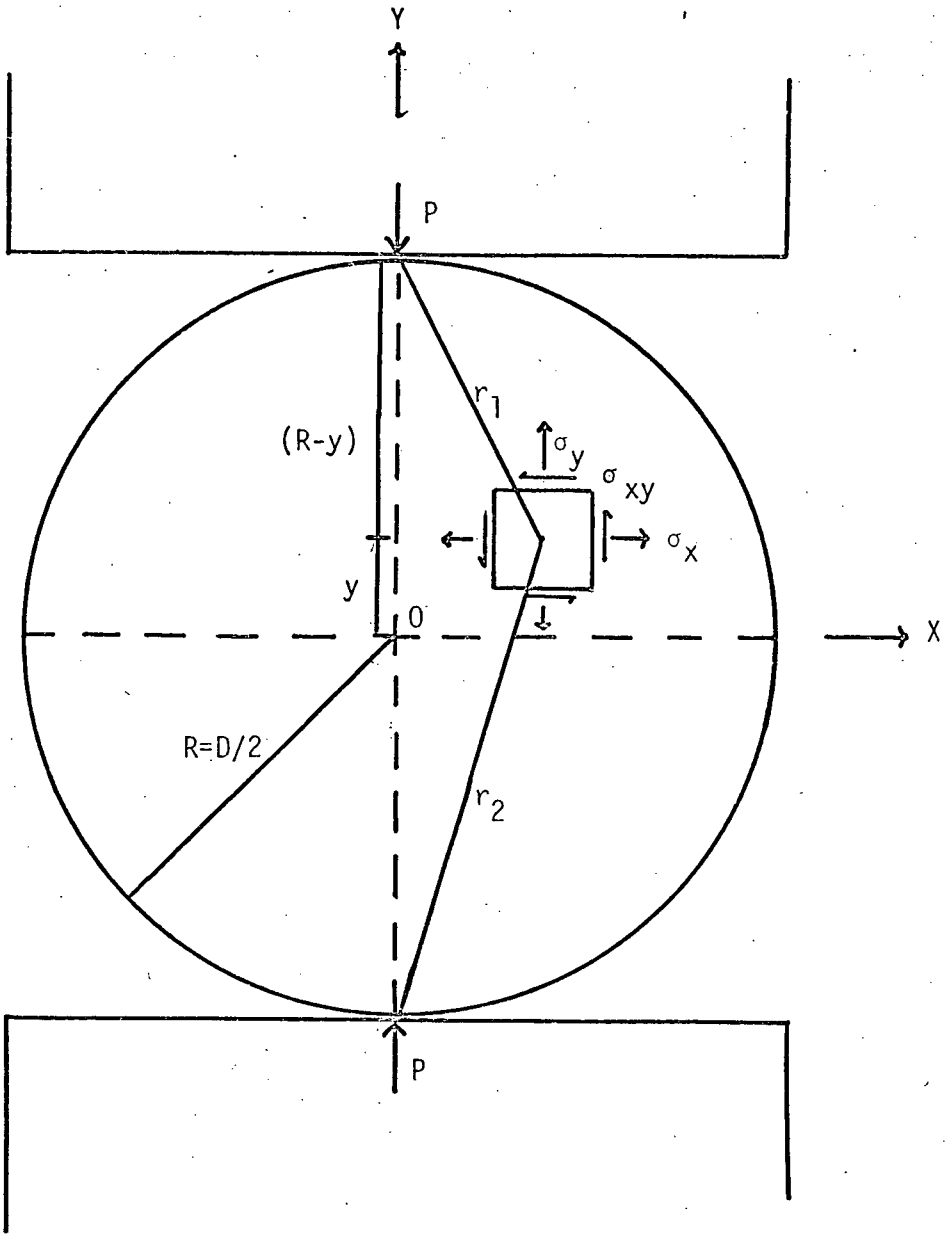

FIGURE 2. THE BRAZILIAN TEST

which occurs normal to the loaded diameter AB. This, in general, has a constant magnitude.

$$\sigma_1 = -\frac{2P}{\pi Dt}$$

where,

σ_1 = Maximum tensile stress

P = Applied load

D = Specimen diameter

R = D/2

t = Specimen thickness

In addition to this tensile stress with point loading, compressive stress acts along the loaded diameter from a minimum of $\frac{6P}{\pi Dt}$ at the centre, to an infinitely high value immediately under the loading points.

In practice it is required that fracture be initiated by these evenly distributed tensile stresses if the test is to yield useful results.

Hence the high compressive stress at the loading points should be dissipated. It has been shown[41,42] that the maximum stress σ_y near the ends can be reduced by distributing the load with pads. However this padding will change the σ_x from tension to compression in the vicinity of the padding. It can be shown[43] that the stress distribution near the centre is unaffected by the stress redistribution due to the pads.

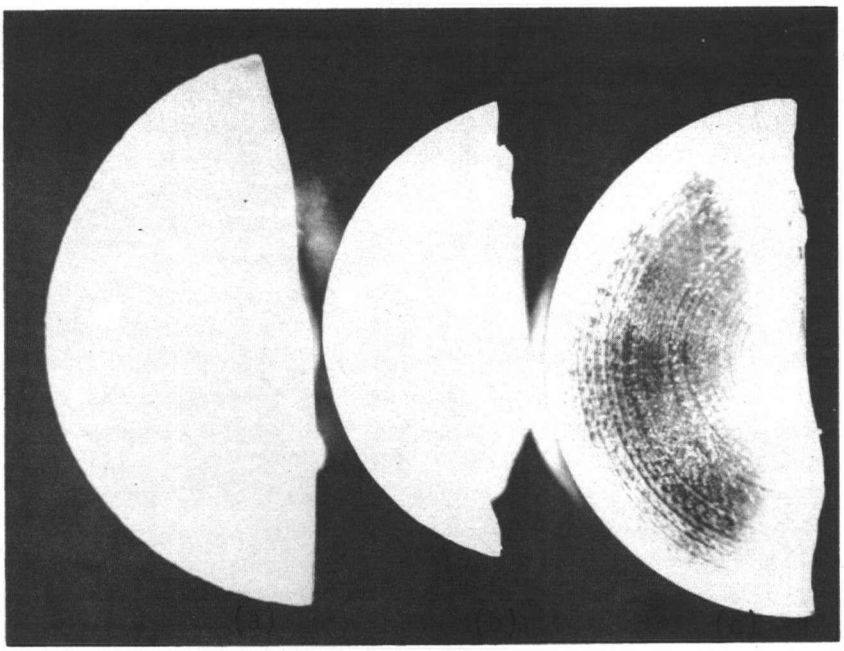

FIGURE 3 TENSILE FRACTURE OF CYLINDRICAL SPECIMENS
(a) Vycor Glass
(b) Kimble Glass
(c) Polymethyl Methacrylate.

It has also been shown[43] that the tensile strength of a specimen decreases slightly with an increasing t/D ratio.

The selection of the Brazilian test for this research project resulted from the fact that corrosion cracking occurs in tension and the above test offers a simple, rapid method of obtaining results. Since comparative results are desired for the tensile strength under varying environmental conditions, a fixed t/D ratio of 1 was selected and padding was not employed.

Figs. 3a, b, and c, illustrate the tensile fracture occurring on the three types of specimens. In all cases the crack propagates along the specimen diameter in the direction of the maximum compressive force, i.e. at right angles to the maximum tensile load.

2:4 Preliminary Experiments

(a) Hydraulic Loading Tests

Cylindrical core samples of rock with a height/diameter ratio of 1 were compressed diametrically using an hydraulic jack and press. Loading to failure was applied at as constant a rate as possible. With the specimens immersed in a variety of aqueous solutions and organic solvents no positive results were obtained in indicating sorption weakening systems. Two factors became apparent however. Firstly, the need for an accurately controlled loading device. Secondly the effects of surfactant environment would be a

function of the state of the original surface. Clean, uncontaminated, reproducible surfaces are essential.

(b) Triple-point Bending Tests

A series of triple point bending tests were carried out on borosilicate glass rods in air to give a direct comparison with the Brazilian test.

Table 1 shows that the Brazilian test gives results with very much less scatter than the bending test. (A coefficient of variation of 15.6% as opposed to 28.7% for the bending test.) This could be due to the effects of flaw geometry. In the bending test the tension is over a smaller area and hence more critically affected by differing flaw size. The statistical distribution of the flaws over the smaller area also accounts for the ratio of the tensile strength to be greater for the bending test than for the Brazilian test, by a factor of 1.8.

2:5 Fracture Apparatus

The experimental apparatus consisted of the following major components.

(a) Constant Strain rate loading device.

(b) Vacuum pumping system.

(c) Load cell and strain indicator.

(d) Vacuum cell.

(e) Gas train.

TABLE 1

Bending Test versus Brazilian Test

	Rod Diam.	No. in Test	Tensile Strength P.S.I.	Coeff. of Variance
Bending Test	.5"	12	10,315.4	28.7%
Brazilian Test	.5"	12	5,730.8	15.6%

Ratio of Tensile Strengths $\frac{\text{Bend}}{\text{Braz}} = 1.8$.

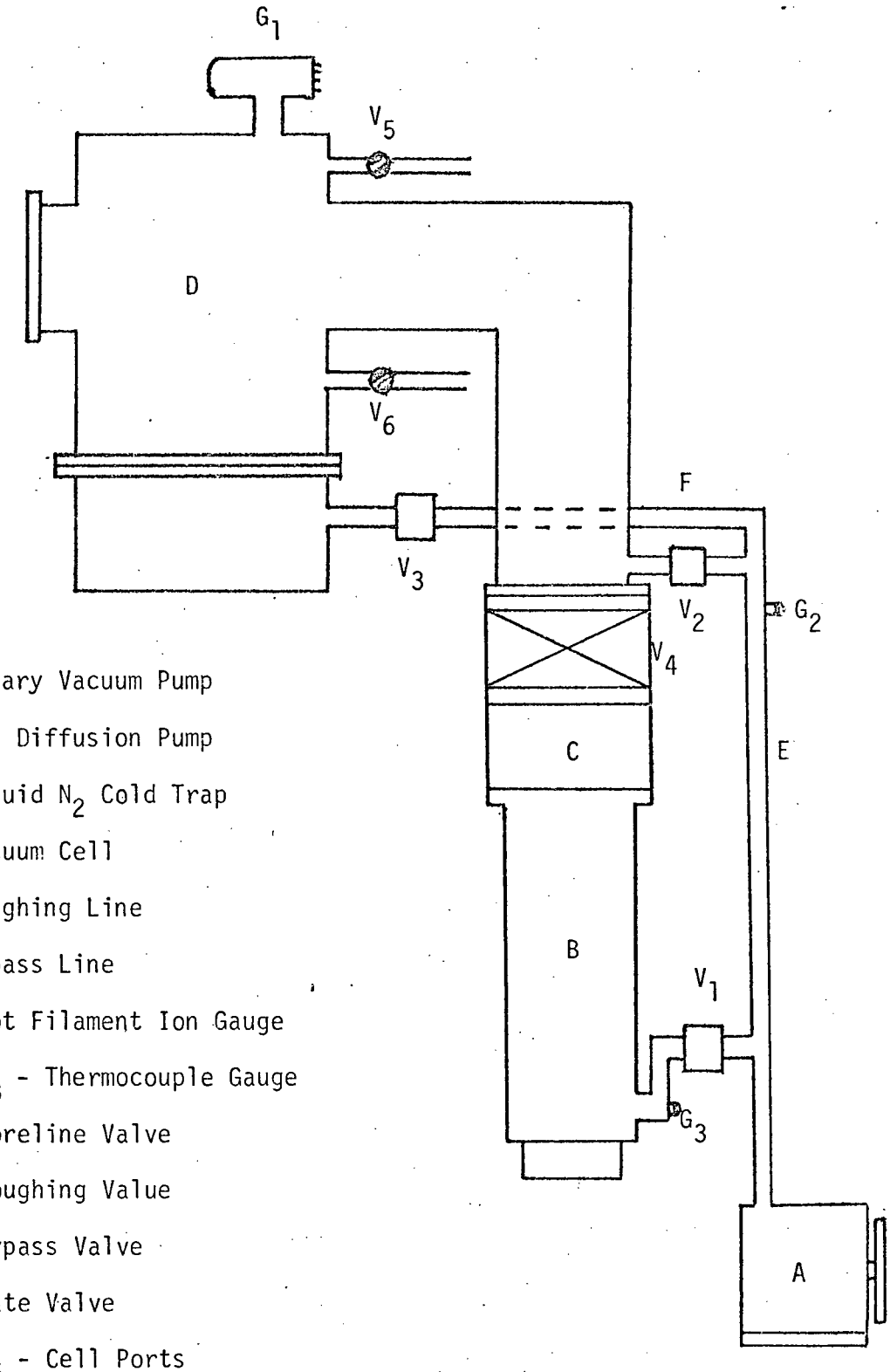

A - Rotary Vacuum Pump

B - Oil Diffusion Pump

C - Liquid N_2 Cold Trap

D - Vacuum Cell

E - Roughing Line

F - Bypass Line

G_1 - Hot Filament Ion Gauge

G_2 & G_3 - Thermocouple Gauge

V_1 - Foreline Valve

V_2 - Roughing Value

V_3 - Bypass Valve

V_4 - Gate Valve

V_5 & V_6 - Cell Ports

FIGURE 4. HIGH VACUUM PUMPING SYSTEM

(a) The Press

Since tensile strength is a function of strain rate it is essential that the strain rate be known. For comparative results employing a variety of chemical environments it is also necessary to use a reproducible constant strain rate for each series of tests.

A Wykeham Farrance Compression Testing Machine, Model T.57, with a load capacity of 5 tons, was selected for these experiments. The machine has a motorised feed and a gear box, which eliminates any hydraulic system. The gear box has six 5-1 reductions and additional change wheels, giving a total of thirty different rates of feed, ranging from 0.3 inches/minute down to 0.000024 inches/minute.

The ram has a 4 inch distance of travel and is driven by a 1 H.P. electric motor. Manual adjustment of the ram is possible in both the coarse and fine ranges prior to activating the motor. A reversible switch allows loading and unloading of the specimen at constant strain rate.

(b) Vacuum System

A schematic diagram of the vacuum system is shown in Fig. 4. Details of the components are given in Appendix A.

The pumping system consists of a forepump A, a foreline valve V_1, a 6 inch oil diffusion pump B, and a liquid nitrogen trap C, coupled directly to the vacuum cell D. The cell may be isolated from the diffusion pump by the butterfly valve V_4.

A roughing line E via valve V_2 allows the cell to be "roughed out" prior to opening the butterfly valve to the high vacuum line.

A separate by-pass line F is provided, to enable the low vacuum chamber to be maintained at roughing line pressures during a run.

A hot filament ionization gauge G, is used to measure high vacua ($> 10^{-4}$ mm Hg), whilst thermocouple gauges at G_2 and G_3 give low vacuum readings.

Valve V_5 allows the vessel to be flushed with N_2, whilst also supplying an inlet port for the introduction of vapours. A mercury manometer, with one leg evacuated, allows vapour pressure differences within the cell to be measured through valve V_6. A separate pump is used for lowering the mercury in the manometer.

(c) Vacuum Cell

A schematic diagram of the high vacuum cell is shown in Fig. 6. Due to the lengthy pump-down times with adsorbants of high surface area, and the statistical nature of the experiment, the cell was designed to enable a sequence of twelve specimens to be fractured in either high vacuum, or a controlled atmosphere.

The specimens are mounted on stainless steel buttons and held in place by light tension clips (Fig. 7). A rotating specimen table holds twelve buttons and can be turned by

means of handle H through a triple O-ring seal.

To avoid leakage around a piston moving in a reciprocating manner into the cell, a Bellofram rolling diaphragm was inserted. A split piston allowed the high vacuum chamber to be separated from a low vacuum chamber by the diaphragm. The low vacuum chamber (10^{-3} mms Hg.), on the underside of the diaphragm, served a double purpose. Firstly it eliminated leakage into the high vacuum chamber and secondly it reduced the pressure differential across the diaphragm. A device of this nature proved successful in maintaining a vacuum down to 8×10^{-7} mm. Hg., whilst allowing a piston motion of approximately 1 inch. Many existing problems in high vacuum experiments could be eliminated by this technique since extremely careful machining is not required. Details of the diaphragm are given in Appendix A.

Unfortunately, as a result of the fracture experiments, fine glass chips caused the diaphragm to tear between the piston and cylinder walls. Repeated attempts to prevent this tearing proved unsuccessful and the design was abandoned.

A split piston push rod was substituted, operating through a triple O-ring seal. Due to the slow operation of the push rod, (.03 inches/min), no leakage occurred. The low vacuum chamber was still incorporated to reduce possible leakage and to act as a vertical guide for the piston.

The cell was constructed of heavy brass tubing of twelve inches diameter with 1/4 inch brass end plates. A six

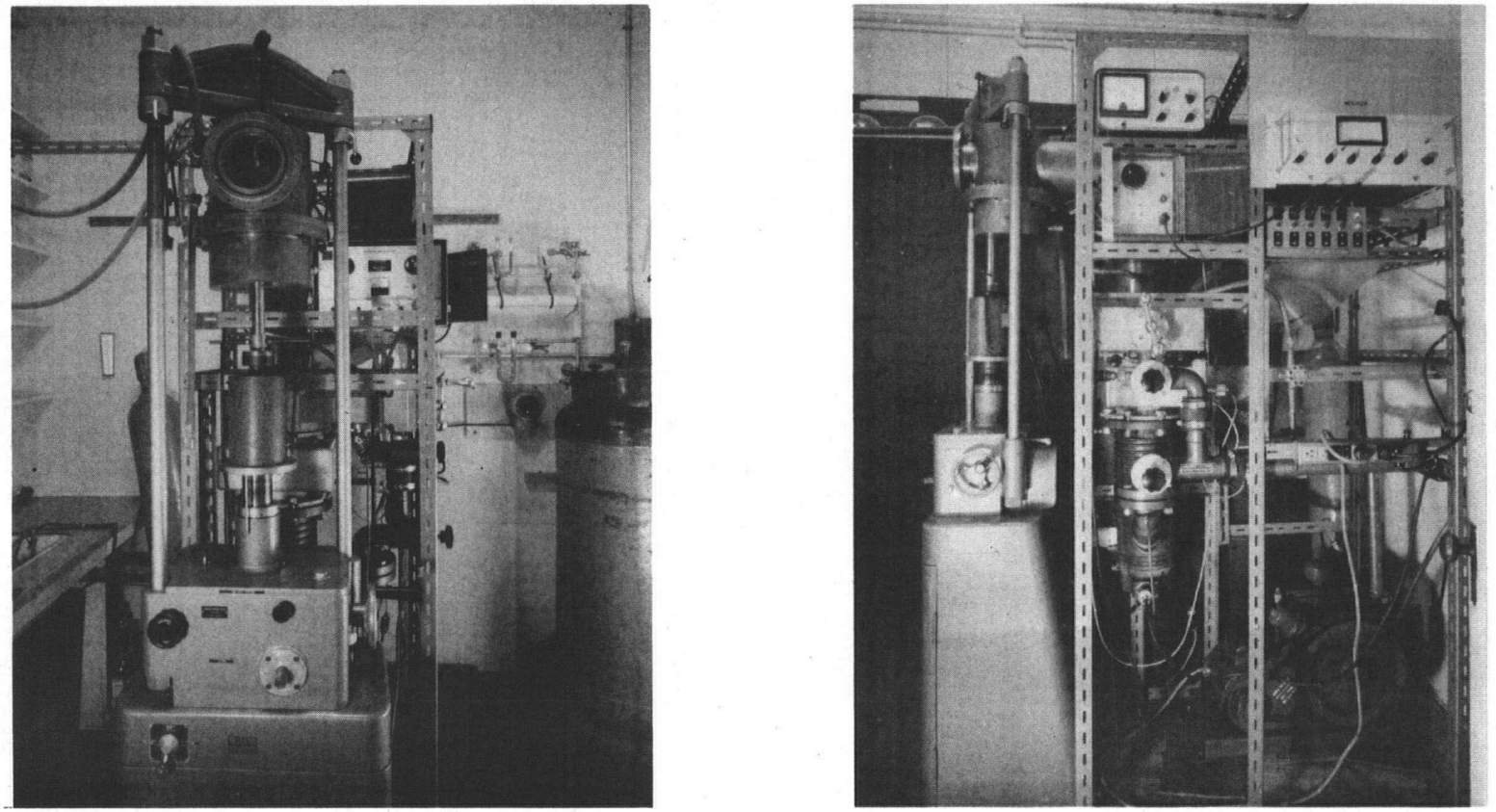

FIGURE 5. HIGH VACUUM FRACTURE APPARATUS.

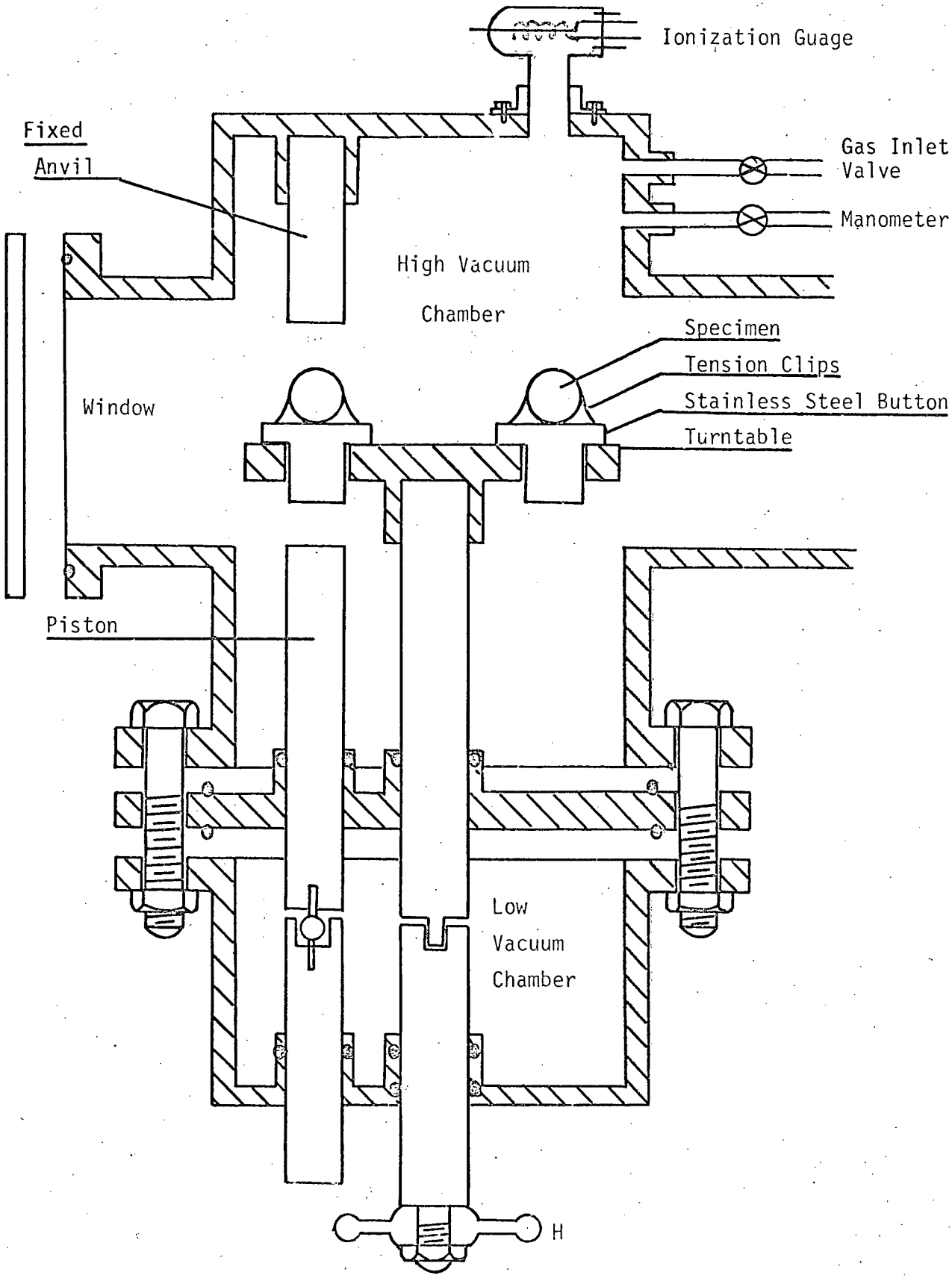

FIGURE 6. HIGH VACUUM CELL

inch window allowed visual observation of the fracture procedure. The upper fixed anvil, specimen buttons and the piston were made of one inch stainless steel rod. A six inch diameter manifold provided connection to the high vacuum gate valve. The hot filament ionization gauge was mounted on a one inch port on top of the cell by silver soldering the Kovar seal to the connecting flange.

The piston was coupled to the ram of the constant strain rate machine by two light springs to counteract the effect of atmospheric pressure forcing the piston into the cell.

Vacuum Seals

All elastomer seals used in the apparatus were standard O-rings of buna-rubber or neoprene. Brass to brass connections were made by soft soldering the pickled components.

(d) Load Measurements

All applied loads were measured using a strain gauge indicator and load cell.

The load cell utilizes the principle that the electrical resistance of very thin wires varies with change in length (strain) as imposed by an applied load. The read-out measures the changes in resistance in terms of microstrains, i.e. micro inches per inch.

Details of the components and their calibration are given in Appendix A and B.

2:6 Experimental Procedure

The specimens were prepared as previously described. To avoid contamination when loading the cell, specimens and buttons were handled with rubber gloves or adsorbent tissue.

The cell was roughed out to backing pump pressures by opening valve V_2, then flushed with dry nitrogen. During loading a positive pressure of nitrogen was maintained in the cell to prevent adsorption of moisture on the specimens and walls of the system. Loading of the cell was most easily accomplished with the cell fully assembled and loading through the 6 inch window port.

With the window in position the cell was pumped down to ~20 microns Hg through the roughing line E. The cell was then flushed once with dry nitrogen, by opening valve V_5. The pump down process was repeated to 20μ Hg, when the butterfly valve to the high vacuum line was opened, after closing V_2 and opening backing valve V_1. The external heating coils were activated and the system allowed to pump for 48 hours, resulting in a vacuum of the order of 8×10^{-7} mm Hg.

The piston was raised manually until a reading registered on the strain indicator. With the clutch of the constant strain rate machine engaged, the load was applied until fracture occurred. The tensile fracture strength could be calculated from the observed strain reading recorded on

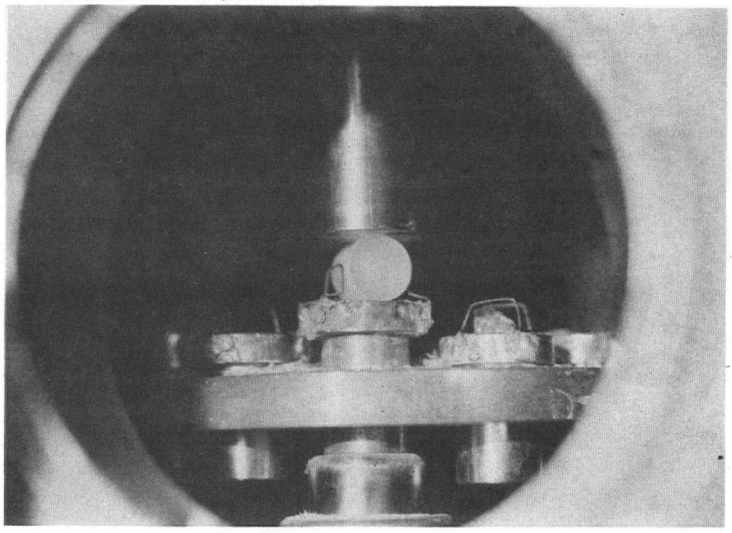

FIGURE 7. SPECIMEN IN FRACTURE POSITION.

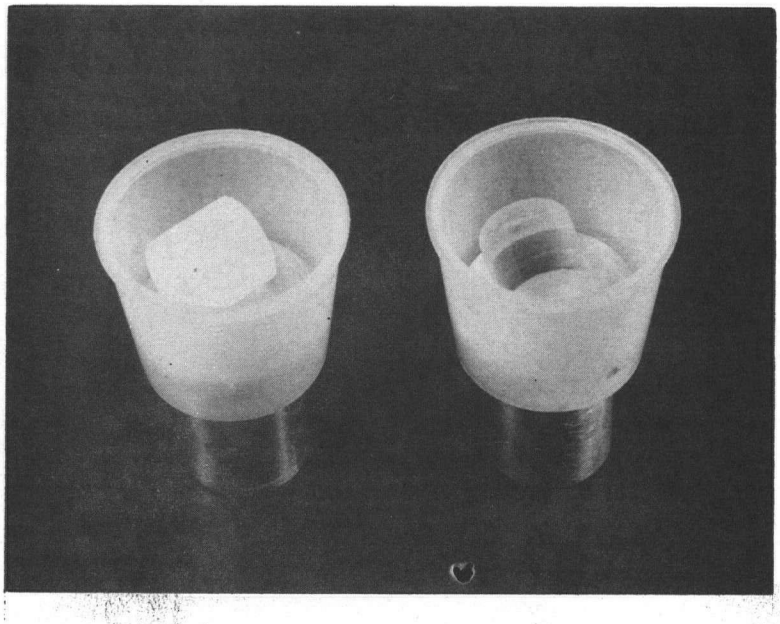

FIGURE 8. CONTAINERS FOR FRACTURE IN LIQUID PHASE.

the strain indicator at failure.

(a) Adsorption from the vapour phase

For vapour phase adsorption experiments the adsorbate was placed in a vessel and subjected to vacuum through valve V_5, before the cell was loaded. After pumping for a short while to remove entrained gases from the liquid adsorbates, the liquid was frozen in a liquid nitrogen dewar. The vessel and line were pumped down during the evacuation of the specimens by opening valve V_5 with the adsorbate in the frozen condition. The vapour could be introduced into the vessel by removing the dewar and warming with the heat of the hand. After the appropriate dosage, valve V_5 was closed.

(b) Adsorption from solution; or experiments in the liquid phase.

(i) Treatment prior to introduction to the cell.

Specimens were evacuated as before. The cell was then filled with dry nitrogen and the specimens removed from the cell and placed in the test solution as quickly as possible. Fracture experiments were then carried out in air by removing the specimens one at a time from the solutions and fracturing in the cell.

(ii) Liquid treatment within the cell.

Small polythene cups were placed around each button. Fig. 8. After specimen vacuum treatment as in previous runs, the cups were filled with solution whilst a positive nitrogen

pressure was maintained within the cell. The solution was admitted through the window port from a polythene container via a length of polythene tubing. Fracture experiments could then be carried out with the specimens immersed.

2:7 The Adsorption Apparatus

An all-glass B.E.T. pressure-volume adsorption apparatus was constructed for the purpose of determining the adsorption properties. The use of a high surface area solid (Vycor glass), and gases and vapours of sufficiently high saturated vapour pressures (Po), at the temperature of the experiment, make a method of this type quite satisfactory.

The details of the apparatus are shown in Fig. 9. The main features are,

(a) Vacuum System

The pumping system consists of two parts:

(i) High vacuum which is maintained by a mechanical pump in series with a six-inch oil diffusion pump.

(ii) Low vacuum line, maintained by a mechanical pump. This line is used to lower the levels of the mercury in the gas burettes and mercury cut-off valves.

(b) Vacuum Measuring Device

High vacuum measurements are made on a hot filament ionization gauge in the main manifold. Checking of vacuum at

roughing pressure was carried out using thermocouple gauges.

(c) Gas Reservoirs

Four 3-litre reservoirs made up the gas storage line. One bulb was kept full of He for calibration purposes. All gases were passed through a purification train before being admitted to the reservoir.

To eliminate leakage the gases were stored at pressures close to atmospheric pressure.

(d) Gas Burettes and Manometers

The gas burettes are a series of bulbs connected by lengths of capillary tubing. Etch marks are made between the bulbs, whose volumes are calibrated prior to mounting in the apparatus. The size of the individual bulbs is of no consequence, but a large number of combination volumes are useful for a complete adsorption isotherm. Mercury cut-off manometers are used whenever possible to eliminate stop-cock grease. To maintain a constant internal volume the mercury in the manometers could be adjusted to fixed reference points after each gas dose and again before each pressure reading.

(e) Sample Vessels

To avoid lengthy pump down times before each determination, three sample vessels were used (Fig. 10). These could be isolated during an adsorption run.

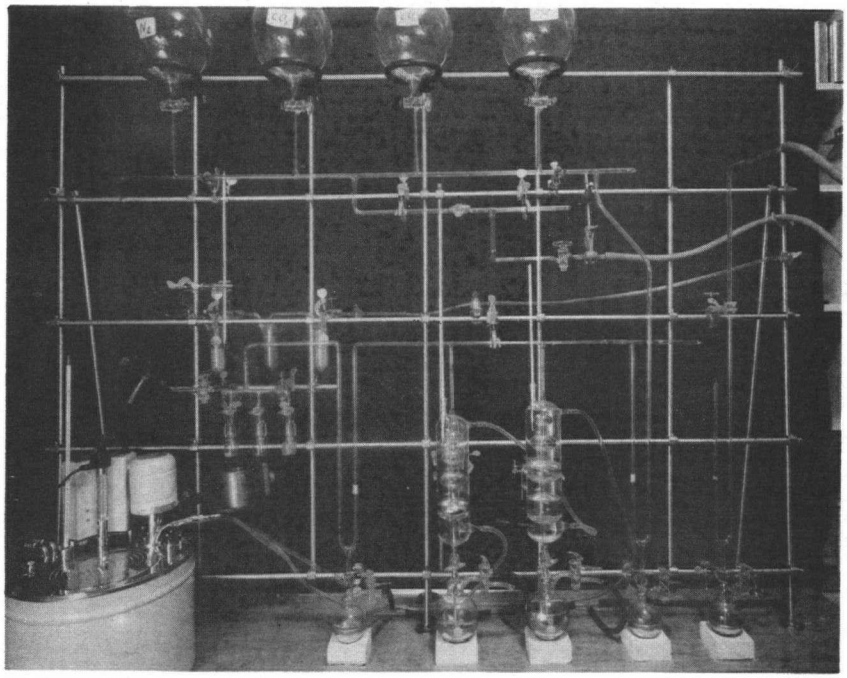

FIGURE 9. THE ADSORPTION APPARATUS

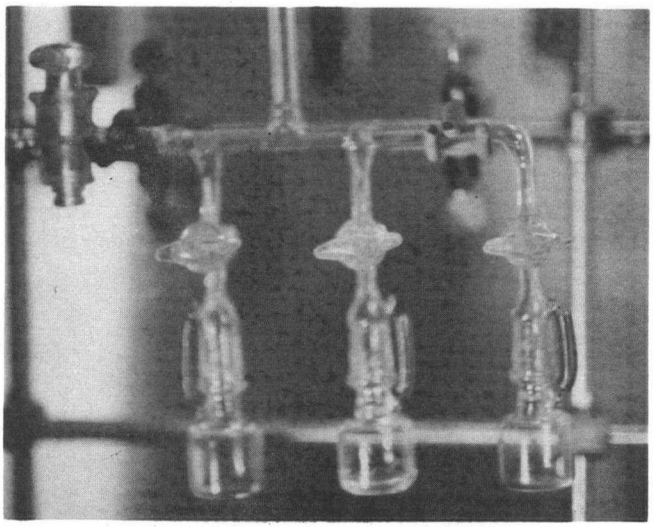

FIGURE 10. THE SAMPLE VESSELS

(f) Furnace

A two inch diameter tube furnace was used to outgas the specimens at an elevated temperature of 180°C.

(g) Thermostating System

The gas burettes were thermostated by circulating water from a constant temperature bath through the water jackets in series. A temperature drop of .5° was experienced across the line.

(h) Pressure Measurements

Pressure differences were read on a 50 cms cathetometer using a vernier scale to three decimal places, in cms.

2:8 Adsorption Procedure

A precleaned weighed sample is evacuated in a sample vessel. A known volume of vapour is then admitted to the sample vessel and the volume not adsorbed is determined from the pressure readings. Knowing the saturated vapour pressure of the vapour at the experimental temperature, allows the adsorption isotherm to be plotted according to the B.E.T. equation in the form,

$$\frac{P}{V(Po-P)} = \frac{1}{VmC} + \frac{C-1}{VmC} \times \frac{P}{Po}$$

P = Corresponding pressure

Po = Sat. Vap. Pressure

Vm = Monolayer Vol.

C = Const. which is a function of the heats of adsorption.

By plotting $\frac{P}{V(Po-P)}$ as a function of P/Po a straight line of slope $\frac{C-1}{VmC}$ and intercept $\frac{1}{VmC}$ is obtained.

The B.E.T. isotherm holds over the pressure range $.05 < P/P_{\odot} < .35$. Deviations from linearity are usually found outside this range.

The parameters of interest from a determination of this type would be,

(1) The volume of gas adsorbed at any equilibrium pressure P.

(2) The monolayer volume (Vm), being the volume of adsorbate to form a mono-molecular layer over the surface of adsorbent.

(3) The surface area (S) obtained by converting Vm to the corresponding number of molecules and multiplying by the cross-sectional area.

CHAPTER THREE

THE THEORY OF BRITTLE FRACTURE

3:1 The Properties of the Solid

(a) Glass

The glass-like or vitreous state is believed to be that of a solid with the molecular disorder of a liquid frozen into its structure.

Random Network Theory

Glass appears to have many of the features of a normal solid, viz., strength, hardness, elasticity etc., but further examination shows it to have an extended melting range, whilst x-ray structural analysis indicates a molecular structure akin to that of a liquid at low temperatures.

Zachariason, (1932)[44], proposed that the atomic or molecular arrangement in the glass like state is an extended network which lacks symmetry and periodicity. He laid down a number of simple rules relating the way in which oxygen anions and the cations must link together for an oxide to exist in the glassy state. Briefly, the glass forming cations (B^{+++}, P^{+++++}, Si^{++++}) are surrounded by polyhedra

of oxygen ions in the form of tetrahedra. The oxygen ions are of two types viz., bridging ions, each of which link two polyhedra and non bridging oxygen ions each of which belong to only one polyhedron. Such a system would produce a polymer structure with long chains cross-linked at intervals. In the structure would be regions of unbalanced negative charge where the oxygen ions are non-bridging. Cations of low positive charge and large size (Na^+, K^+, Ca^{++}) may exist in holes in the network, where they compensate the excess negative charge.

Oxides forming the basis of the glass are known as network formers and those soluble in the network as network modifiers.

In 1947 Sun[45] advanced a theory that glasses are only formed from those oxides in which the bond strength between the oxygen and the cation reaches a certain minimum value.

Oxides lowering the bond strength may act as network modifiers, or intermediates, but not as network formers. The bond strength $M^+ - O^-$ of all glass formers is greater than 80 Kcals per Avogadro number of bonds, whilst that of the modifiers below 60 Kcals. The classification is arbitrary.

Using x-ray analysis Warren[46] has confirmed the Zachariason model on the structure of glass.

Screening Power

When a group of atoms interact chemically, single molecules will be formed only if the cation is a proton (NH_3), or if the number of anions required to neutralize the charge of the cation, at the particular temperature, is sufficiently great to provide proper shielding of the cation force field (SiF_6). Unless both conditions, electroneutrality and adequate screening are met, the interaction of the atoms does not lead to the formation of molecules, but to an indefinite array of ions, i.e. a solid.

Silica glass is therefore better described by the formula $Si^{++++}\ (O^{2-}/2)_4$. This expression indicates that the cation is screened by four O^{2-} ions. Since the composition is SiO_2, each O^{2-} ion is shared by two Si^{++++}, and is therefore depicted as $O^{2-}/2$ for each Si^{++++} ion. This formulation indicates the screening of the co-ordinate requirements of the cations and the nature of the building units.

The freshly fractured surface will be a region of incomplete screening, resulting in higher reactivity and a greater electron redistribution in lateral surface bonds. A contraction of these bonds results, the surface remaining in tension. Certain spontaneous surface reactions will serve to withdraw electrons from these lateral bonds, a relaxation and swelling of the solid results. Obviously the stronger the surface interaction, (the screening power), the greater the

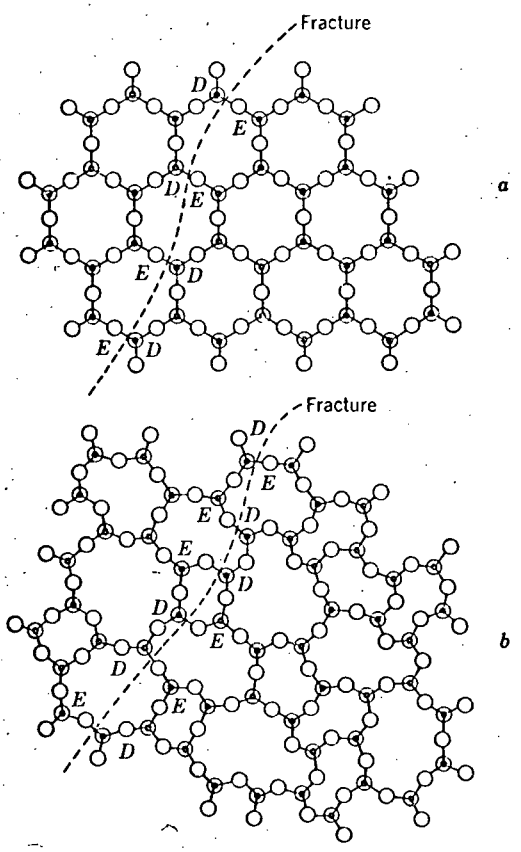

FIGURE 11. SCHEMATIC PICTURE OF THE FRACTURE OF SILICA

(a) Quartz (b) Silica
o Oxygen ⊙ Silicon

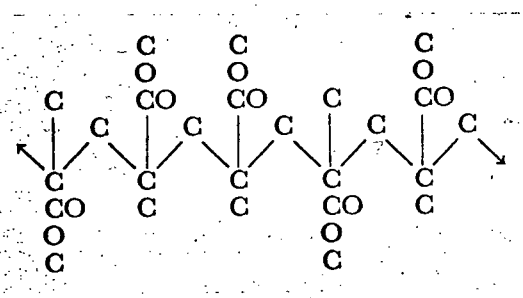

FIGURE 12. THE STRUCTURE OF POLYMETHYL METHACRYLATE.

electron withdrawal.

The effects of the screening of the force field of the Si^{++++} cores on the mechanical strength properties of the material, will be dealt with in the section on adsorption.

Surface Structure

A freshly formed surface of silica contains two kinds of structural units called E-centres and D-centres (Fig. 11).

The E-centre, (excess oxygen centre), consists of an Si^{++++} ion that is screened by four O^{2-} ions. The Si^{++++} ion shares only three of its four O^{2-} ions with neighbouring tetrahedra, its fourth O^{2-} ion is not shared with another cation. The structural unit may be written

$$(Si^{++++} O^{2-}_{2.5})^{-}$$

The D-centre (deficient oxygen unit) has a positive excess charge. The Si^{++++} ion is incompletely screened, hence these units are responsible for the high surface energy of silica surfaces. The structural unit has the formula

$$(Si^{++++} O^{2-}_{1.5})^{+}$$

In the absence of reactive molecules the surface of freshly broken silica consists of an array of E-units and D-units having excess positive and negative charges.

The possibility of an electron transfer from an E to a D unit is not likely, since this would result in the formation of Si^{+++} ions having 8+1 outer electrons.

Chemical Reactivity of the Glass Surface

An E-centre contains three bridging O^{2-} ions stabilized by two Si^{++++} ions. In addition, the unit contains one O^{2-} exposed to only one Si^{++++} ion. This O^{2-} ion has greater polarizability and screening power than the other two and is termed a 'basic' active centre, with a negative excess charge.

Thus the D-centre, or 'acidic' active centre is positive, due to the incompletely screened Si^{++++} ion. The simultaneous occurrence of basic and acidic sites in the same surface leads to many interesting chemical reactions.

(i) Water Vapour

It is a well established fact that the surface of glass is covered with a layer of hydroxyl groups which affect many of the solid's properties. This layer may be depicted as

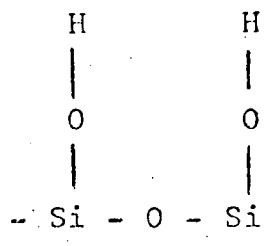

and is generally termed the "bound water". Many of the

reactions occurring at the glass surface involve the silanol surface. The work of Dzisko, Vishnevskaya and Chesalova[47] shows,

(1) Physically adsorbed water is removed by drying to constant weight at 115°C.

(2) The bound water is proportional to the surface area.

(3) Between 115°C and 600°C the hydroxyl groups are evolved without serious loss of surface area.

(4) Above 600°C surface area is destroyed.

(ii) Adsorption Reactions

Many of the adsorption reactions with glass may be regarded as secondary reactions since the surface must first adsorb a hydroxyl ion, or lose a proton, in order to provide a site for cationic adsorption. The fractured surface is usually distorted in such a way as to bring the more polarizable O^{2-} ions to the surface in order to screen the smaller Si^{++++} ions. Thus the surface is essentially negatively charged. Non-ionic organic compounds are attracted to the silanol surface, usually in the more stable micellar form[48]. The adsorption of long-chain substituted ammonium ions has been employed for the flotation of silica from ores for many years, the adsorption taking place from aqueous solution.

Adsorption from solution involves a competition for the surface site between the solvent and solute molecules.

Thus in general, the less polar the solvent the greater the adsorption of the active solute species. Amines are, however, strongly adsorbed from the gas phase, a monolayer being formed at very low partial pressures[49].

Yates[50] has demonstrated the importance of hydrogen bonding in explaining volume changes accompanying adsorption on Vycor glass rods.

The difficulties encountered in studying interactions on glass surfaces arise from the presence of water vapour and the extremely high reactivity of the surface.

Stress Corrosion of Glass

Mechanical forces acting on the solid change the interatomic distances, causing the solid to change its optical and electrical properties, as well as its chemical reactivity. For silicas under a tensile stress the Si^{++++} ions are screened to a lesser degree and are therefore more likely to increase their co-ordination by adding $(OH)^-$ ions. The polarizability of the O^{2-} ions is increased due to the increase Si-O-Si distance in the direction of the force. A proton will now preferentially enter the electron cloud of the more polarizable O^{2-} ions. Therefore the mechanical forces aid chemical corrosivity by increasing the internuclear distances. One would thus expect any environment with an affinity for the glass surface to decrease the tensile strength by screening the effects of attractive cohesive

forces; the greater the screening, the greater the decrease. C.J. Culf[51] has measured the effect of several liquids and dried gases upon the mechanical strength of plate glass. Moisture gave the major decrease in mechanical strength (a fracture energy of 2900 dynes/cms), with dry ammonia gas, (an effective screener), having a lesser effect, but similar to many liquids, (4200 dynes/cms).

The static fatigue phenomenon, to be discussed subsequently, is a direct consequence of the mechanochemical reaction of the glass surface with the ambient moist atmosphere.

(b) Plastics - Polymethyl Methacrylate

This acrylic thermoplastic $[-CH_3-C(CH_3)COOCH_3)-]_n$ possesses many remarkable properties and is chosen for this study for its brittleness at room temperature. Polymethyl methacrylate has a molecular shape of long continuous carbon chains to which the methyl and ester groupings are attached. Fig. 12 shows the structure, which is large in the transverse direction. There is evidence that the polymer exists largely in a coiled configuration. Every second carbon of the chain is asymmetric, with resulting isomeric d and l arrangements randomly located down the chain. This randomness makes an ordered arrangement of the molecular chains difficult. Steric effects associated with the ester grouping are also non-conducive to crystallization. Thus polymethyl metha-

crylate is completely non-crystalline.

General Considerations in Polymer Failure

The forces of attraction between the polymer molecules are of two types; hydrogen bonds and Van der Waal's forces. The Van der Waal's, or secondary forces, are due to a combination of several forces, namely, the orientation effect (attraction between dipoles), the induction effect (attraction between a dipole and an induced dipole), and the London dispersion effect (attraction between non-polar molecules because of electron induced fluctuating dipole moments). The presence of polar groups in macro-molecules greatly increases their net attraction.

The point of initiation of the fracture process may be quite arbitrary, usually commencing from structural imperfections. These imperfections are frequently at the surface and rupture is usually a surface initiated effect.

The tensile strength refers to the ultimate property of the material, normally expressed in terms of the tensile load at fracture divided by the initial undeformed area of cross-section.

Factors influencing the tensile strength of plastics are, polymer constitution, crystallinity, degree of cross-linking, molecular weight, temperature, rate of test, geometry of the test piece and the type of surrounding environment.

Fracture in the Glassy Region

When the rate of the strain becomes high, or the test temperature sufficiently low, a material that was formerly rubbery, begins to behave as a glass. Due to the restricting effect of internal viscosity, the chains of the network are unable to uncoil and stretch in a rubbery fashion. Under such conditions fracture is of a brittle nature and the network chains are far from fully extended at the moment of fracture.

Beuche[52] has derived a theoretical treatment for the brittle failure of polymers using a statistical mechanical approach very similar to that of Poncelet for glass.

Environmental Stress-cracking of Plastics

The term environmental stress cracking applies to accelerated surface initiated brittle failure, which occurs when the material is subjected to a tensile stress in an 'active environment'. The effect of this environment is to induce cracking which would not occur in its absence, or to cause failure at lower stress, or in shorter times, than would normally be experienced in an inactive environment.

The molecular mechanisms involved in crack initiation and propagation would be expected to be similar to the non-environmental case, the distinction lying in the catastrophic reduction in crack resistance in the presence of an active environment.

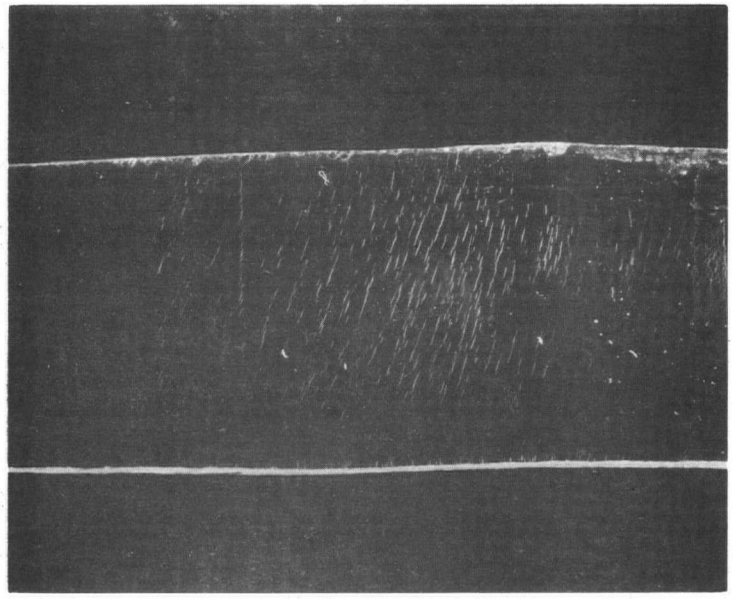

FIGURE 13 CRAZING OF POLYMETHYL METMACRYLATE

Richards[53] in 1946 was the first to note the failure of polyethenes of low molecular weight in soap solutions. A review by Howard[54] (1959) covers the studies to date, which mostly involve polyethylene.

At the present time, theoretical understanding of environmental stress cracking is very sketchy. Hittmair and Ullman[55] report on the effect of crystallinity and molecular weight on stress cracking of polyethylene. The theoretical reasons for the effects are discussed in terms of the Griffith theory of fracture, suggesting the role of the active species to be that of reducing the surface energy so that the stress at which brittle failure occurs is reduced. As discussed elsewhere, this may be partly correct but is obviously an insufficient reason for cracking.

Polymethyl methacrylate exhibits the effect of crazing, i.e. the appearance of fine cracks on the surface in either random or patterned formation, Fig. 13. The effect is similar to stress cracking since it is environment sensitive.

(i) Structural Effects

Average Molecular Weight is known to be one of the major factors in determining stress cracking resistance. Howard[54], Spohn and Frey[56], and Lander[57] have all shown the deleterious effects of low molecular weight fractions on crack resistance of polyethylene.

Long chain networks with high degrees of cross-linking serve to reduce the stress cracking effects.

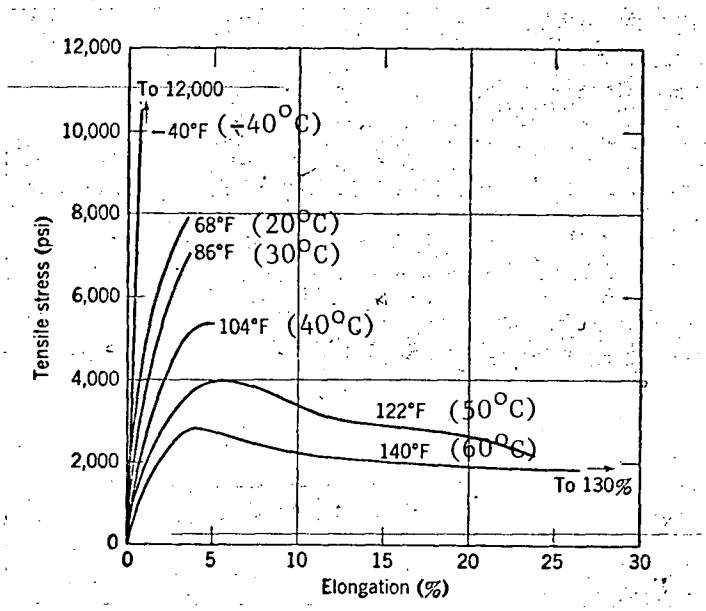

FIGURE 14. EFFECT OF TEMPERATURE ON TENSILE STRESS-STRAIN CURVE OF POLYMETHYL METHACRYLATE (58).

(ii) Temperature Effects

Fig. 14 shows the effect of temperature on the stress-strain curve of polymethyl methacrylate. In a group of specimens broken between 23°C and 80°C, Wolcock et al[58] have shown the nature of the fracture to go through a transition stage between 40°C and 50°C. Below 40°C the fracture surface is flat and perpendicular to the faces of the specimen, indicating essentially brittle failure. Above 40°C there is an indication of shear with the material becoming tougher and the critical crack size greater, so that the mirror area is increased in size. The ductility also increases thereby reducing stress concentration at the tip of the crack by flow.

It is obvious from Fig. 14 that the elongation at failure rises sharply in the region 40°C-50°C. There would appear to be a change in the mechanism of failure in this region, as yet unexplained.

3:2 Brittle Fracture

(i) Introduction

Metals, plastics, concrete, ceramics, glass, wood, rocks etc., are all solids whose utilization is governed by the presence of cracks or flaws within them. Some cracks are initiated by the concentration of stresses around flaws, that are either natural to the material or built into it inadvertently during manufacture or fabrication. Others are

initiated by plastic deformation of the material caused by the stresses themselves. Under stress once a crack is initiated, it grows slowly until the strain energy at the tip reaches a limiting value, at which point the crack becomes unstable and propagates at high velocity of its own accord. The nature of this process differs from material to material but depends upon the manner in which the load is applied, as well as the temperature and chemical environment. The latter two factors are less well understood and it is the object of this work to investigate further the role of chemical environment.

To avoid confusion occurring from the use of fracture terminology, definitions of the terms used in the thesis are given below.

(ii) Definitions

Fracture is defined as the separation or fragmentation of a solid body into two or more parts under the action of a stress. The different types of fracture arise from differences in the modes of crack nucleation and crack propagation; these processes depend on the nature of the applied stress, strain rate, temperature and specimen environment.

Fracture may be either ductile, where the separation occurs after extensive plastic deformation; or brittle, with little, or ideally no plastic deformation accompanying the break.

Various conditions and stages of fracture may be

visualized,

(a) Crack Initiation. A failure process by which one or more cracks are formed in a material free from any cracks. (Poncelet)[59].

(b) Fracture Initiation. A failure process by which one or more existing cracks in the material begin to extend. (Griffith)[3].

(c) Fracture Propagation. A failure process subsequent to fracture initiation in which the cracks are extending in the material. A distinction may be made between two types of fracture propagation:

(i) Stable fracture propagation is the failure process in which crack extension is a function of the applied load and can be controlled accordingly.

(ii) Unstable fracture propagation is the failure process in which crack extension is governed by factors other than loading and thus becomes uncontrollable.

(iii) Fracture Initiation

Brittle failure often occurs at unpredictable levels of stress, by the suden propagation of a crack. It is believed that in crystalline materials some dislocation process sets up stresses that are relieved by atomoc separation instead of atomic slip. A crack forms. The question is then whether the crack can spread catastrophically across the crystal as a cleavage

crack. If it can, brittle fracture ensues.

Amorphous materials, such as glass, are completely brittle, whilst crystalline materials usually exhibit some plastic deformation prior to fracture.

An approximate calculation of the theoretical cohesive strength of a perfect material results in values several orders of magnitude larger than the measured values. The first explanation given for the discrepancy was derived by Griffith[3] from the assumption that all brittle materials contain a host of fine elliptical cracks.

The Griffith Criterion

Microcracks pre-existing on the surface, or in the bulk of a material, act to concentrate applied stresses at the flaw apex[101]. The Griffith criterion for fracture initiation predicts that at a particular level of applied load, a critical energy value will cause the crack to propagate. It should be noted that a fracture initiation criterion is not necessarily a strength failure criterion. As a result of the stress concentration the cohesive strength of the material may be exceeded at this localized area at low applied loads. The critical stress value, as shown by Orowan[60], represents the molecular cohesive strength of the material.

The Energy Approach

The concept of the original Griffith hypothesis is based on the condition that the energy W applied by loading a structure, is balanced by the elastic strain energy W_e stored in the structure and the surface energy W_s in the free faces of the existing cracks.

$$W = W_e + W_s$$

If the load is increased the corresponding increase dW in the applied energy W may be balanced either (i) by an increase dW_e in the strain energy W_e only or, (ii) by an increase dW_s in the crack surface energy W_s or, (iii) partly by an increase dW_e and partly by an increase dW_s.

In case (i) $dW = dW_e$, $dW_s = 0$ and the crack does not extend. In the other two cases dW_e can equal 0 and the crack surface energy can only increase by extending the crack, i.e. if the crack half-length c increases to (c + dc).

Balancing the energies we have

$$dW = dW_e + dW_s$$

$$\frac{dW}{dc} = \frac{dW_e}{dc} + \frac{dW_s}{dc}$$

It can be shown that $\frac{dW}{dc} = 2\frac{dW_e}{dc}$.

hence $\frac{dW_e}{dc} = \frac{dW_s}{dc}$.

For a thin plate Griffith gave[3]

$$W_e = \pi c^2 \sigma_o^2 / E$$

$$W_s = 4\gamma c$$

where σ = Applied uniaxial tensile stress.

E = Modulus of Elasticity.

γ = Surface Energy per unit length of crack surface.

c = Crack half length.

Solving by substitution we have,

$$\sigma = \left[\frac{2E\gamma}{\pi c}\right]^{1/2} = \sigma_{in} \qquad (1)$$

σ_{in} = Stress necessary for fracture initiation

We then have the Griffith criterion for fracture initiation.

For $\sigma < \sigma_{in}$ the crack does not extend ($dW_s = 0$) i.e.(ii)

For $\sigma > \sigma_{in}$ we have fracture propagation.

Then the stress necessary to propagate a crack is inversely proportional to the crack length. The tensile strength of a completely brittle material will thus be determined by the length of the largest crack existing prior to loading.

Griffith's experiments on glass fibres showed that when surface cracks are absent, an increase in strength results to values approaching the theoretical cohesive

strength.

Since the Griffith equation only applies to completely brittle materials, a new treatment must be used for crystalline materials, which appear to fail in a brittle fashion, but which usually have an amount of plastic deformation next to the fracture surface. The theory must therefore take into account not only the energy necessary to create new surface (2γ), but also to produce plastic deformation in the vicinity of the crack (p).

Orowan[60] modified the Griffith equation to,

$$\sigma = \left[\frac{2E(\gamma+p)}{\pi c}\right]^{1/2} \qquad (2)$$

where p is the work of plastic deformation at the tip of the growing crack. Roesler[22] has shown that the energy dissipated in plastic deformation is much larger than the surface energy changes unless the material is very brittle.

Therefore, the function of an embrittling species is not only to reduce γ, but also to decrease p to a value close to zero. In a fracture of this nature the stress concentration at the tip of the microcrack is initially accommodated by plastic deformation. When equation (2) is satisfied, the crack will propagate spontaneously. The speed at which this spontaneous propagation occurs increases rapidly from zero to a limiting value, about one-third of the speed of longitudinal sound waves in the medium. Since yield stress is strongly dependent on strain rate, the velocity of the

crack increases to the extent that plastic deformation cannot accommodate the stress concentration at the head of the crack, and the crack spreads in a brittle manner.

(iv) Fracture Propagation

Subsequent to fracture initiation is fracture propagation, which consists of stable and unstable crack growth.

As long as the condition $\sigma > \sigma_{in}$ is maintained by a definite relationship existing between c and the applied stress σ the propagation is controllable and stable.

Irwin[61] proposed the relationship,

$$\sigma = \sqrt{\frac{GE}{\pi c}} \qquad (3)$$

where G is the energy released per unit crack area.

Thus an amount of energy G is released from the stored elastic strain energy W_e and used to form new surface.

The similarity between the Griffith and Irwin formulae is obvious, but whilst equation (1) is a formula specifying a criterion, equation (3) constitutes a relationship between c and σ.

When the unique relationship (3) between c and σ ceases to exist unstable propagation ensues.

Stable propagation is usually a slow process whilst unstable propagation is rapid[65].

Irwin postulated that when G attains a critical value G_{CR}, the transition from stable to unstable propagation

ensues.

$$G_{CR} = \pi\sigma^2_{CR}\, C_{CR}/E \qquad (4)$$

Velocity of Crack Propagation

Unstable fracture propagation occurs when other quantities, e.g. crack growth velocity, play a contributing role, and the fracture can no longer be controlled by the applied load.

When a bond in the material breaks under the action of a tensile stress, the two freed atoms accelerate away from one another. Since they are part of the same body they cannot travel very far, each movement causing a disturbance to propagate through the body situated on either side of the broken bond. This diturbance may be described by the theories of elasticity.

Perpendicular to the free boundary the disturbance propagates as a longitudinal wave, the front of which carries a displacement of the same orientation as the displacement of the freed particle. Along the free boundary the disturbance propagates as a transverse wave whose front carries a displacement that also has the orientation of the freed particles. The longitudinal waves superimpose a compression on the bonds of the body previously extended by the imposed tensile stress. They act therefore as a stress relieving mechanism liberating the strain energy of the body as a consequence of the creation of new surface. As the reflected transverse waves on each

side of the crack reach the crack tip simultaneously, each carrying displacements in opposite directions, they superimpose on the unbroken bonds at the edge of the crack, (already extended by the tensile stress), thus furthering the break. The irreversibility of the fracture process results from the effects of these emanating transverse waves that prevent the bond from reforming.

By relating the kinetic energy to the velocity of movement of the material on either side of the propagating crack Mott[62] derived the equation

$$V = \sqrt{\frac{2\pi}{k}}\, V_1 \left[1-\left(\frac{\sigma_c}{\sigma}\right)^2\right]^{1/2}$$

where V = Crack propagation velocity

V_1 = Velocity of sound in material

σ_c = Critical stress level

σ = Stress on pre-existing flaw.

Roberts and Wells[63] gave $\sqrt{\frac{2\pi}{k}} = B = .38$ and expressed $V = .38\sqrt{\frac{E}{\rho}}\,(1-c_o/c)$.

Thus the terminal velocity will be

$$V_T = .38\sqrt{\frac{E}{\rho}}$$

The terminal velocity is thus a characteristic property of the material, being a fraction of the velocity of the longitudinal wave in a rod of this material.

The value of .38 for B compares well with Schardin and Struth's[64] value of .4 for vitreous silica. A similar

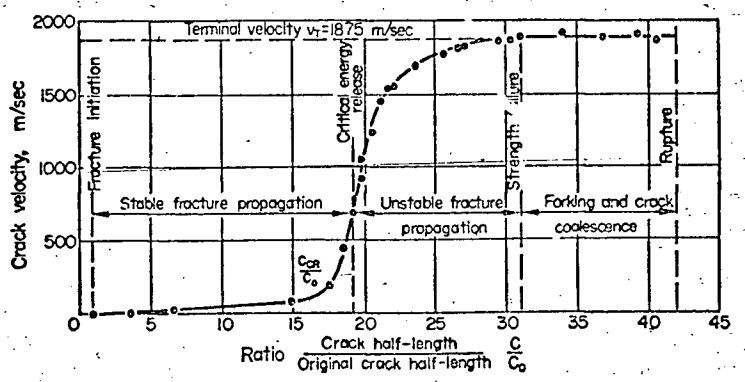

FIGURE 15a. CRACK VELOCITY RELATED TO CRACK-LENGTH RATIO (65).

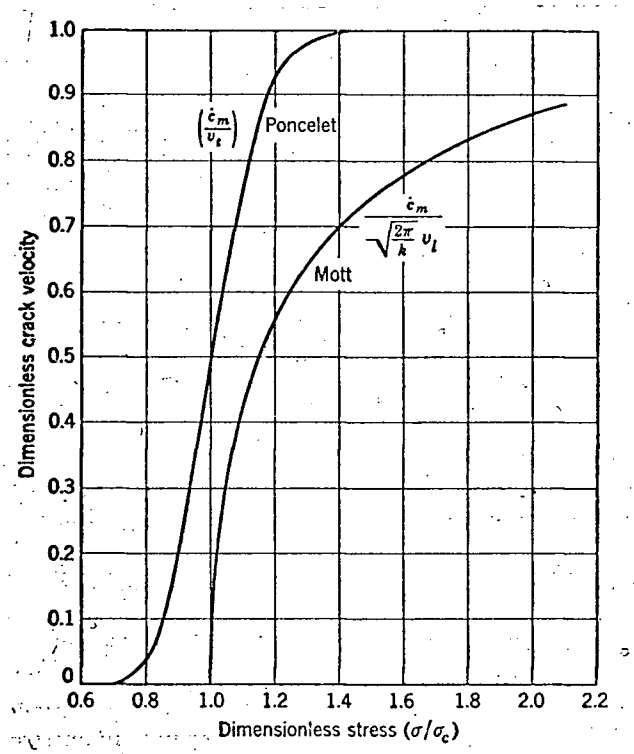

FIGURE 15b. MAXIMUM CRACK VELOCITY VERSUS STRESS (62).

result was obtained by Bieniawski[65] for rocks.

Fig. 15a[65] shows that fracture propagation starts with low velocity which later increases rapidly to a constant value. The turning point in the curve marks the transition from stable to unstable propagation, i.e. when $c/c_o = c_{CR}/c_o$ and $G = G_{CR}$.

Therefore, whilst the influence of crack velocity is small during stable propagation it will be a governing factor in the unstable fracture propagation process.

Once the crack approaches its terminal velocity the kinetic energy of crack extension must also approach a limiting value. Since the released energy increases with crack length the crack tends to increase its surface area in order to dissipate the additional energy. Branching or forking occurs.

(v) Alternatives to the Griffith Theory

Various other theories[66][67] have arisen to explain brittle failures, many of which involve slight variations of the basic Griffith hypothesis. The theory of Poncelet[68], however, does not utilize the concept of pre-existing cracks and warrants more detailed attention. This statistical mechanics approach states that nonequilibrium processes are determined by the difference between the forward and backward reaction rates, in this case the difference between the rate at which bonds are broken and the rate at which these bonds are reformed. With no stress these rates

would be equal, but with stress the rates are biased; a process which is stress and temperature sensitive.

(vi) The Poncelet Flaw Genesis Theory

An ideal brittle solid may be regarded as being composed of a collection of identical particles held together at definite spacings by bonds of an electrostatic nature. These bonds may be pictured in the usual way on a Morse diagram. Fig. 16. Electrostatic repulsions exist between the nuclei of both particles and also between the electrons of both particles, whilst electrostatic attractions occur between the electrons of one particle and the nucleus of the other. The equilibrium distance between the particles is stable, since the Morse resultant of the bond urges the particles back toward their equilibrium spacing, no matter where their actual spacing may momentarily be.

Under the influence of these restoring bonds the particles vibrate. The energy involved in these oscillations is represented by the area subtended by arc AB or arc AC and is usually referred to as the thermal energy level of the particles. According to statistical mechanics the probability that a given bond has a thermal vibrational energy in excess of an arbitrary value $E_{(r)}$ is given by

$$P = e^{-E(r)/KT}$$

where T is the temperature in degrees Kelvin and K is Boltzmann's constant (1.372×10^{-16} ergs/degree).

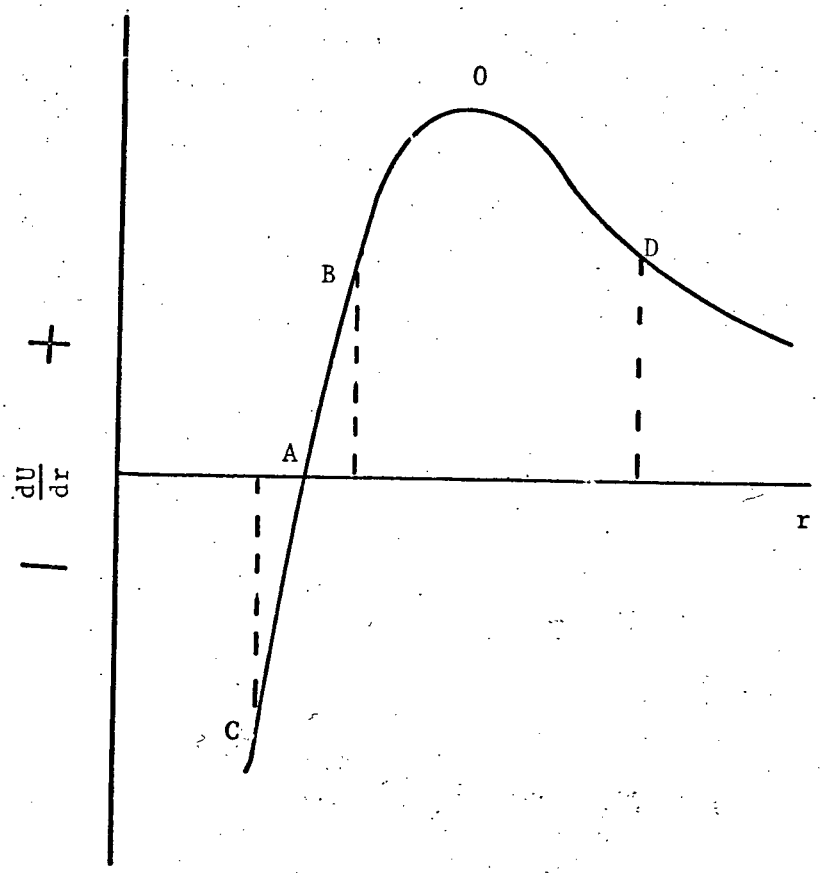

FIGURE 16 THE MORSE CURVE FORCE (U) = f(r)

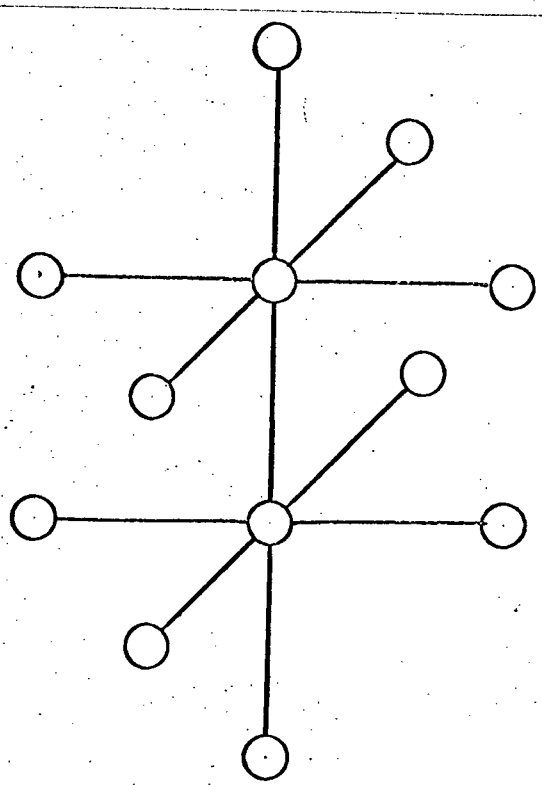

FIGURE 17 PRINCIPAL BOND DIAGRAM

While the energy levels of the various particles are changing continuously and independently as the particles interfere with one another, the distribution of the various levels follows a well determined pattern referred to as the Maxwell-Boltzmann Law.

The computations of the energy level of a particle is a very complicated matter, but may be simplified by calculating the energy levels of the bonds rather than those of the particles, a bond joining two particles. The energy of a particle is thus half the sum of the energy levels of the bonds joining it to other particles.

The vibrational energy levels of the various bonds of a particle do not depend solely on the vibration and energy levels of the particle being considered, but also on the vibrations and energy levels of the other particles to which the one in question is bound.

It follows that the vibration and energy levels of any one bond varies independently of any other bond, and the bonds may thus be considered one at a time.

The principal bonds of a particle may be regarded as the 6 mutually perpendicular bonds lying along the co-ordinate axis. The principal stresses may be regarded as the vector-pairs of forces acting along the principal bonds (Fig. 17).

Since solids fail, the principal bonds must become unstable when subjected to specific stress tensors. Due to the increasingly steep nature of the negative Morse resultant the

continued contraction of bonds is precluded. Unstable bonds must therefore keep on expanding.

There may be nothing to prevent the bond from reaching a third equilibrium spacing whilst expanding, which equilibrium would again be a stable equilibrium. On reaching such an equilibrium the bond starts to oscillate about it and then becomes a "long" bond. It consequently ceases to be a principal bond, some other bond becoming the principal bond. Such bonds are termed "swapped" bonds.

The failure of solids resulting in broken bonds we call fracture, and the failure giving swapped bonds, flow. Since brittle solids do show other phenomena than fracture when submitted to stress-tensors, we accept the possibility of flow, although not necessarily of a viscous or plastic nature.

In the case of simple tension the stress acting along one axis is positive, with both the other axial stresses being zero. As the vibrating bond reaches spacings greater than the primary equilibrium spacing, its Morse resultant, urging a contraction, at first increases from its value at B until a maximum spacing at point 0 is reached.

For greater bond expansions the Morse resultant decreases asymptotically to zero. As the spacing of the primary bond increases under the influence of its thermal energy there is only one position greater than the primary equilibrium for which the resultants and the stress are again in equilibrium,

as shown by D on the Morse curve. This is an unstable equilibrium and when the bond exceeds this length it becomes a broken bond.

The unstable equilibrium is reached when the thermal energy level is sufficient, as given by the area under the Morse curve. This required energy level varies with the tensile stress applied, and can therefore be expressed as a function of stress.

The Maxwell-Boltzmann Law gives the time during which a bond possesses sufficient energy to overcome the energy barrier in proportion to the total duration of the tensile load.

It is found that the duration varies steeply with the stress. Theoretically the smallest tensile stress is sufficient to break a bond but the required duration might be millions of years.

At the surface where we have an absent bond the required energy would be appreciably less than if all the principal bonds were present. Thus the first bonds to break will normally be surface bonds.

At the tip of an existing crack where the bond is perpendicular to the crack plane, the principal bond in the crack plane cannot remain perpendicular to the vibrating bond subject to the tensile stress, since the link has been severed by the crack. As a result this bond becomes oblique and contributes to the applied stress. Thus bonds perpen-

dicular to a crack tip will break even more readily than surface bonds.

Physical Nature of Strength in Brittle Solids

In brittle solids where the elastic flow in failure is very slight, the limiting stress which may be applied to the solid refers to the fracture stress.

The fact that identical brittle solids in identical tests will not give identical strengths follows from the variation in the energy levels of the various particles. An average strength may however be computed on a statistical basis. Since the first bond to break sets the fracture phenomenon in motion the duration of a specific stress required to fracture identical solids may vary greatly.

The condition of the outer surface obviously affects the strength considerably, as will the surrounding atmosphere. It is well established that the strength of solids is greater in vacuo or an atmosphere with no affinity for the solid. This aspect will be discussed in further detail later.

(vii) A Comparison.

Poncelet objected to the Griffith existing flaw hypothesis on the grounds that the initiation of a crack is an atomistic approach and not treatable by the macroscopic equations of thermodynamics.

Orowan approached the problem from an atomistic point of view and demonstrated that when the stress reaches a value predicted by the Griffith formula the material will break.

In the Poncelet approach, although the crack geometry assumption is removed, others are added in the form of activation energy and the manner in which intrinsic energy is biased by the macroscopic load.

The interesting feature of the flaw genesis theory is that it leads to virtually the same conclusion as the pre-existing flaw theory. Any disagreement is a reflection in the differences in the point of view between statistical mechanics and classical thermodynamics.

(a) Existence of Microcracks

Gordon, Marsh and Parratt[69] have presented experimental evidence that stress creates flaws. They also showed, using a sodium vapour decoration technique, that long (50μ), narrow (200A°) and shallow (1000A°), cracks do exist in glass prior to the application of the stress. A further conclusion supporting the existing flaw hypothesis shows that low crack density results in the glass breaking at high stresses. Elliott[70] showed that flaws no more than several atomic diameters would account for loss in strength. The results of Shand[71], leave no doubt that the presence of minor surface flaws has a drastic effect on the strength of glass. No direct evidence for the existence of

surface flaws has resulted from electron microscopic examination, but the decoration techniques of Andrade and Tsien[72] showed orientated cracks on the inside of glass tubes when abrasion was absent.

Thus it would appear that in glass specimens cracks do exist and operate to reduce the strength.

Bieniaskwi[73] shows the existence of microcracks in rocks, the cracks lying on grain boundaries between the constituent minerals, and concludes that their presence results in the modulus of elasticity of the material being lower than that of a solid continuum.

(b) Crack Propagation Velocity

In comparing the equation of Mott[62] (based on the initial flaw concept of Griffith) with the Poncelet equation using the flaw genesis hypothesis, the differences are found to be very small, Fig. 15b.

Poncelet assumes that there is no flaw until it is created by a stress, at about $.7\sigma_c$ whereupon it spreads catastrophically to a limiting value of .5 of the transverse wave velocity.

Thus the limiting values of .38V and .5Vt in the case of Mott and Poncelet respectively, are reasonably close (in view of the theoretical assumptions made).

(c) Static Fatigue

Static Fatigue is that phenomenon particular to inorganic glass where the average breaking strength at constant load as opposed to alternating load in cyclic fatigue, depends upon the time. From the pre-existing flaw point of view, the phenomenon can be related to slow fracture growth, i.e. the size of c_o depends on time. The magnitude of c_o depends on the stress and atmosphere, such that a lower stress will cause fracture after a longer time interval. Thus the stress-time equation results from the gradual penetration into the cracks of substances that will be adsorbed on the crack walls. At a stress level of about 1/3 the breaking stress at rapid loading the glass appears to withstand fracture indefinitely. Orowan[60] showed that the factor 1/3 was equal to the square root of the ratio of γ in moist atmosphere to γ in vacuum. Thus it seemed that the change in γ was responsible for static fatigue. Experiments of Gurney and Pearson[74] confirmed Orowan's[75] prediction that static fatigue will not occur in vacuum. They were able to show that the fatigue effect could not be ascribed entirely to gaseous attack on the crack, and is possibly due to the atmospheric constituents in the surface layers.

Elliott[66] proposed that the crack depth may be deepened by the diffusion of corrosion products at the crack tips.

Thus the loss of strength with time may be due to the growth of the crack size or the decrease in the surface

energy, or both. In any event, the Griffith hypothesis of pre-existing flaws seems to explain adequately the phenomenon of static fatigue.

CHAPTER FOUR

ADSORPTION

4:1 Introduction

The study of environmental effects on fracture involves the contact of solid surfaces with a gas or liquid phase, resulting in adsorption at the interface. The adsorption characteristics constitute important parameters in deducing the mechanism by which the fracture takes place.

Adsorption in the solid/vapour system may be defined as the concentration of vapour at the solid surface resulting from the residual attractive forces in the solid surface. The phenomenon is customarily divided into two broad categories of physical adsorption and chemisorption. Physical adsorption, barring hysteresis in porous solids, is reversible and involves essentially non-specific forces. Chemical adsorption involves electron transfer in the formation of a chemical bond and is often referred to as localised or fixed site adsorption.

The thermodynamic terminology of surfaces is normally applied to liquid interfaces. When dealing with solids misuse of terms has led to a great deal of confusion in the literature[77][92]. The terminology to be used in this

thesis is defined as follows.

4:2 Definitions

(i) Surface free energy. The work necessary to form unit area of surface by a process of division, in vacuo. The specific surface free energy is the free energy per $1 cms^2$ (F).

(ii) Surface Tension. (γ) The work necessary to form unit area of surface in a multi-component system.

(iii) Surface Stress. (f) Lateral forces operating in the solid surface, which must be balanced by external forces, or by volume stresses in the body.

Therefore, in a one component system (vacuo), the specific surface free energy and surface tension are identical. In an environment we have,

$$F = \gamma + \mu_s \Gamma_s$$

where μ_s is the chemical potential and Γ_s is the concentration excess of the adsorbed species, i.e. γ decreases due to the adsorption term $\mu_s \Gamma_s$.

4:3 The Surface Tension, Surface Free Energy Concept

Contrary to the situation with liquids the surface tension (γ) and surface free energy (F) values for solids are not necessarily equal. Gibbs[76] gave the relationship between the quantities,

$$\gamma = F + A\, dF/dA$$

where A is the surface area.

The difference may be seen by imagining the process for creating fresh surface to be comprised of two steps. Firstly the solid or liquid is cleaved, keeping the atoms in fixed positions as they appeared in the bulk and secondly the atoms are allowed to rearrange themselves to their final equilibrium positions. For liquids, due to the high mobility of the atoms, equilibrium is established immediately and the two steps occur as one. In the case of solids, the second step may occur only slowly and in this instance the surface free energy and surface tension will not be equal. Therefore for liquids dF/dA is zero, and $\gamma = F$, whilst for solids Shuttleworth has shown[77] that F and dF/dA are of the same order of magnitude. Nicolson[78] has calculated the quantities for NaCl and showed its surface tension to be about three times as large as its surface free energy.

Typical studies of solid surfaces are frustrated by the lack of a suitable absolute technique for measuring solid surface tensions. Zero creep experiments conducted near the melting point would yield very different results from the non-equilibrium conditions with incomplete relief of surface stresses.

4:4 The Surface Stress, Surface Tension Concept

The surface stresses (f_i) are forces acting within the surface of a material and are not to be confused with

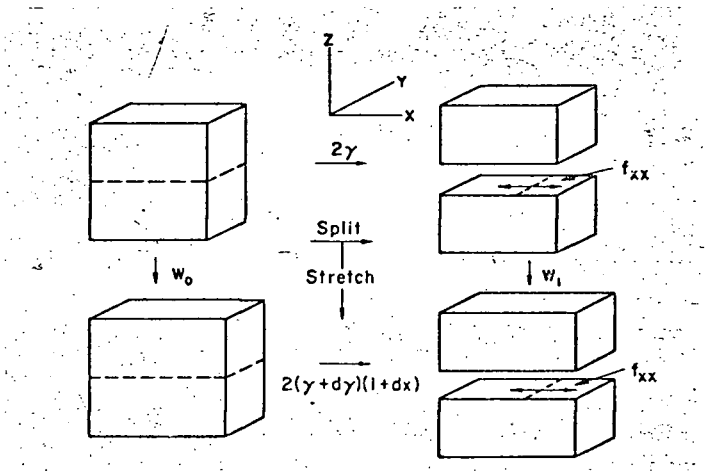

FIGURE 18a. CYCLE RELATING SURFACE TENSION AND SURFACE STRESS (77).

surface tension (γ).

"Consider a unit cube with edges parallel to the x, y, z axes of the Cartesian co-ordinate system (77) Fig. 18a. The cube is reversibly stretched along the x axis by an amount dx under the constraint that the y edge (but not the z edge) maintains constant length, with the corresponding work done being Wo. With the cube in its original position let it be separated into two halves along the x-y plane, and let these halves be stretched by an amount (dx) under the same constraint as before. In general the work required, W_1, will differ from Wo. This difference is attributed to a force component fxx within the newly formed surface acting in the x direction across a unit length normal to the x axis. We have,

$$f_{xx} = \frac{W_1 - W_o}{2\,dx} = \frac{W_1 - W_o}{2\varepsilon_{xx}}$$

where ε_{xx} is the linear strain.

Similarly the work required to perform a pure shear ε_{xy}=dy on the same faces of the original cube W_o' in the y direction of the xy plane and the work W' required to effect the same shear on the separated halves results in a stress component,

$$f_{xy} = \frac{W' - W_o'}{2\varepsilon_{xy}}$$

Since the f's may be regarded as the components of a tensor it may be concluded that surface stress and surface tension are not in general even the same type of physical quantity; the former is a tensor whilst the latter is a scalar. Shuttleworth(77) expressed the relationship between f and γ by equating the work required to go from the original unstrained cube to the final state of two separated halves stretched along the x-direction by two different paths.

I The cube is first stretched and then separated

$$W_I = W_o + 2(1+\varepsilon_{xx})(\gamma+\Delta\gamma)$$

$$W_o+2\gamma+2\Delta\gamma+2\gamma\varepsilon_{xx}$$

II The cube is first separated and then stretched

$$W_{II} = 2\gamma+W_1$$

Equating W_I and W_{II} we get

$$f_{xx} = \gamma + \frac{d\gamma}{d\varepsilon_{xx}}$$

Considering the shear ε_{xy} and since the area of the xy plane remains unchanged the equation for shear is

$$f_{xy} = \frac{d\gamma}{d\varepsilon_{xy}}$$

The general relationship,

$$f_{ij} = \delta\gamma_{ij} + \frac{\delta\gamma}{\delta\varepsilon_{ij}}$$

where $\delta_{ij} = 1$ if $i = J$ and zero otherwise, and where all strains except ε_{ij} are held constant in the partial differentiation.

For the liquid case $d\gamma/d\varepsilon_{ij}$ will be zero since new atoms are readily supplied to the surface and a change in area will not result in a change in surface tension. For solids having long range order the state of the surface will be altered by an extension and $\frac{d\gamma}{d\varepsilon} \neq 0$ and the surface stress

will be different from the surface tension.

Thus the surface tension does not necessarily lead to surface stress. Since f_{ij} and $d\gamma/d\varepsilon_{ij}$ may have either sign, compressive as well as tensile stresses are possible in the surface. In glass, both solid-like behaviour ($d\gamma/d\varepsilon \neq 0$) and liquid-like behaviour ($d\gamma/d\varepsilon = 0$) may be achieved by varying the temperature and the rate of strain.

4:5 The Effect of Adsorption

In the creation of fresh solid surface the cohesive forces are disrupted, resulting in the surface itself constituting a reactive or excited state. Vapour molecules reacting with the surface can again lower the surface tension. Obviously, the stronger the reaction the greater the decrease in surface tension, since adsorption is a spontaneous exothermic event. Thus chemisorption would be more likely to influence the physical properties involving the solid surface, (e.g. fracture).

Fig. 30a shows the relative change in surface enthalpy for the events discussed. In general therefore, physical adsorption will not greatly affect the surface configuration and influence surface sensitive properties.

Once the surface is covered with an adsorbed monolayer the stronger interactions must cease, unless new surface is created. The decrease in the surface tension will, however, continue until a steady state is reached at which

the chemical potential of the adsorbate is that of the condensed liquid.

The Gibbs adsorption isotherm[76] relates the decrease in the surface tension to the concentration excess of the adsorbed species, Γ, over the bulk, in equilibrium at any pressure p, by,

$$-d\gamma = RT\Gamma d\ln p$$

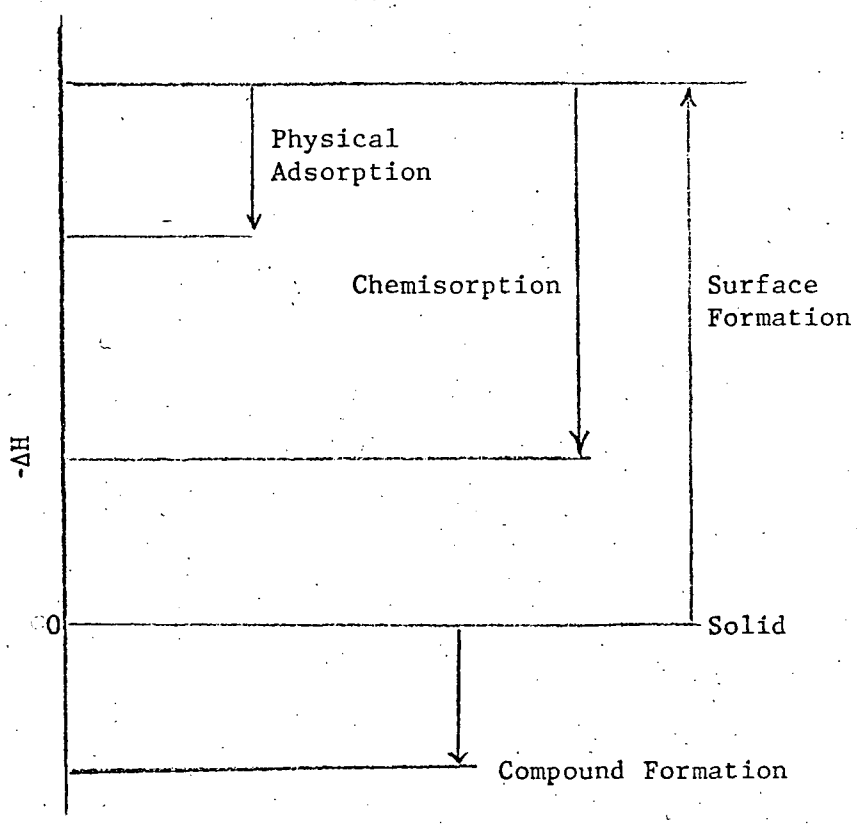

FIGURE 30a. ENTHALPY CHANGES IN SURFACE FORMATION, ADSORPTION AND COMPOUND FORMATION.

The change in surface tension on adsorption is indicated in Fig. 30b where p' is the half-coverage value and γ_o is the surface tension of the clean solid surface. For a continuous curve of this nature it is assumed that the heats of adsorption are the same for all surface sites.

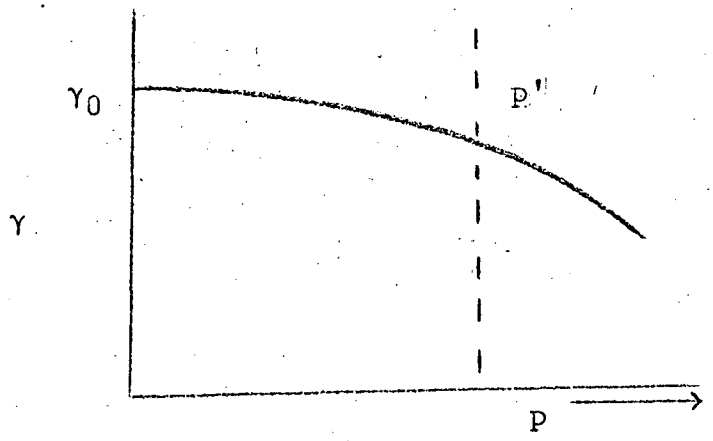

FIGURE 30b. SURFACE TENSION CHANGES ON ADSORPTION.

The change in surface tension accompanying adsorption may or may not bring about a change in surface stress. The change in the surface stress will occur when the absolute value of $\frac{\Delta\gamma}{\Delta\varepsilon}$ is different from γ in the equation

$$f = \gamma + \frac{\Delta\gamma}{\Delta\varepsilon}$$

Variations in surface stress will be manifested in bulk volume changes, especially in isotropic materials. Bangham and Razouk[79] found the fractional change in length, of a charcoal rod, to be proportional to the reduction in the surface free energy with adsorption

$$dl/l = \pi_e \lambda$$

where π_e = surface pressure and λ is a constant depending on the elastic properties of the solid. It should be mentioned that their calculations involved the Gibbs adsorption equation and hence the conclusion should involve the surface tension reduction and not surface free energy.

Maggs[80] concluded that if length changes be confined to directions parallel to the axis of the rod then λ is simply related to Young's modulus (Y). This would be reasonable if Young's modulus did not change with adsorption. As γ varies, the surface stress may vary, and since Young's modulus is a relationship involving stress and strain one might expect Y to vary. M. Sato[81] has shown varying moduli with adsorption.

Yates[82] confirmed Bangham's equation, but by regarding the glass as an isotropic solid, found the bulk modulus to be a more realistic value, since Young's modulus only takes into account a linear increase in length.

CHAPTER FIVE

RESULTS AND DISCUSSION

5:1 Interpretation of Results

The theory of the strength of solids in relation to structure has always been unsatisfactory. Large differences result between computed values of the mechanical strength from atomic and structural data, and experimental observations.

Glass, which does not have a simple ionic crystal structure, yields still greater discrepancies in experimental results. Although the ideal material for studies of brittle fracture, glass would not appear to be suitable for studies in mechanical strength.

G.O. Jones[119] in an excellent review on the interpretation of data on the strength of glass, has demonstrated the difficulties of analysis of results on strength measurements under prolonged loading conditions, i.e. loading of the specimen to some fraction of the ultimate breaking load and measuring the time to failure. The variation in times will be large due to inherent variations in the strength properties. (Times vary from a fraction of a second to thousands of hours for the same test). Fatigue types of experiments should be

avoided in the case of glass.

Glass differs in strength properties from most materials, particularly polycrystalline metals, since,

(1) Surface condition is of major importance.

(2) The strength is reduced 3 to 4 times under conditions of prolonged loading.

(3) The strength is not strongly temperature dependent in the solid state.

(4) Heat treatment resulting in surface compression increases the strength.

(5) Strength depends on specimen size. The larger the size the smaller the strength.

(6) Their fibres show strengths of 50 to 100 times those of "massive" glass.

Due to the wide variation in the effectiveness of flaws - not always surface - strength values for glass exhibit considerable scatter. Experiments must be performed on a statistical basis.

Table 2 gives the results of the statistical evaluation of tensile fracture data. All subsequent values quoted in the text will be the numerical mean of three determinations with the standard deviation occurring in Table 2 being applied.

Since the strength of glass is strain rate dependent, the effect of strain rate variation was determined. Table 3 lists the effect of strain rate on the statistical scatter. At high and low loading rates the scatter is largest, due

TABLE 2

Statistical Analysis

Strain Rate .03"/min.

Solid	Environment	No. of Measurements	Mean Strain μ"/"	Std. Dev.	Coeff. of Variance %
Vycor Glass	Vacuum 8×10^{-7}mm Hg	15	268	48	18
	Air	15	193	51	24
	H_2O	15	161	27	15
	CCl_4	15	216	37	17
Kimble Glass	Vacuum 8×10^{-7}mm Hg	15	294	44	15
	Air	15	165	28	17
	H_2O	15	138	15	11
Plexi-glass	Vacuum 10^{-3} mm Hg	10	128	9	7
	Air	10	132	12	9

TABLE 3

The Effect of Strain Rate on

the Tensile Fracture Strength of Kimble Glass

(In Air)

Strain Rate "/Min.	No. of Measurements	Mean Strain μ"/"	Std. Dev.	Coeff. of Variance %
0.15	15	176	42	24
0.03	15	165	28	17
0.006	15	142	47	33

to the critical dependence on flaw geometry. An intermediate rate of 0.03"/min was selected for all further measurements, unless otherwise stated.

5:2 Vycor Glass

The porous glass, vacuum treated and not heated above 200°C, will have a surface almost completely covered with hydroxyl groups. The hydrogen in these hydroxyls are partly protonized and are electron acceptor centres[85]. This results in an increased adsorption of substances having electron donor properties, such as water, alcohols, amines, and aromatic hydrocarbons. Removal of the silanol surface sharply decreases the adsorption of the above mentioned substances[86].

Infra and spectral studies on porous glass[87][88] indicate that a large percentage of the surface OH groups interact with others resulting in two types of surface hydroxyl groups, the free groups and the hydrogen bonded groups. Fig. 18b shows a suggested model for the surface[89].

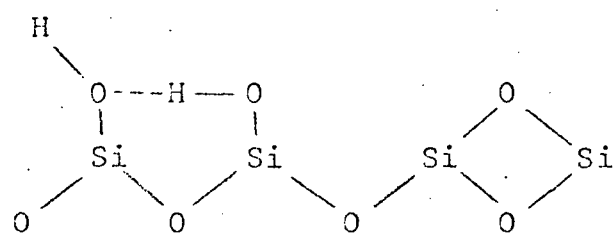

FIGURE 18.b. MODEL OF SILANOL SURFACE

If we represent a hydrogen bonded system as X-H...Y where H...Y is the hydrogen bond and X-H the normal bond, then the strength of the hydrogen bonding will be given by a shift to lower frequencies of the X-H bond stretching frequency.

Table 4 gives the results of various workers in order of increasing hydrogen bond strength for the systems studies. A value for n-butylamine is not available but might be expected to be of the same order as the ammonia group. The importance of these results will lie in the effective screening power of the adsorbed species. The stronger the interaction with the surface, the greater the screening power. However the bond strength refers to individual bonds formed and does not take into account the adsorbate size or orientation on the surface. Hence a more effective screener might be a group of lesser hydrogen bond strength but capable of adsorbing on more active sites due to the proper steric factors, e.g. water will be a better screener than acetone.

The nature of the adsorption process is best studied through the adsorption isotherm. This plot of volume adsorbed at equilibrium pressure p and constant temperature, may be comprised of three phenomena; the increasing adsorption to the monolayer, a multilayer build up, and a condensation effect in capillaries or pores.

Brunauer et al[94] classified the isotherms in five main types. Typical isotherms on porous glass exhibit the

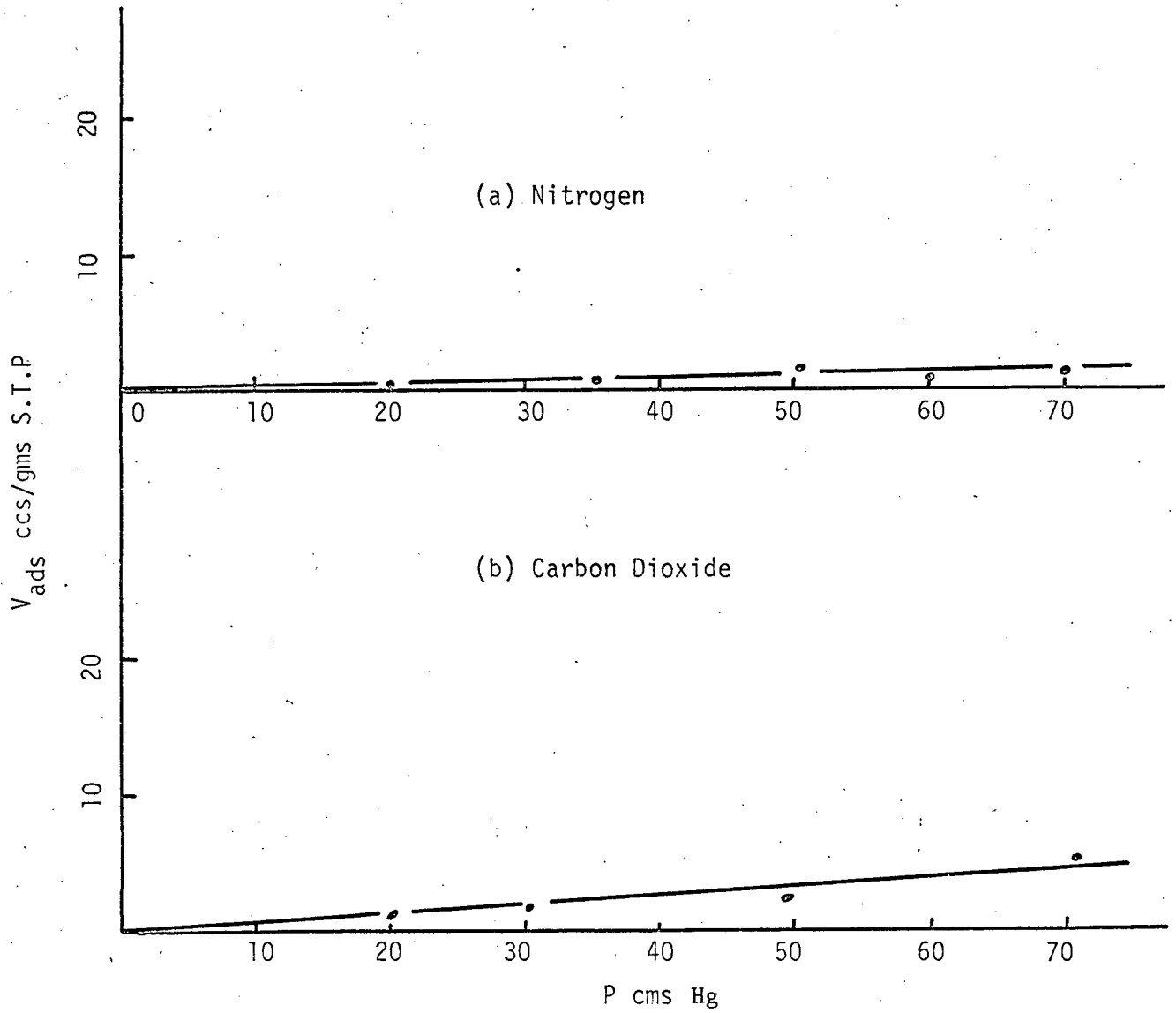

FIGURE 19 ADSORPTION ISOTHERMS ON VYCOR GLASS (25°C)

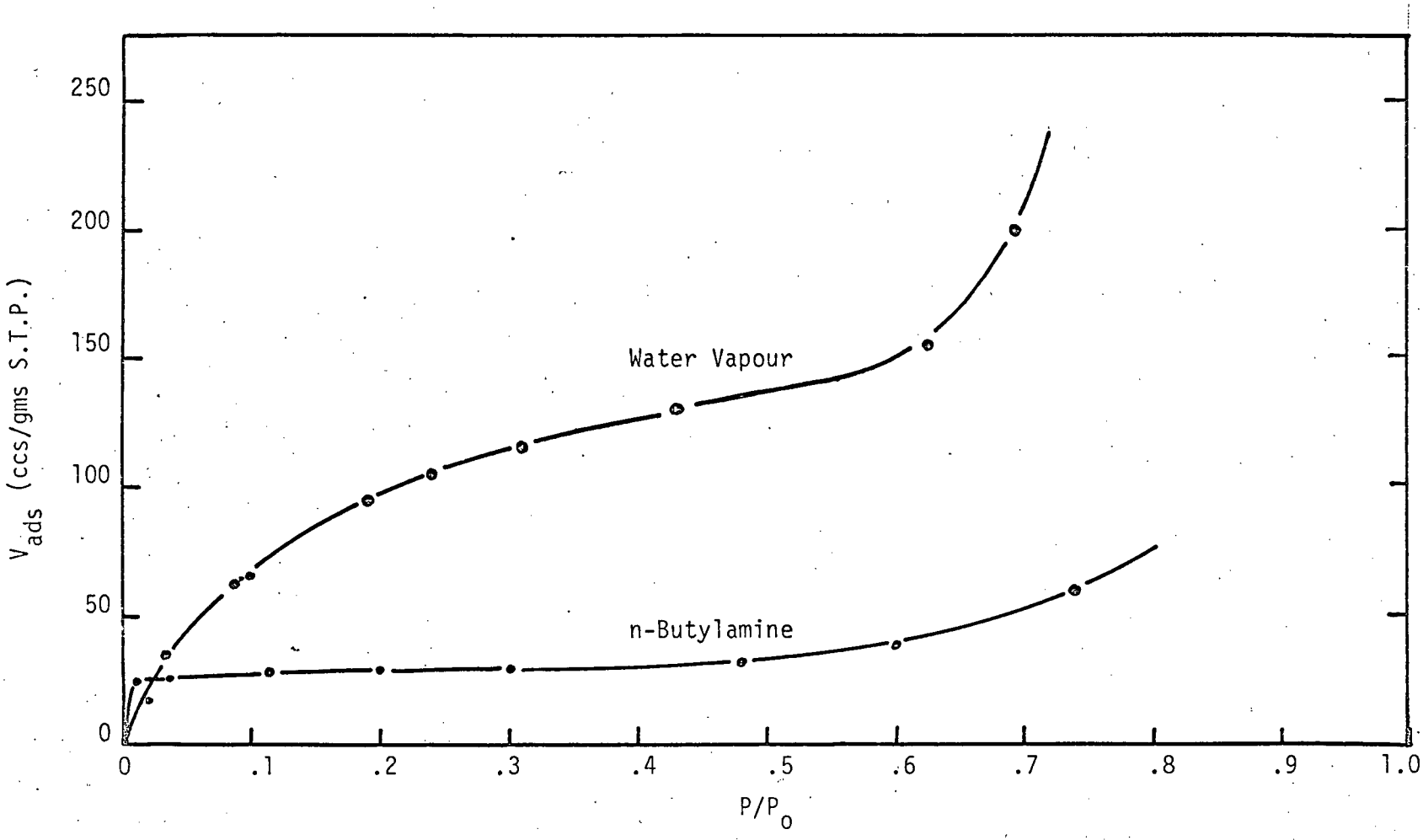

FIGURE 20 ADSORPTION ISOTHERMS ON VYCOR GLASS (25°C)

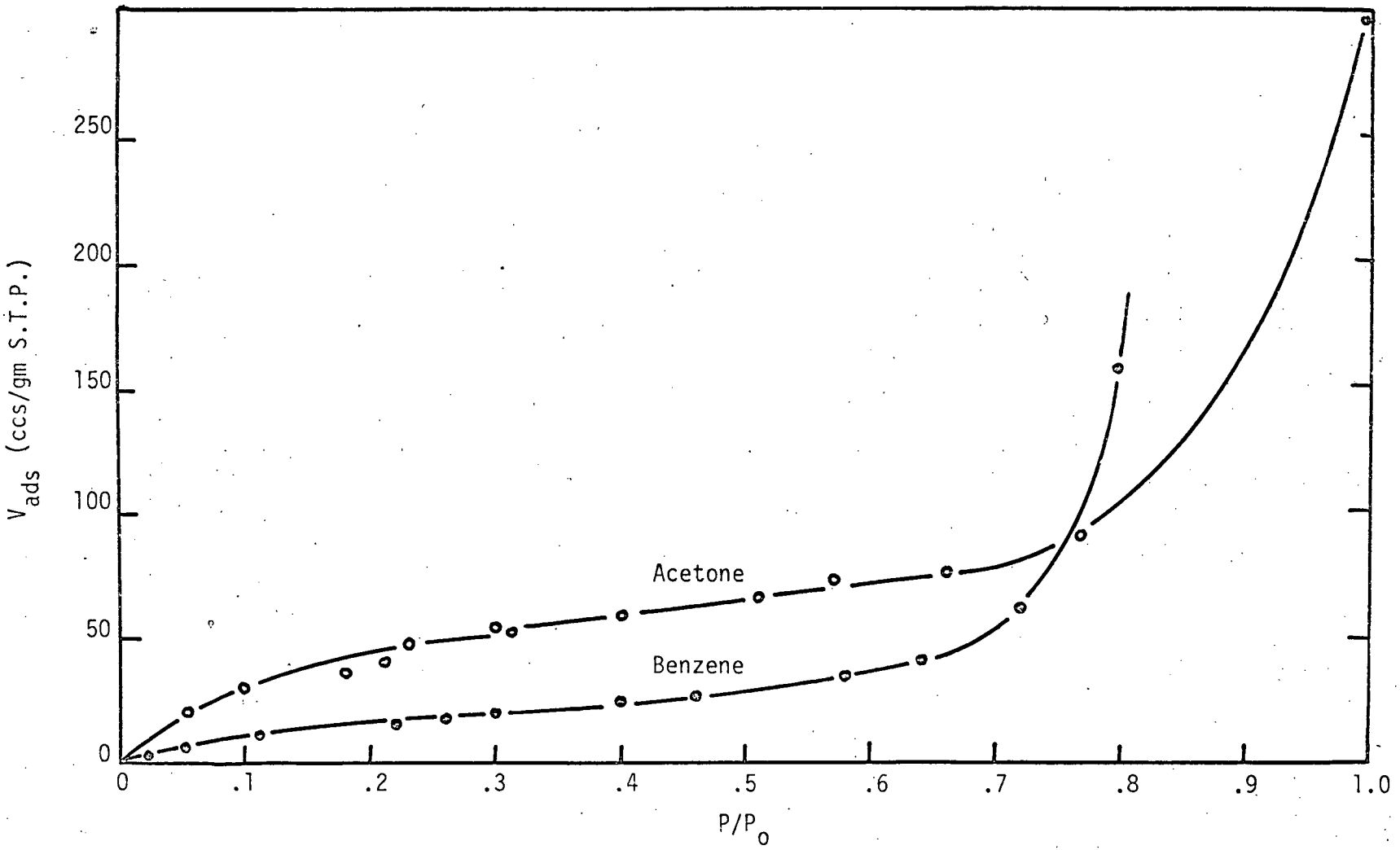

FIGURE 21 ADSORPTION ISOTHERMS ON VYCOR GLASS (25°C)

TABLE 4

Shifts in Frequency of Surface OH Groups on the Adsorption of Gases at Room Temperatures on Porous Glass

Adsorbate	Shift cms^{-1}	Reference
N_2	24 (-170°C)	90
Benzene	110	91
Water	290	93
Acetone	330	89
Ammonia	820	89

sigmoid or S-shaped, type II isotherms, with the exception of benzene, which appears to be more of a type V, due to the small monomolecular forces of adsorption (Figs. 19, 20, 21).

All isotherms were measured at thermostated ambient temperature. In the case of the gases N_2 and CO_2, pressures were increased up to one atmosphere. Since the saturated vapour pressure of these gases at 25°C is greater than 50 atmospheres, very little adsorption could be detected.

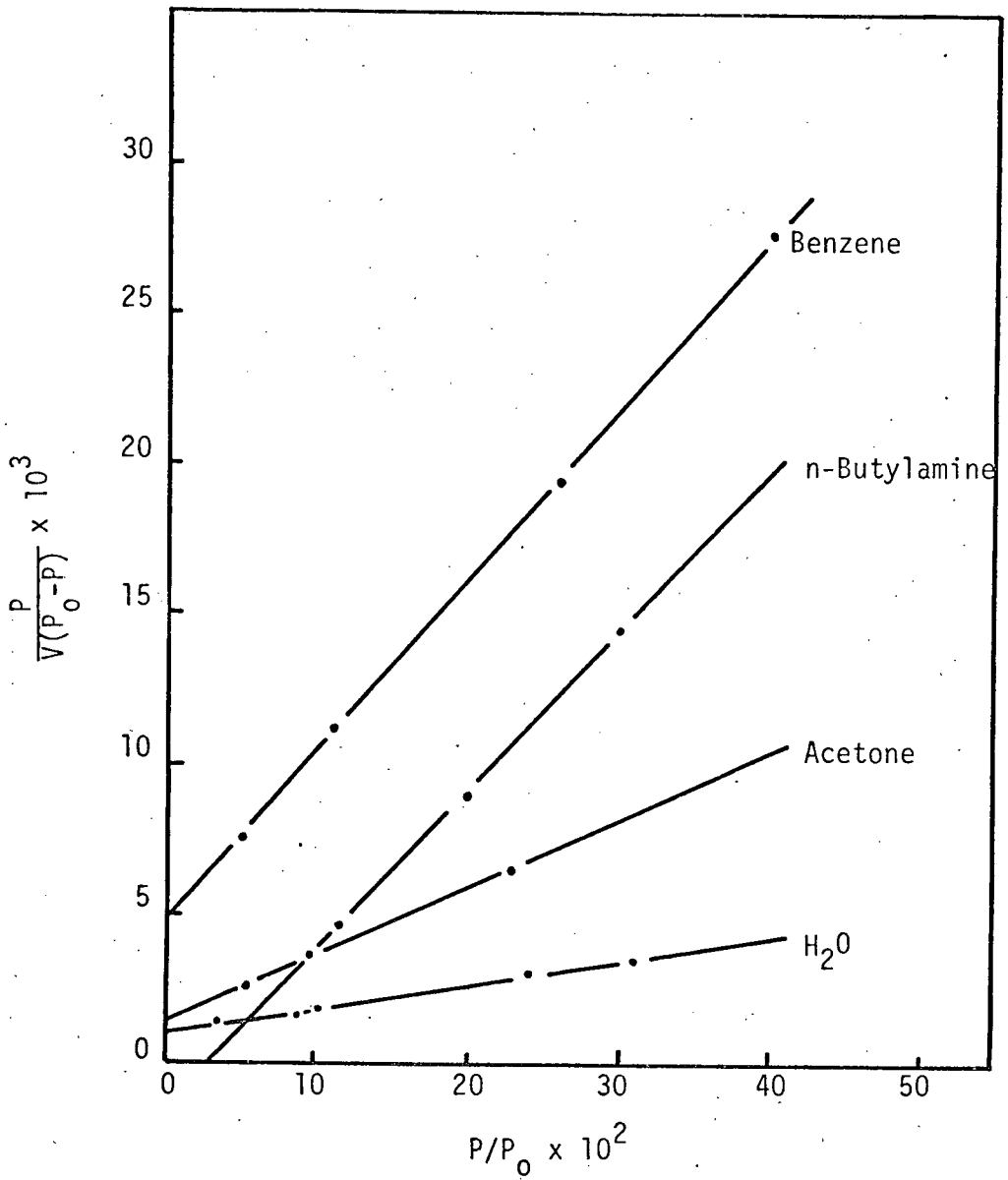

FIGURE 22 B.E.T. LINEAR PLOTS

TABLE 5

Equilibrium Adsorption Rates on Vycor Glass

Adsorbate	Time to Equilibrium
N_2	Immediate
CO_2	Immediate
H_2O	20 minutes
Benzene	Immediate
Acetone	10 minutes
Ethanol	10 minutes
n-Butylamine	180 minutes

Equilibrium was achieved when three consecutive pressure readings over a period of 15 minutes were identical, having allowed a 15 minute period for thermal equilibrium to be achieved. Table 5 lists the varying equilibrium times. Physical adsorption is normally rapid whilst chemisorption may be rapid or slow. The rate behaviour is indicative of the presence of an activation energy.

Table 6 gives the various parameters of interest calculated from these isotherms. Details of the calculations are given in Appendix D.

The decrease in surface tension on adsorption may

TABLE 6

Relative Vapour Pressures

at Monolayer Volumes (Vm)

Vapour	Monolayer Vol	P/P_o
	Vm ccs S.T.P.	
H_2O	90.9	.180
n-Butylamine	22.5	.005
Acetone	36.4	.130
Benzene	17.0	.225

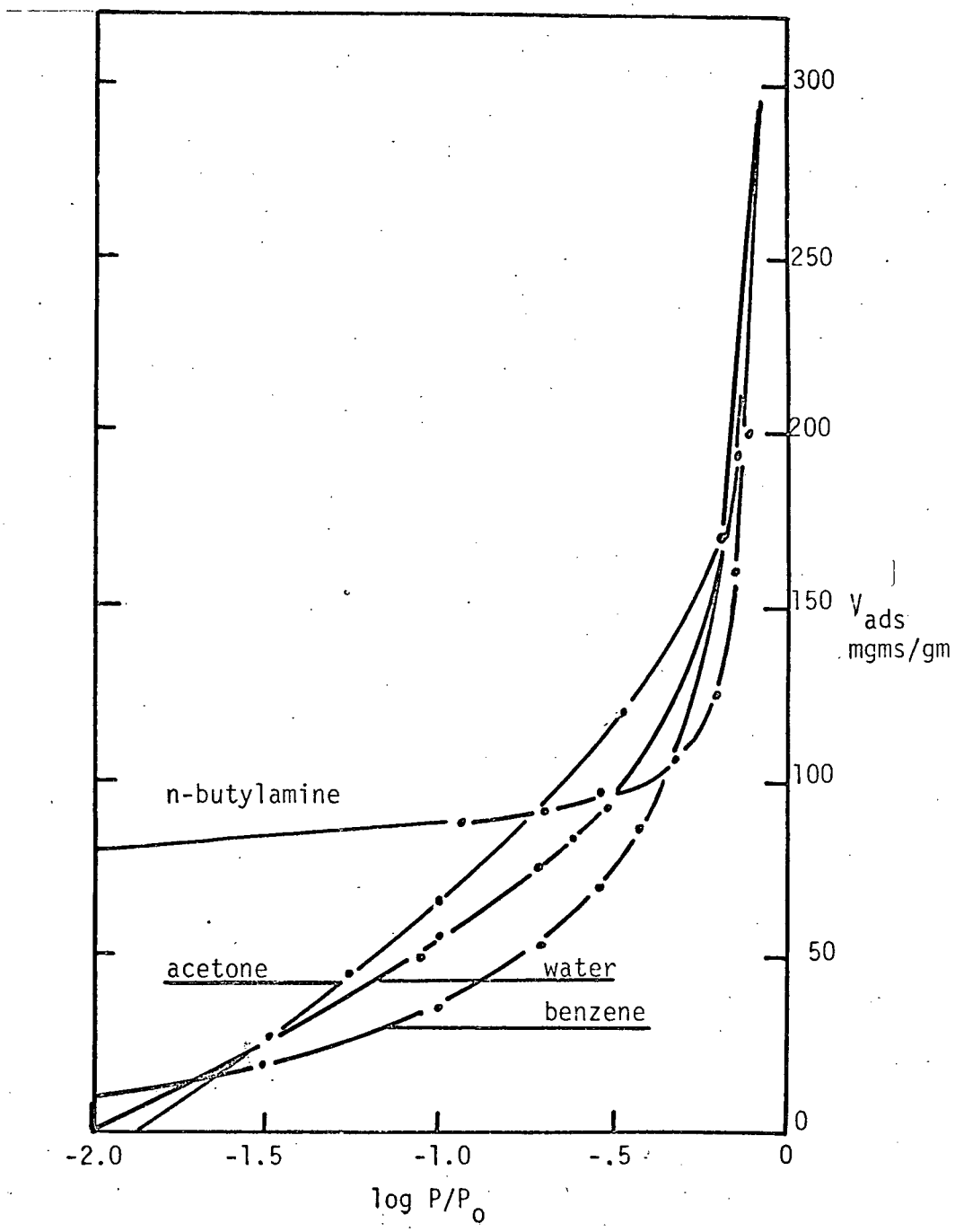

FIGURE 23 V_{ads} vs log P/P_o
(Vycor Glass)

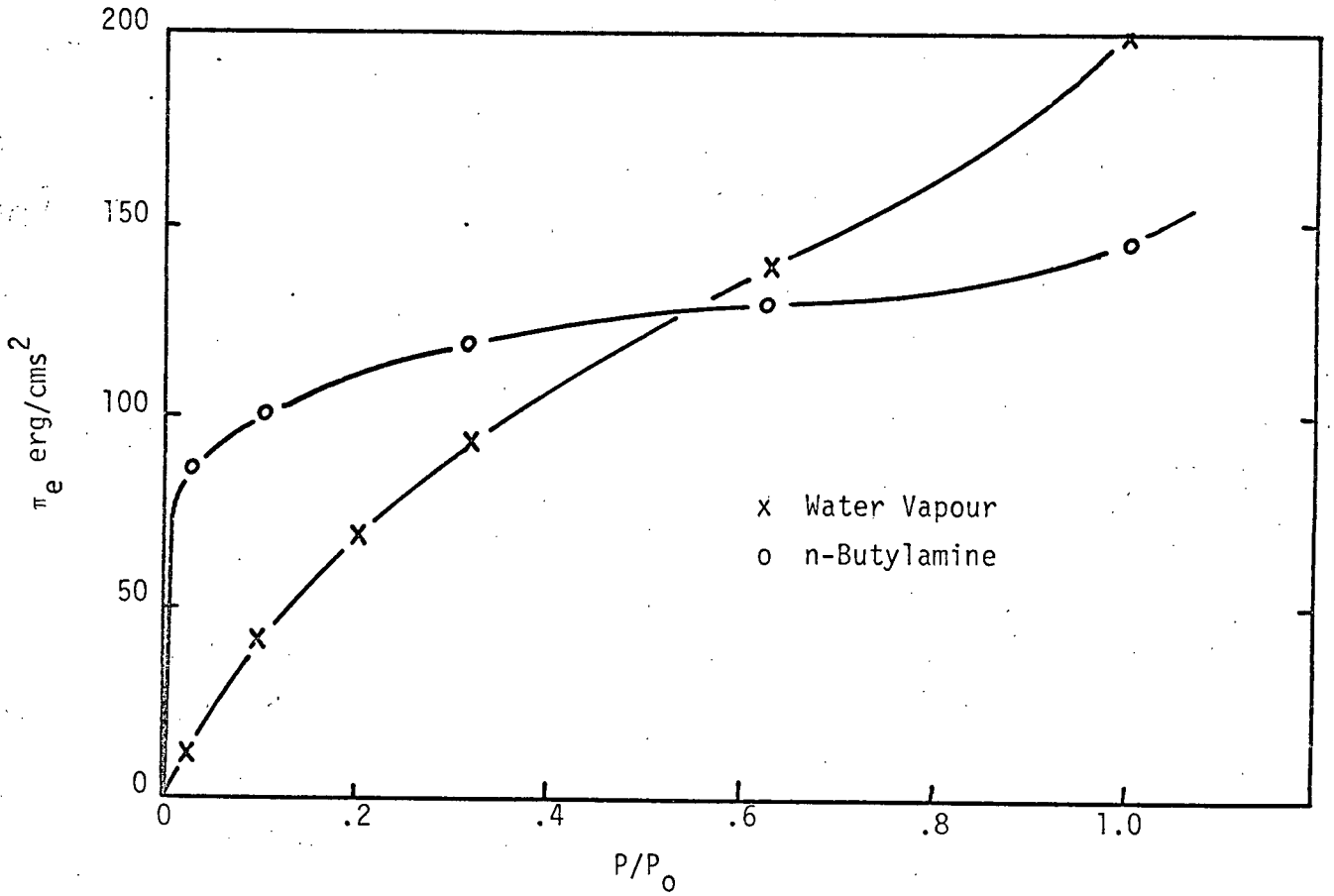

FIGURE 24 CHANGE IN SURFACE TENSION WITH INCREASE IN VAPOUR PRESSURE
(Vycor Glass)

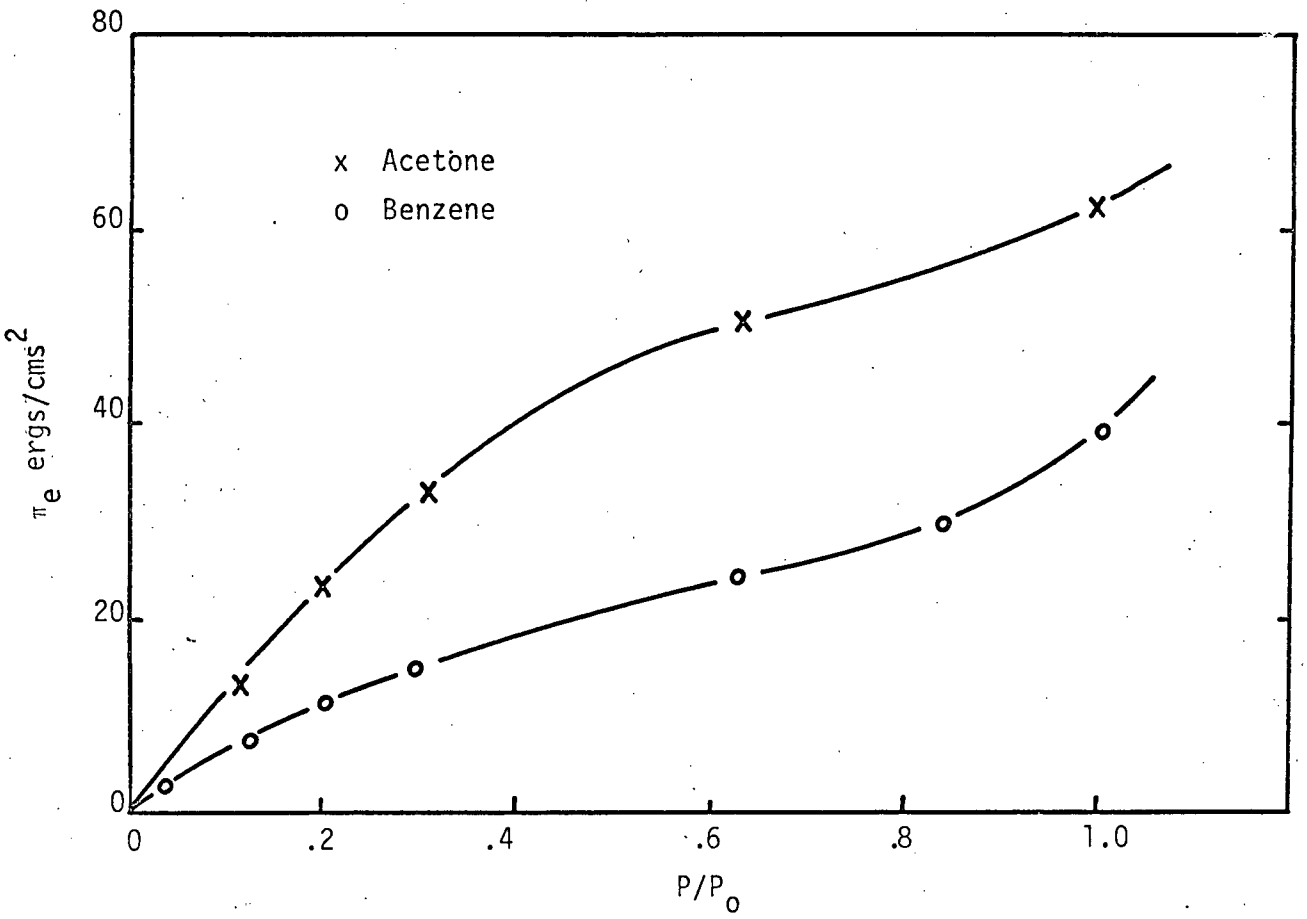

FIGURE 25 CHANGE IN SURFACE TENSION WITH INCREASE IN VAPOUR PRESSURE
(Vycor Glass)

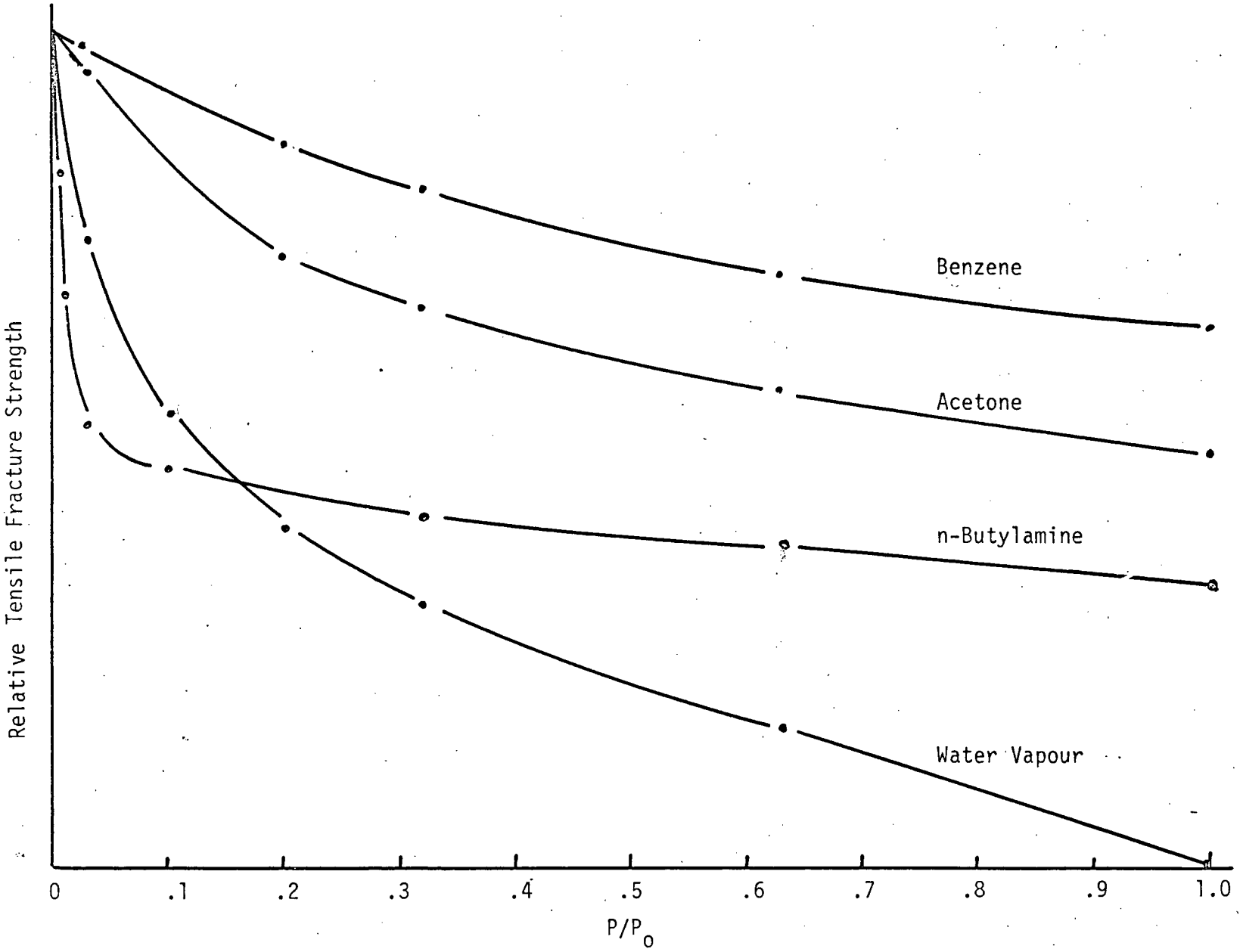

FIGURE 26 PREDICTED SHAPE OF FRACTURE ISOTHERM FROM SURFACE TENSION CHANGES
(Vycor Glass)

be computed from a plot of Vads versus log P/P_o by applying the Gibbs equation in the form(95)

$$-\Delta\gamma = \frac{RT}{MS} \int_{o}^{P/P_o} V d\ln P/P_o$$

(See Appendix D for details of the computation).

Typical plots are shown in Figs. 24 and 25. Some uncertainty in estimating the area under the curve is evident since on a log scale zero pressure corresponds to minus infinity. However extrapolation to zero amount adsorbed is sufficiently accurate for the purpose of this work.

Maximum decrease of surface tension (γ) is not reached until well into the condensation region. At low coverage the lowering of γ is very small. In the light of the Griffith equation it might be expected that maximum weakening would occur at multilayer adsorption values.

Fig. 26 illustrates the shapes of the predicted fracture isotherms calculated from the Griffith equation, by assuming a constant critical crack size and using the surface free energy changes computed above. The fracture isotherm is the variation in tensile fracture strength with increasing concentration of environment.

The fracture data were measured for the systems studied in the adsorption experiments. The various results will be discussed by correlating the data from (a) Adsorption

TABLE 7

(a) The Effect of Dry N_2 on the Tensile Fracture Strength of Vycor Glass

Strain Rate 0.03"/Min.

Environment	Tensile Strength (p.s.i.)
Vacuum	8692
15 cms Hg	8627
25 cms Hg	7968
70 cms Hg	8755

(b) The Effect of Dry CO_2 on the Tensile Fracture Strength of Vycor Glass

Strain Rate 0.03"/Min.

Environment	Tensile Strength (p.s.i.)
Vacuum	8692
25 cms Hg	7822
40 cms Hg	8055
70 cms Hg	7991

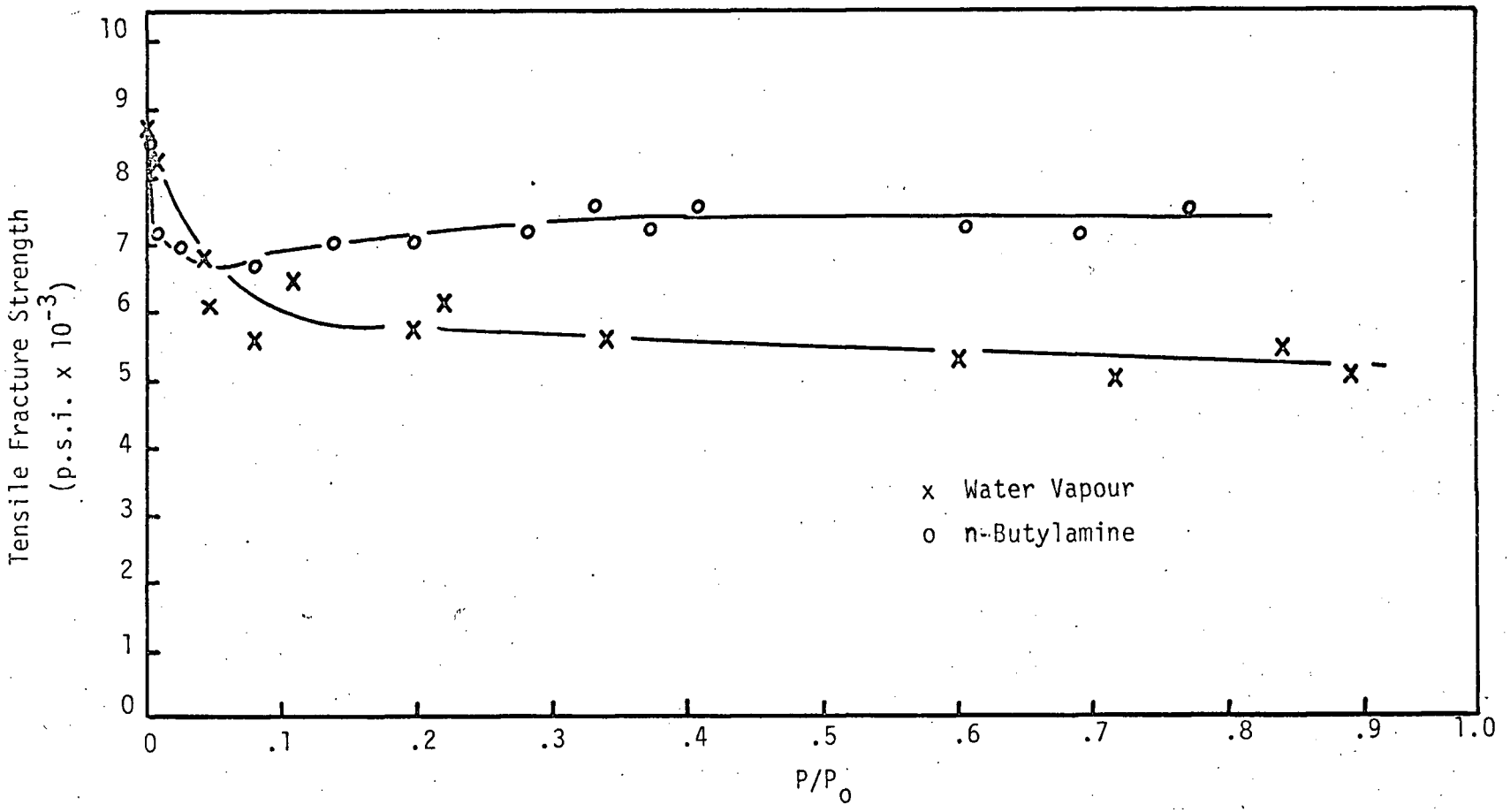

FIGURE 27 TENSILE FRACTURE STRENGTH vs. RELATIVE PRESSURE FOR VYCOR GLASS

Studies; (b) Surface free energy changes and, (c) Fracture isotherms.

(i) Dry Nitrogen and Carbon Dioxide

At 25°C very little adsorption occurs on the glass surface (Fig. 19). The dry gases show no effect on the fracture strength to a pressure of 1 atmosphere. [Table 7 (a) and (b)].

(ii) Benzene

Benzene reacts with the silanol surface by forming π-bonded complexes with the acid hydroxyls of the surface.

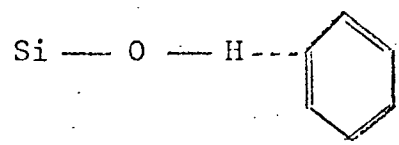

The interaction is relatively weak as evidenced by the small reductions in surface tension of the solid surface, (Fig. 25). The relative decrease in the fracture energy accompanying adsorption (Fig. 28), shows a slight gradual decrease to a minimum corresponding to a relative pressure of $\frac{P}{P_o} = .8$. Fig. 26 demonstrates the deviation from the experimental curve.

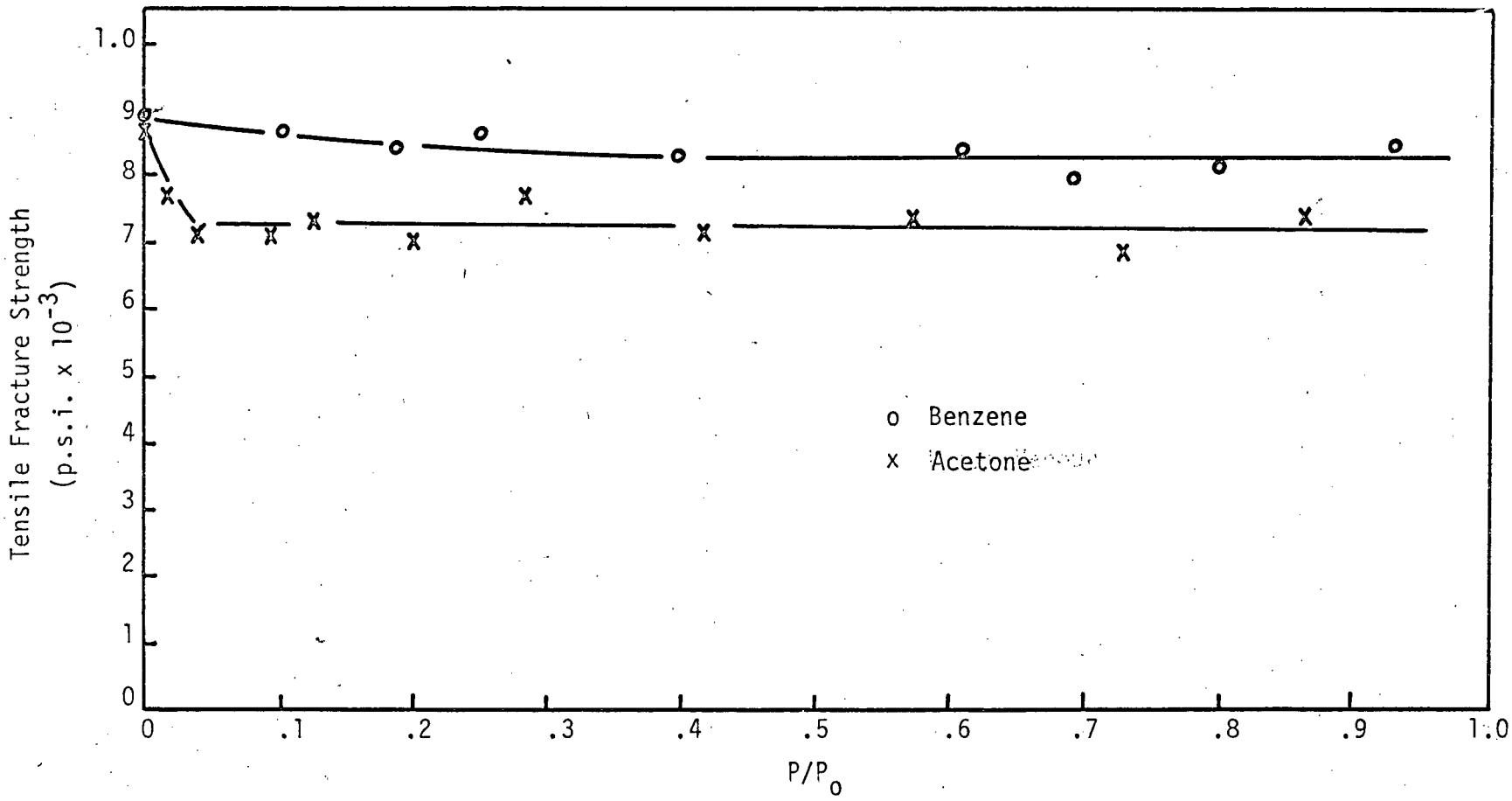

FIGURE 28 TENSILE FRACTURE STRENGTH vs. RELATIVE PRESSURE FOR VYCOR GLASS

(iii) Acetone

Strong hydrogen bonding, (Table 4), results in a larger surface tension reduction than with benzene. (Fig. 25.) The maximum reduction of tensile fracture strength occurred at approximately P/P_o = .05, which corresponds to a value of only 6 erg/cms^2 in the surface tension reduction. The strength of the hydrogen bond formed (a shift of $\Delta\nu$= 350 cms^{-1}) is slightly greater than that formed with water (290 cms^{-1}). The strength reduction however is only 40% of that caused by water. This is possibly due to the larger acetone molecule adsorbing on fewer OH sites and hence screening the surface to a lesser degree.

(iv) n-Butylamine

The amine adsorbs strongly from the vapour phase, forming a monolayer at a very low relative pressure (0.005) (Fig. 20 and Table 6). Traces of the amine cause a reduction in tensile fracture strength to a value of 75% of the vacuum fracture strength. Subsequent increases in vapour concentration appear to cause a slight strengthening effect. Lateral interaction of the adsorbed species could explain this increase, which is not large enough to lie outside of the standard deviation for the measurements, and hence may be due to scatter in fracture measurements.

(v) Water

Water reacts strongly with the silanol surface. At a relative pressure of 0.05, the strength reduction has reached 70% of its maximum decrease (Fig. 27). A minimum tensile strength value is reached at P/P_o = .8. The surface tension reduction at the point P/P_o = 0.05 is only a fraction of the maximum reduction close to saturated vapour pressure (Fig. 24).

A comparison between the fracture isotherms for water and n-butylamine, would lead one to predict, in the light of the Griffith equation, a far greater strength decrease at low coverages for the amine vapour. Results show water to give the greater strength decrease. Thus a mechanism in terms of surface energy reduction alone would not be valid. This conclusion might be drawn by considering the fracture isotherm for water and comparing the strength values with the surface tension reduction at various relative pressures. Obviously the largest decrease would be expected in the vapour phase at values close to saturation pressure. It must be emphasized, however, that great care should be exercised in applying bulk measurements to fracture theories.

Since the fracture process in active environment involves a mechano-chemical mechanism, the processes occurring in the stressed zone might be very different from those occurring in the bulk of the solid. The concentration of adsorbing species in the stressed zone will be higher than indicated from an ad-

sorption isotherm at the same relative pressure. Hence the surface tension decreases in the stressed region will be very much greater than those indicated, since the relative pressure in a surface flaw may be close to saturation or even that of the condensed liquid phase. Hence a substitution of the surface free energy values into the Griffith equation and assuming a constant critical crack size, will not be a valid test for the Griffith approach. Firstly, the assumption of a constant critical crack size is erroneous, since the environment influences the crack growth phenomenon as well as the specimen's limiting strength. Secondly, for the reasons stated above, a comparison of the calculated strength value with the measured strength, could not be explained in terms of plastic flow at the crack tip.

For water, the value of the tensile fracture strength at the saturated vapour pressure is the same as for soaking in the liquid, whilst for all other adsorbates measured, the vapour phase gave higher strength values than the liquid. Such differences are attributed to the presence of water in the various solvents. In all experiments in the vapour phase the effect of the environment was very much less than that reported by various other workers. It is felt that the differences are caused by different levels of moisture contamination, since moisture is the dominant adsorbate for glass systems.

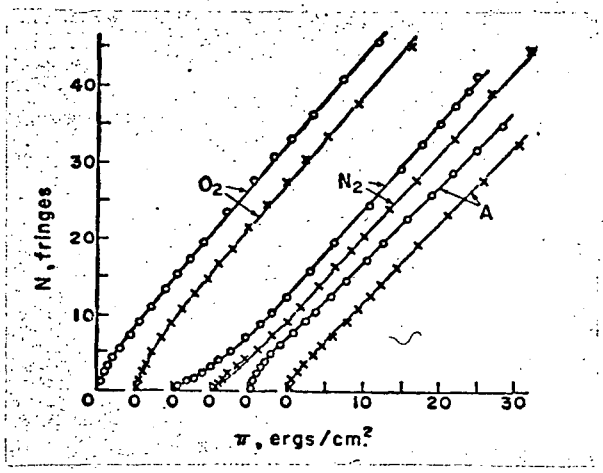

(a) Nitrogen, Oxygen and Argon

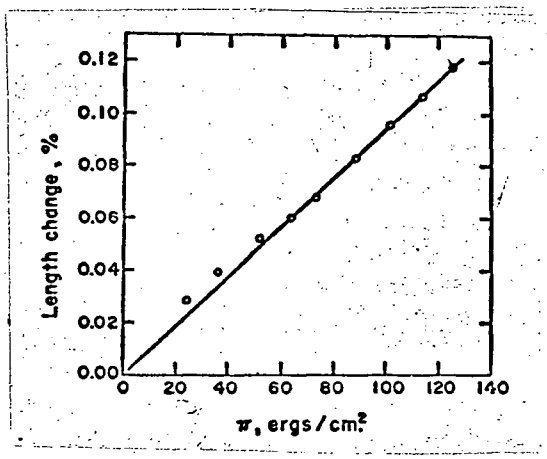

(b) Water Vapour

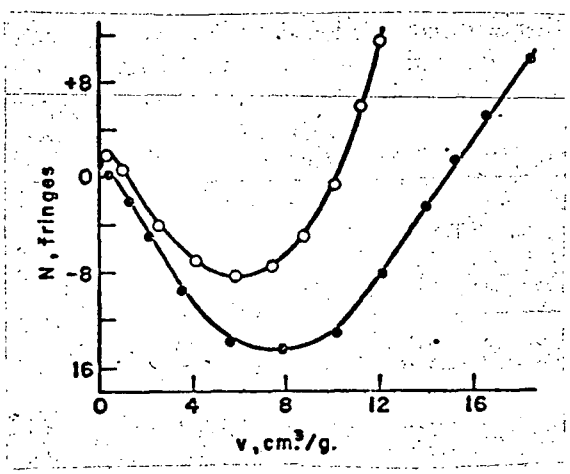

(c) Acetone

FIGURE 29. VOLUME CHANGES OF VYCOR GLASS WITH ADSORPTION. (84)

Volume Changes on Adsorption

The work of Yates[84], in studying volume changes on porous glass accompanying adsorption, demonstrates the important aspects of the depth action of chemical binding in physical adsorption. Even noble gases were capable of adsorption on the high energy surface and screening the Si^{++++} cores.

Figs. 29a,b,c show the length changes of porous Vycor glass after the adsorption of the corresponding vapours used in this study, as obtained by various workers[83][84]. The adsorption of N_2, CO_2, and water result in expansions which are a linear function of the free energy lowering. Acetone gave large contractions in the low coverage regions, followed by an expansion as adsorption increased. One might therefore expect very different strength properties in the expansion and contraction regions of the isotherm. Adsorption results in a decrease in the surface tension bringing about a change in the surface stress and the solid expands. An expansion will result in an increase in the tensile stresses at an existing surface crack tip, thereby resulting in a weakening effect. Conversely a contraction, although arising from an increase in surface tension, causes a compressive action across surfaces flaws and should bring about a strength increase. As shown in Figs. 28, no such strength increase was experienced with acetone. The following course

of events is suggested.

The volume changes measured are bulk effects resulting from an overall interaction of the vapour with the solid. At very low coverages ($<< V_m$), molecules will be adsorbed at preferential high energy sites. Surface flaws would constitute such sites. If a tensile load is applied to the solid, a concentration of adsorbate will occur in the stressed region, due to the increased interatomic distances. The greater the load the greater the reactivity of this stressed zone. The concentration of adsorbate in this zone will then be very much larger than in the bulk specimen, thereby excluding any contractions from occurring in the stressed region, since contractions were experienced at very low coverages. Thus working from an ideal vacuum cleaned specimen, all adsorbates will result in a strength reduction mechanism.

5:3 Fracture Isotherms on Kimble Glass

The results experienced with Kimble glass are shown in Figs. 32 and 33. In all cases the effects are similar to those obtained with Vycor glass, with the exception of n-butylamine. Water, acetone and benzene resulted in larger decreases in strength than with the porous glass. The difference may be attributed to two factors. Firstly, due to the high surface area of the porous specimens, the removal of surface moisture was incomplete. The vacuum strength

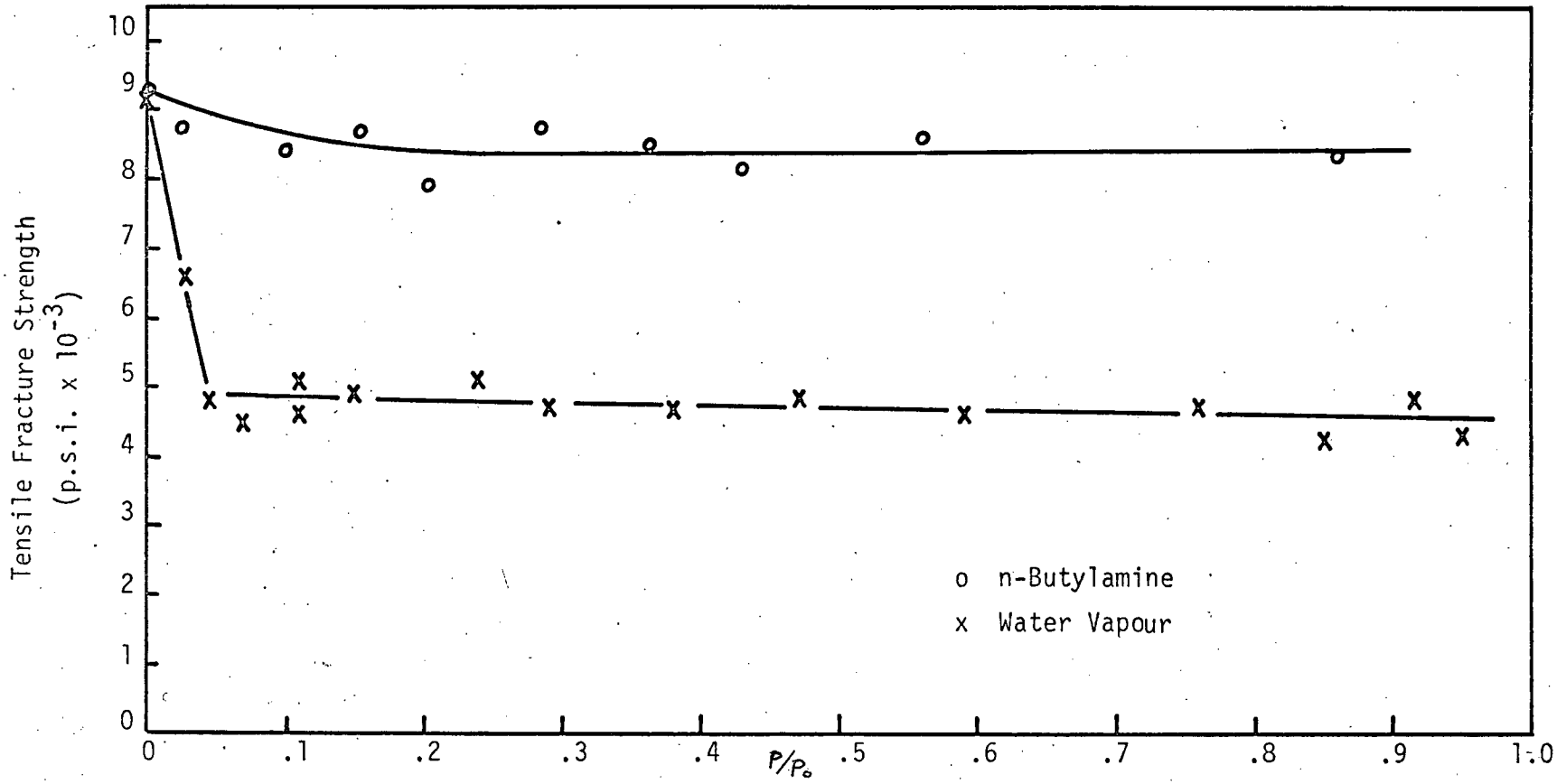

FIGURE 32 TENSILE FRACTION STRENGTH vs. RELATIVE PRESSURE FOR KIMBLE GLASS

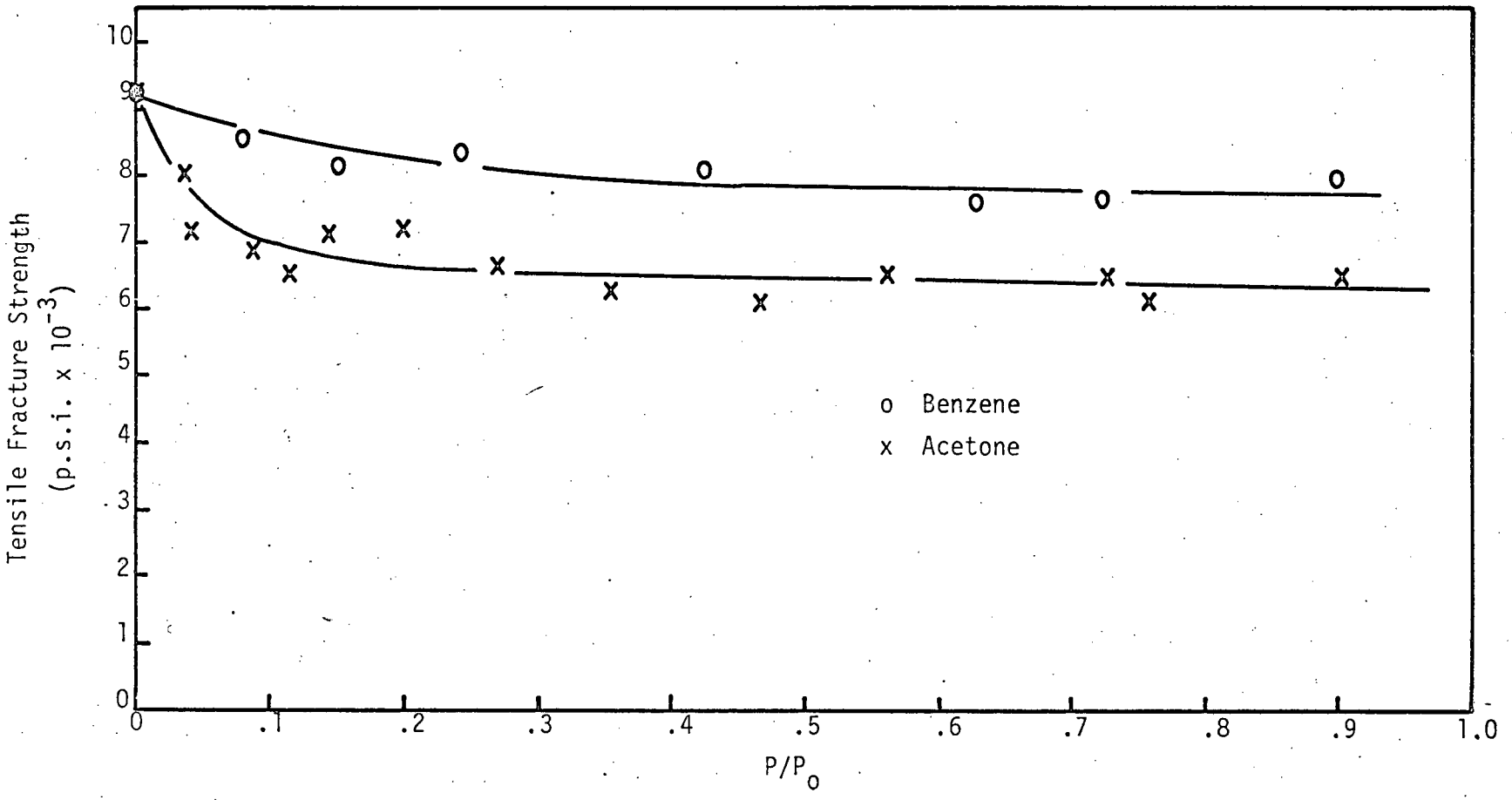

FIGURE 33 TENSILE FRACTURE STRENGTH vs. RELATIVE PRESSURE FOR KIMBLE GLASS

TABLE 8

Effect of Adsorption from

Aqueous Solutions

Vycor Glass		Kimble Glass	
Environment	Tensile Strength p.s.i.	Environment	Tensile Strength p.s.i.
H_2O	5096	H_2O	4368
10^{-4}M C_{12}TAB	5262	10^{-4}M C_{12}TAB	4416
10^{-3}M C_{12}TAB	5216	10^{-3}M C_{12}TAB	4343

value of the Kimble glass was greater than that of the Vycor cylinders. The latter's strength could be increased with prolonged pumping (8,800 psi after 168 hrs.). Secondly, the high surface area glass would contain a greater number of surface flaws and the probability of being weaker would be high, whilst changes in surface stress would be cushioned by the porous nature of the material.

n-Butylamine resulted in only small reductions in strength of the Kimble glass. The presence of the network modifiers Na_2O and Al_2O_3, might reduce the adsorptivity of the solid for the amine.

Adsorption from aqueous solution failed to provide any additional weakening of either the Kimble or the Vycor glass (Table 8). Since the solvent, water, would be preferentially attracted to the surface any additional surface free energy decrease would be small. These results have been substantiated on a quartzitic rock specimen.

5:4 Polymethyl Methacrylate

Fracture isotherms were measured on polymethyl methacrylate as described elsewhere. Due to the low energy surface it was found the high vacuum pretreatment was not necessary.

Table 9 gives the effects of four vapours on the tensile fracture strength. Increasing vapour concentration showed no measurable strength reduction compared with the

TABLE 3

Effect of Vapour Environment on

the Tensile Strength of Polymethyl Methacrylate

Environment	Relative Pressure	Tensile Fracture Strength (p.s.i.)	
		Vapour before load	Load before vapour
Benzene	.15	4375	
	.42	4288	4326
	.56	4294	
	.84	4316	4294
Acetone	.08	4321	
	.36	4311	4305
	.59	4286	
	.79	4282	4301
Carbon Tetrachloride	.17	4314	
	.33	4318	4296
	.65	4297	
	.77	4292	4287
Water	.15	4366	
	.46	4305	4294
	.68	4291	
	.88	4361	4311

TABLE 10

The Effect of Immersion on Tensile Strength of Polymethyl Methacrylate

(Strain Rate 0.03"/Min.)

Immersion Liquid	Tensile Fracture Strength p.s.i.
Vacuum	4454
H_2O	4362
Acetone	1562
Benzene	1634
Carbon Tetrachloride	1618

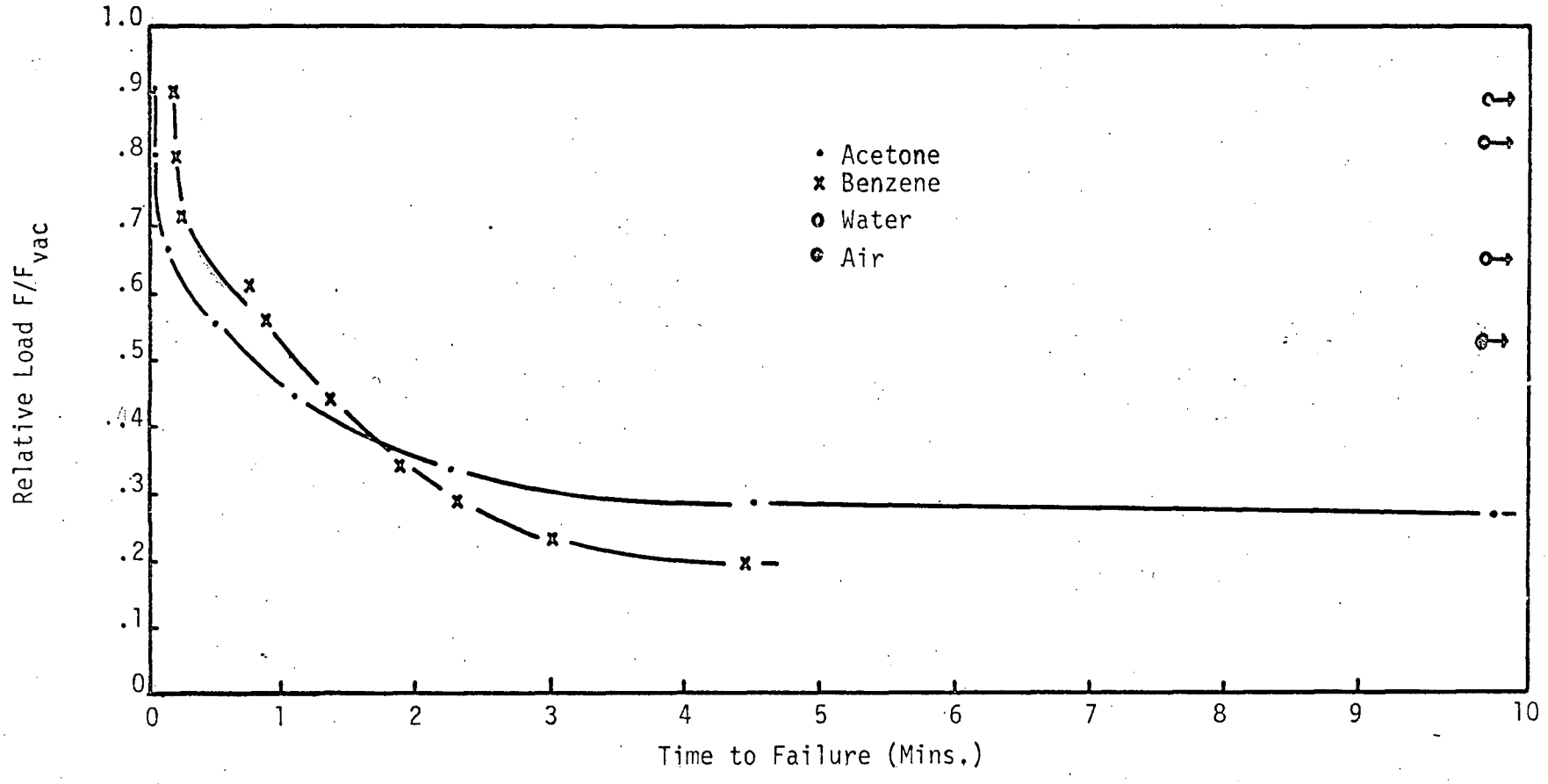

FIGURE 31 STATIC FATIGUE CURVE FOR POLYMETHYL METHACRYLATE

clean specimen (10^{-3} mm Hg vacuum). In each case the load was applied subsequent to the introduction of the vapour. Since polymethyl methacrylate is known to craze under stress, a series of measurements were made by applying the load before introducing the vapour. Again failure did not occur in the vapour phase at reduced loads. With the noted exception of water, immersion in the liquid resulted in failure at approximately a 60% reduction in Load (Table 10). Water had no influence on the strength properties, illustrating wetting to be an important aspect of stress environmental cracking. Water does not wet polymethyl methacrylate.

Fig. 31, shows the results of two typical fatigue curves. The specimens were loaded to a fraction of the breaking load in vacuum, and the time to failure measured on introducing acetone and benzene. Failure times of greater than 10 minutes were not recorded. Acetone with a strong affinity for the plastic, (being a solvent for polymethyl methacrylate), causes failure with explosive violence at higher loads ($\frac{F}{F_{vac}} = .8$), and in shorter times than immersion in benzene. At a relative load of .38 the curves intersect and benzene gives failure in shorter times than acetone.

Due to the solvation process in acetone, longer immersion times lead to a crack healing mechanism, the Joffé effect. At low relative loads ($\frac{F}{F_{vac}} = .4$) the crack could be seen to form on introducing the liquid but the specimen did not fail within the 10 minute period. It would appear under

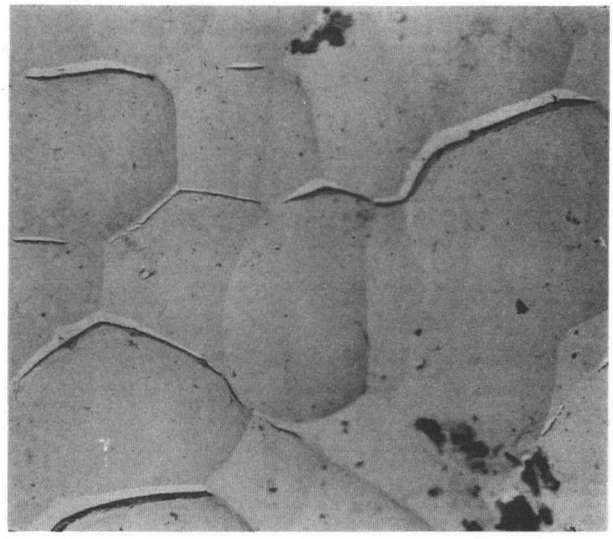

(a) Specimen Untreated

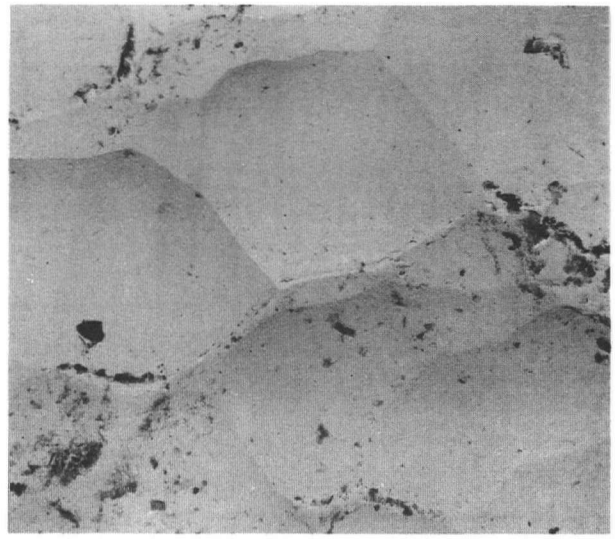

(b) Specimen Soaked in 2N NaOH for 1HR

FIGURE 34 ELECTRON MICROGRAPH OF END FACE OF VYCOR GLASS CYLINDER (X2,000)

these conditions that the crack propagation rate was slower than the rate of dissolution of the plastic, in the stressed region, in acetone. Results presented in the section on the Joffé effect reinforce the above conclusion.

The crack propagating stage is therefore the critical factor in determining the strength characteristics. Berry[96] has shown that polymethyl methacrylate undergoes plastic flow at the crack tip in the process of fracture. A layer of material with altered structure is clearly visible and the apparent surface energy is extremely high. The crack propagates from the surface into the bulk with very low velocity compared with the unstable fracture velocity. The low rate of propagation is a function of the applied load[97].

5:5 The Effect of Immersion

The Joffé Effect

Joffé, in 1928[98], demonstrated the increase in fracture strength of NaCl crystals broken under water or in saturated NaCl solution. The effect is attributed to the decrease in stress concentration at the crack tip, by blunting of the tip, in one of two ways. Firstly, a dissolution process in the stressed region and secondly, deposition of precipitate from solution within the crack, both effects resulting in a reduction in stress concentration and increase in strength. Both porous glass and polymethyl methacrylate exhibit the Joffé effect.

FIGURE 35 EFFECT OF SOAKING TIME ON TENSILE FRACTURE STRENGTH (VYCOR GLASS)

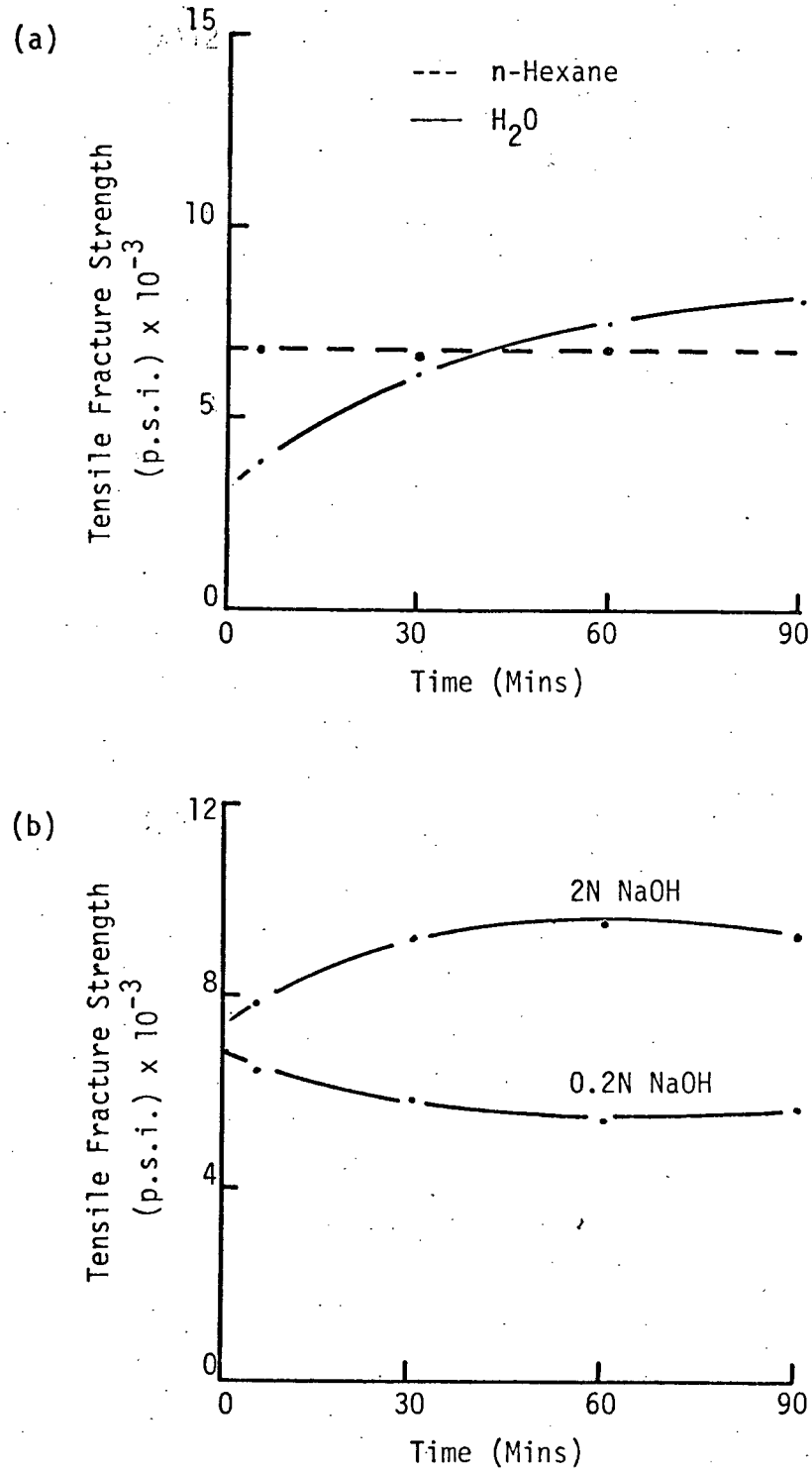

FIGURE 35 (Cont'd)

(c)

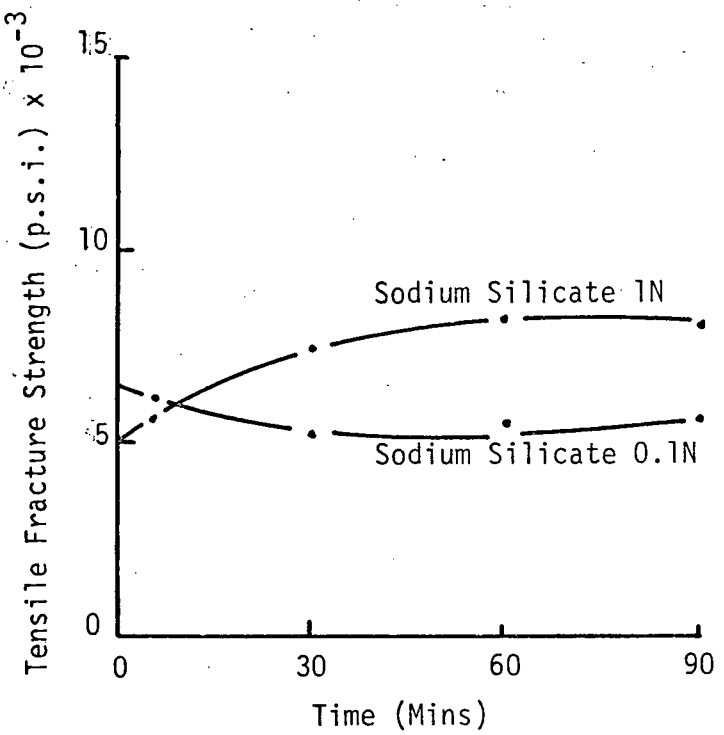

(i) Vycor Glass

Fig. 35 shows the effect on the tensile strength properties of the glass on soaking in various liquids. All specimens were soaked in the solution and broken in air. The immediate effect of immersion in water is a decrease in strength from the vacuum strength value. Hexane, having no affinity for the glass, shows no strength changes with time. Distilled water shows an increase of approximately 45% after a soaking period of 1 hour. Dilute (0.2N) NaOH causes a rapid initial increase from the distilled water value, with no further increase with time occurring.

2N NaOH, which causes the glass to fuse, adequately demonstrates the importance of surface defects. Fig. 34a is an electron micrograph of the end face of the porous glass prior to soaking in 2N NaOH. Fig. 34b illustrates the dissolution process resulting in a blunting of sharp edges. The overall increase in strength results from rapid dissolution in the highly alkaline medium.

Dilute $Na_2O.SiO_2$ gave a slight decrease in strength with time. Since a more concentrated solution (more alkaline) resulted in a strengthening effect, Fig. 35c, a wetting mechanism suggests itself in the case of the dilute silicate. Wetting and spreading will be dealt with subsequently.

The Mechanism of Dissolution

The dissolution of solid silica involves a simultaneous hydration and depolymerization.

$$(SiO_2)_n + 2nH_2O = nSi(OH)_4$$

A chemical reaction of the surface of the solid phase with water results in the hydration of the surface layer of SiO_2 and as each silicon atom is removed, together with its surrounding oxygen atoms, further reaction leads to the formation of monosilicic acid. Dienert and Wandenbulcke[99] report the dissolution to be catalysed by bases and alkali salts, especially carbonates. Alexander, Heston and Iler[100] report a slightly increased solubility in the acid (pH < 4.2) and high solubility in the alkaline regions (pH > 9).

The increase of tensile fracture strength of Vycor glass, with time, in various solutions, is therefore associated with the dissolution effects resulting in a decrease in stress concentration at operative flaws. Very slight increases in the radius of curvature at the flaw apex will greatly reduce its effect as a stress concentrator[101]. It should be emphasized that bulk dissolution rates may not be applied, since the strength is flaw sensitive. Reactions within the flaw may be very different from reactions of the bulk solid.

TABLE 11

Effects of Alkali Solutions

Environment	Load	Tensile Strength
H_2O	2250.0	5730.8
0.2N NaOH	2125.0	5412.4
2N NaOH	3700.0	9423.9
$Na_2O.SiO_2$ ~ IN	1737.5	4425.5
$Na_2O.SiO_2$ ~ IN	2625.0	6685.9

Time of soaking: 60 mins.

Strain rate: .03 inches/min.

TABLE 12

Effect of Strain Rate on Fracture of Polymethyl Methacrylate

Acetone		Benzene	
Strain Rate "/Min	Tensile Strength psi	Strain Rate "/Min	Tensile Strength psi
.03	1562	.03	1634
.015	1615	.015	1752
.006	3774	.006	1761
.0012	4154	.0012	2019

(ii) Polymethyl Methacrylate

The acrylic plastic fractured in liquid acetone shows an interesting feature of the Joffé effect. Using rapid strain rates (> .015 inches/min), catastrophic failure of the solid occurs at very low loads (approximately 50% of the load required to fracture in air). At slow strain rates (< .006 inches/min), strengthening occurs to a value equivalent to the vacuum breaking strength. (Table 12). Using benzene no strengthening occurs, since polymethyl methacrylate is not solvated.

These results add further support to the flaw theory mechanism of the Joffé effect, since the rate of dissolution is the controlling step and must be allowed to proceed faster than the crack propagating rate for the effect to be evident.

5:6 The Spreading or Wetting Effect

A liquid will wet a solid when the work of adhesion between the solid and the liquid is greater than the work of cohesion in the liquid. Since it is essential for the effects of the environment to be felt at the crack tip for a reduction in strength to occur, for liquid adsorbates spreading of the liquid on the solid is a necessary aspect of stress-sorption failure. It may readily be shown that non-spreading liquids do not cause failure at lower loads, e.g. water and

polymethyl methacrylate.

The thermodynamic treatment of Young[102] and Dupré[103] in deriving their classical wetting equation from surface tension concepts alone, ($\gamma_L \cos\theta = \gamma_S - \gamma_{SL}$), does not take into account the nature of surfaces forces. Weyl et al[104] were able to demonstrate that it is not possible to relate wettability of high energy surfaces to the surface tension properties of the liquid. The modern approach[105] concludes that chemical bonds between the solid and liquid phases are responsible for adequate wetting.

Recently Fowkes[106] has shown the importance of the London dispersion forces in adhesion. Regardless of the nature of the solid and of the liquid, the two phases will always attract one another through their dispersion forces. Superimposed on these forces will be the stronger mechanisms supplying cohesion. Thus the surface tension of all materials is the sum of the dispersion forces (γ^d) and other attractive forces (γ^a).

Fig. 37a illustrates the model used by Fowkes for predicting wetting, spreading and adsorption behaviour of many fluids.

The surface tensions of the phases are given by,

$$\gamma_i = \gamma_i^d + \gamma_i^a$$

Thus the interfacial tension between phases 1 and 2 will be given by,

$$\gamma_{12} = \gamma_1 + \gamma_2 - 2\sqrt{\gamma_1^d \gamma_2^d}$$

The reduction in surface tension on adsorption π_e, allows an evaluation of the polar interactions at the solid/liquid interface

$$\pi_e = 2\sqrt{\gamma_S^d \gamma_L^d} - 2\gamma_L$$

where $2\sqrt{\gamma_S^d \gamma_L^d}$ is the dispersion force interaction and $\pi_e + 2\gamma_L$ is a measure of the polar interactions in ergs per square cms.

Types of Attractive Forces

(a) Van der Waal's forces, which operate between all atoms, ions, or molecules, and are due to attractions between oscillating dipoles in adjacent atoms. They are relatively weak forces.

(b) Hydrogen bonds. Since the silanol surface contains hydroxyl ions many of the surface properties will be determined by the ability to form hydrogen bonds. These are relatively weak attractive forces (2-7 Kcals/mole), but their formation is a process requiring low activation energies. Hydrogen bonds form rapidly at room temperature.

(c) Dipole-dipole and Electrostatic Attractions. A solution process involves a penetration of exchanged cations (protons) into the lattice, followed by an expulsion of cations into the liquid. As opposed to the previously mentioned types of

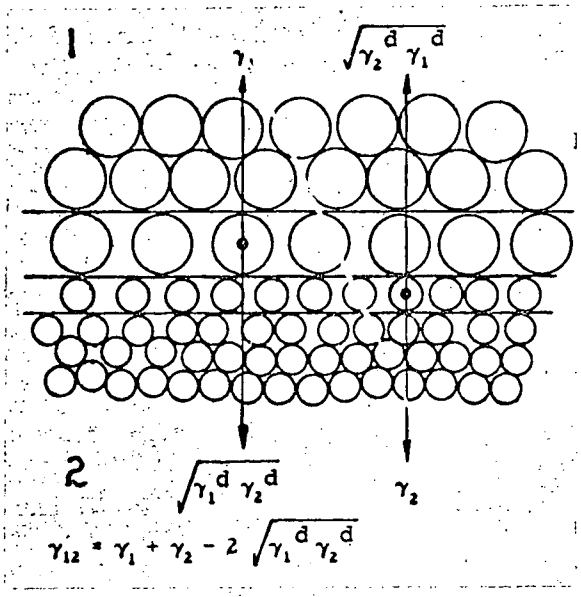

FIGURE 37a. ATTRACTIVE FORCES AT THE INTERFACE.

TABLE 14

Polar Interfacial Interactions at Solid/Liquid Interfaces.

Solid	Liquid	$2\sqrt{\gamma_S^d \gamma_L^d}$	$\pi_e + 2\gamma_L$	Excess
Silica	n-Heptane	100	100	0
	Benzene	118	138	20
	Acetone	98	156	58
	n-Propanol	98	182	84
	Water	94	462	368

bonding, which are strictly surface effects, the electrochemical attack is a depth process.

Any one of these reactions, or combinations of them, with the solid surface, may result in a change in strength properties by changing the state of stress of the surface. This strength change may be positive or negative.

Many researchers[12][24][20] have shown that a linear relationship exists between the decrease in tensile fracture strength and the surface tension of the wetting liquid. C.J. Culf[51] has pointed out the difficulties in removing water from the hygroscopic solvents used, e.g. acetone, benzene and ethanol. To eliminate this uncertainty, values of the tensile fracture strength of Kimble glass were measured by adsorbing from the vapour phase, at the saturated vapour pressure of the liquid. Fig. 36(a) curve illustrates the non linearity of the results obtained. For liquids involving essentially the same type of bonding, viz. ethanol, n-propanol and water, the curve does appear linear. Liquids of differing polar properties and similar surface tensions yield different strength decreases, although each liquid may be classed as "wetting" the glass surface from surface tension considerations. Curve (b) and (c) in Fig. 36 show the effect of drying the solvents on the relative strength changes. Benedicks[24] showed a large increase in the strength of glass using kerosene. In the present study I have found light oils to cause only slight effects, always decreasing the tensile

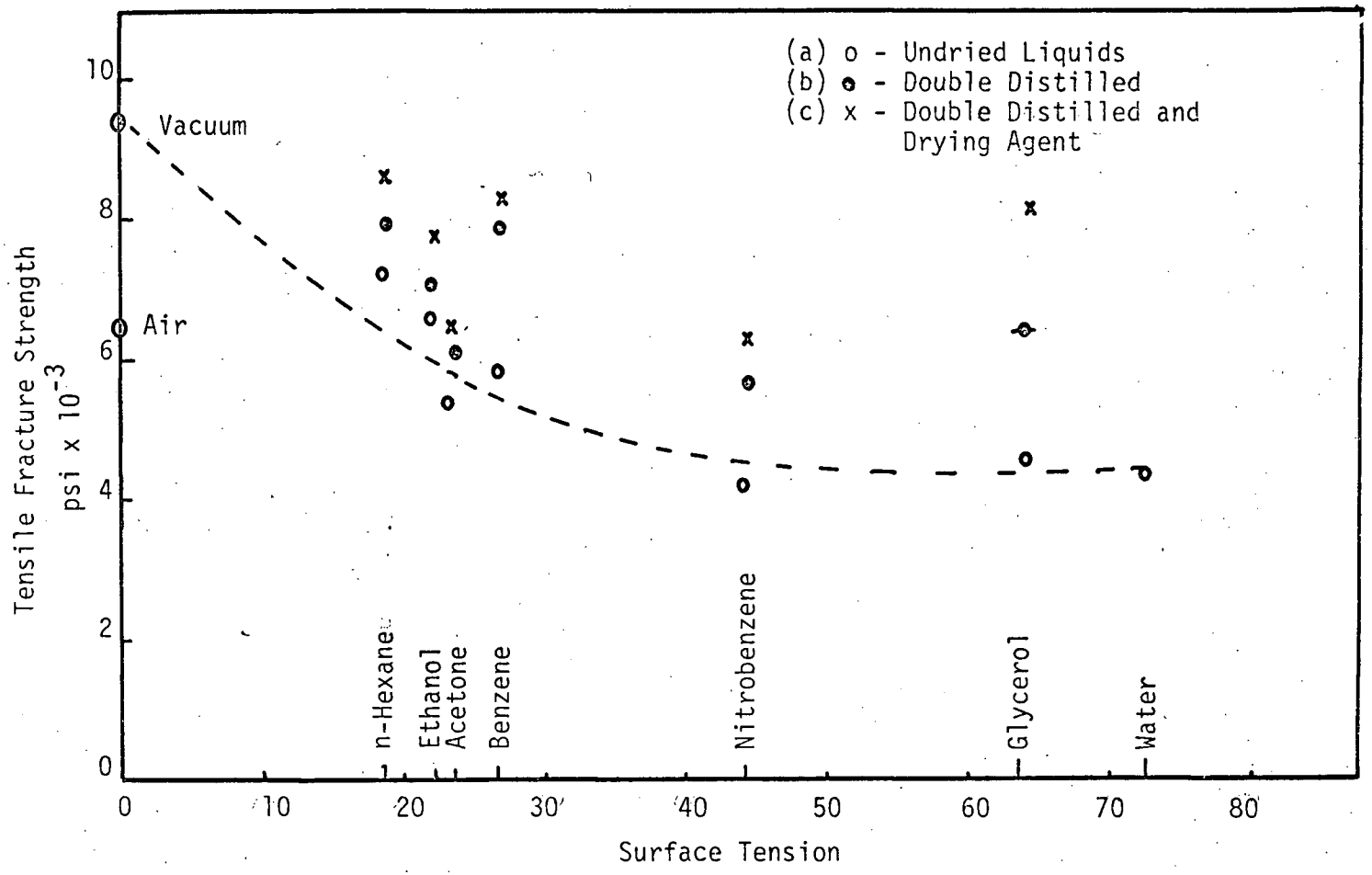

FIGURE 36 TENSILE FRACTURE STRENGTH vs. SURFACE TENSION OF THE WETTING LIQUID
(Kimble Glass)

TABLE 13

The Effect of Paraffin Oil on Tensile Strength of Kimble Glass

(Strain Rate .03"/Min.)

Solid Treatment	Environment	Tensile Fracture Strength (p.s.i.)
Vacuum 8×10^{-7} mms Hg	Nil	9329
	Paraffin Oil (Untreated)	7354
	Paraffin Oil (Na metal)	8785
Vacuum then adsorbed with H_2O vapour	Nil	4836
	Paraffin Oil (Untreated)	4986
	Paraffin Oil (Na metal)	5963

fracture strength of specimens which were vacuum treated (Table 13). For specimens preadsorbed with water vapour and using paraffin oil dried with Na metal, strength increases do occur, although only a fraction of the value reported by Benedicks. The undried oil had little effect. The increase is therefore associated with some dehydration of the silanol surface due to the slight solubility of water in oil.

It appears that the strength reduction on Kimble glass is not a linear function of the wetting liquid, but a more complex relationship, involving the size factor and strength of attraction of the adsorbing species.

The energy required to produce 1 cms^2 of new surface must be greatest if the glass is broken in vacuo, and will decrease with increasing ability of the environment to screen the field of the Si^{++++} ions as previously described. Therefore depending on the screening power of the liquid the tensile fracture strength of the glass will vary. The screening effect is difficult to interpret in terms of steric factors and strengths of adhesion, since the complexity of the mechanism is enhanced by the distribution and varying size of operative flaws within the specimen.

The high dipole and small size of the water molecule cause the greatest strength reduction of glass[107][108]. Due to the rapid contamination of a freshly formed surface by hydroxyl ions the effects of other species may not be detected unless complete elimination of all moisture is

maintained. Culf[51] showed a 50% decrease in fracture energy of glass in dry gaseous NH_3, whereas only small differences were found with other gases (CO_2, N_2 and SO_2). The high screening power and small steric factor for NH_3 satisfy the requirements for an effective strength reducer.

Following the treatment of Fowkes[106], Fig. 37a, in which the surface tensions of the various phases are divided into two parts, Table 14, shows the polar interfacial interactions between silica and various liquids. The London dispersion contribution for each of the liquids shown, $[2\sqrt{\gamma_S^d \gamma_L^d}]$ is approximately the same, whilst the polar attractions vary vastly. Water is by far the most active species. Fig. 37b shows the correlation between these values and the decrease in tensile fracture strength. Although not linear, probably due to a steric effect, the curve does exhibit a correlation for all points. Miss Culf obtained a correlation between the heats of wetting, a bulk equilibrium effect, and the decrease in fracture energy, a dynamic event at the existing flaw. Acetone was the exception.

It is evident that the strength of attraction of the adsorbent for the adsorbate is of primary importance in a strength reducing mechanism. It may be concluded that wettability based on surface tension differences alone, is not a criterion for strong interaction between the solid and liquid phases. Therefore wettability is a necessary but insufficient criterion for stress-sorption cracking.

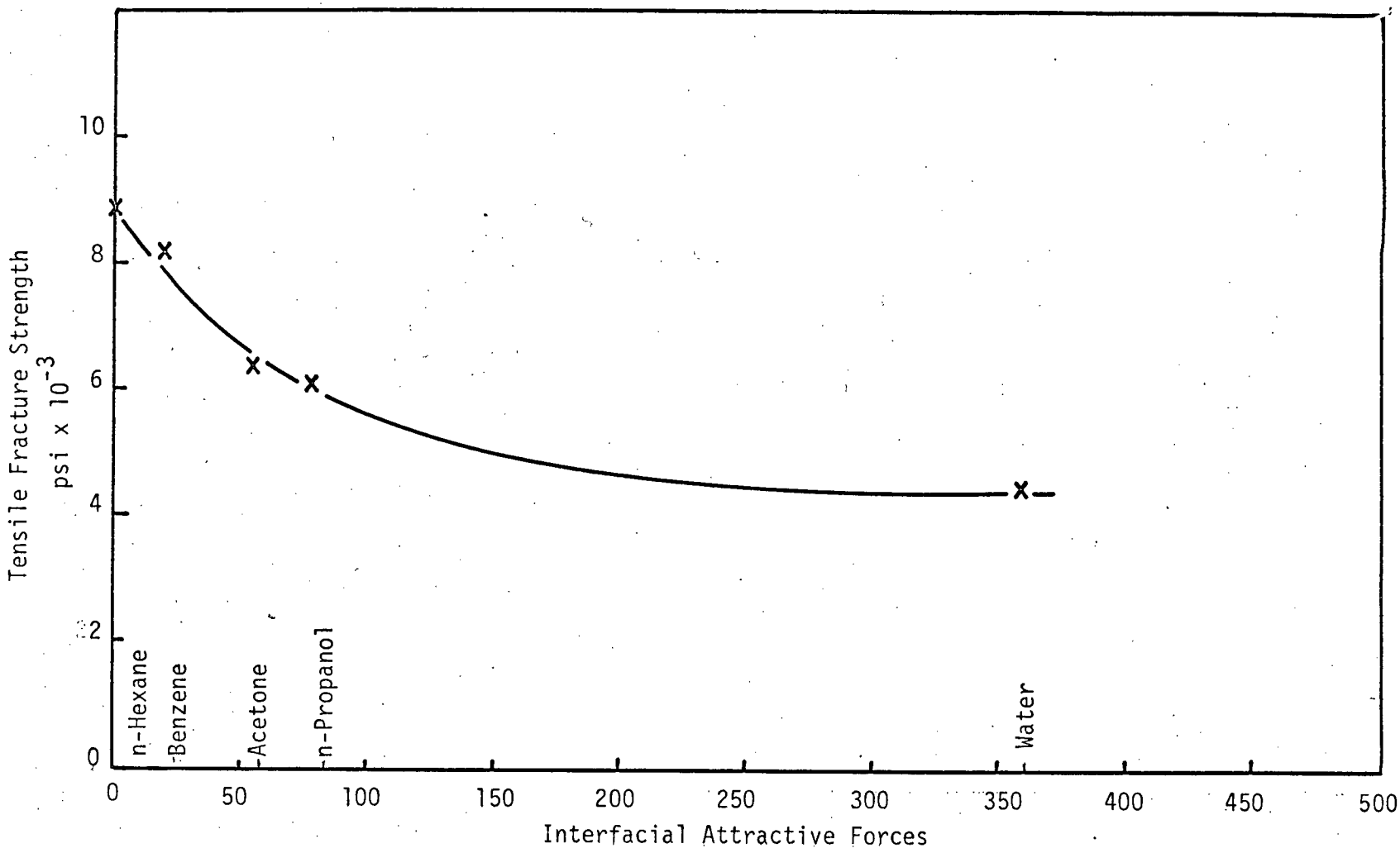

FIGURE 37b TENSILE FRACTURE STRENGTH VERSUS INTERFACIAL ATTRACTIVE FORCES

5:7 Quartzitic Rock Specimens

A brief series of experiments were carried out to test the validity of the fracture process on rocks. A granodiorite core of 1" diameter was fractured in vacuum and in selected environments, after pre-treatment as described elsewhere.

The results shown in Table 15, lead to the following conclusions:

(1) Moisture exhibits the largest reduction in tensile fracture strength of any of the environments tested.

(2) All environments have a decreasing effect with reference to a vacuum treated specimen.

(3) Adsorption from aqueous solution has negligible effect due to the major reaction of the water molecule with the silica surface.

(4) Strength decreases in various solvents are often due to the presence of moisture in the solvent. It is my experience that the tensile fracture strength versus surface tension plot is not linear, e.g. n-hexane, with a surface tension of 18.4 dynes/cms. causes approximately the same decrease as glycerol (γ = 63.4 dynes/cms.) if the liquids are carefully dried (Table 15).

(5) The confusion resulting in the literature from a wide variety of experiments is probably due to the variation in surface conditions, both physical and chemical,

of the starting material. All results should contain details of specimen history and pre-treatment.

TABLE 15
THE EFFECT OF ENVIRONMENT ON THE TENSILE STRENGTH OF ROCK

Environment	Tensile Fracture Strength p.s.i.	Surface Tension dynes/cms.
Vacuum 1	7290	--
Vacuum 2	7860	--
H_2O	5540	72.8
n-Hexane	6974	18.4
10^{-4}M C_{12}TAB	5592	--
Glycerol	6885	63.4
Ethanol	6255	22.8

C_{12}TAB = Dodecyl trimethylammonium bromide
Vacuum 1 = 24 hours at 8×10^{-7} mms Hg
Vacuum 2 = 48 hours at 8×10^{-7} mms Hg.

5:8 The Appearance of Fracture Surfaces - Fractography

The fracture surface of a crack opening under the influence of a steadily increasing crack-tip stress shows three distinct zones[110].

(1) A region in which the velocity of the crack propagation is increasing rapidly resulting in a smooth mirror on the fracture surface.

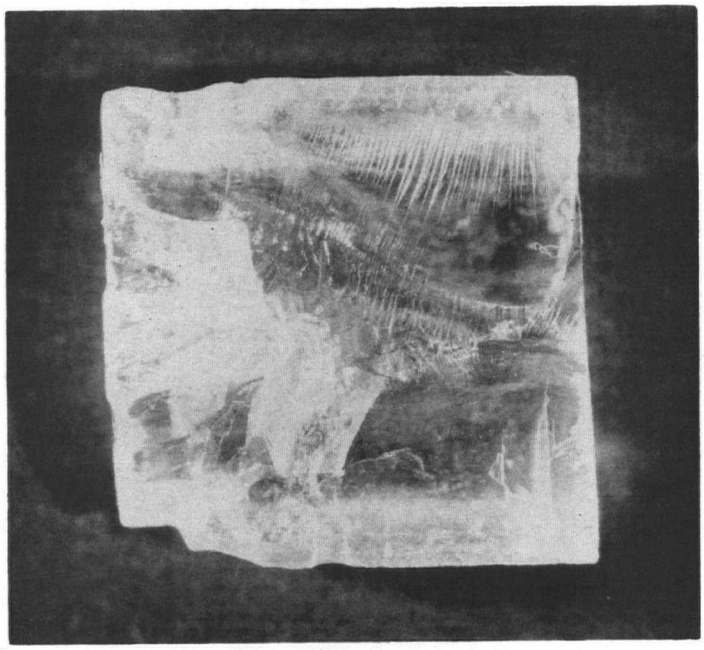

FIGURE 38a FRACTURE SURFACE OF GLASS IN WATER VAPOUR ATMOSPHERE

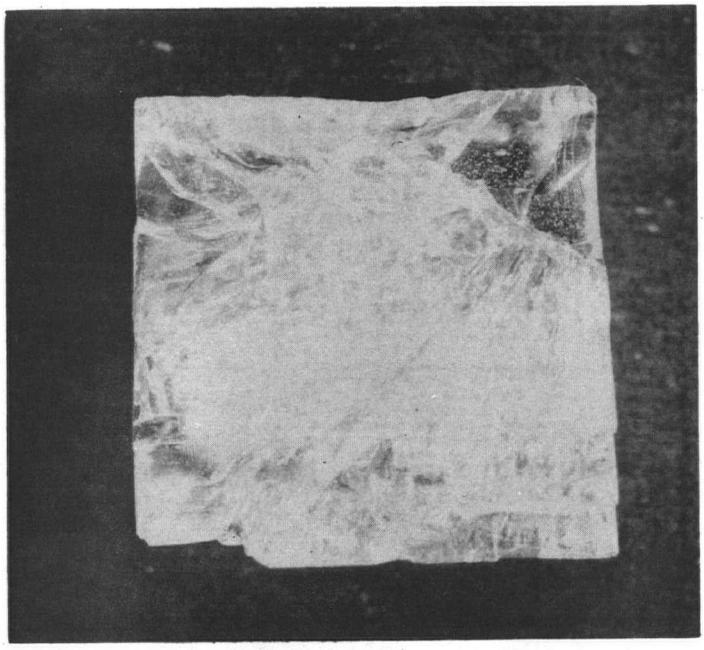

FIGURE 38b FRACTURE SURFACE OF GLASS IN VACUO

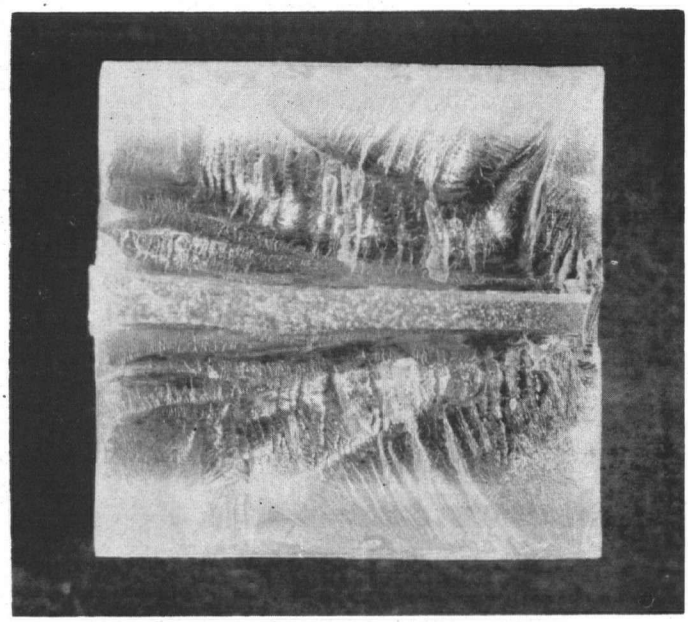

FIGURE 39 FRACTURE SURFACE OF POLYMETHYL METHACRYLATE IN AIR

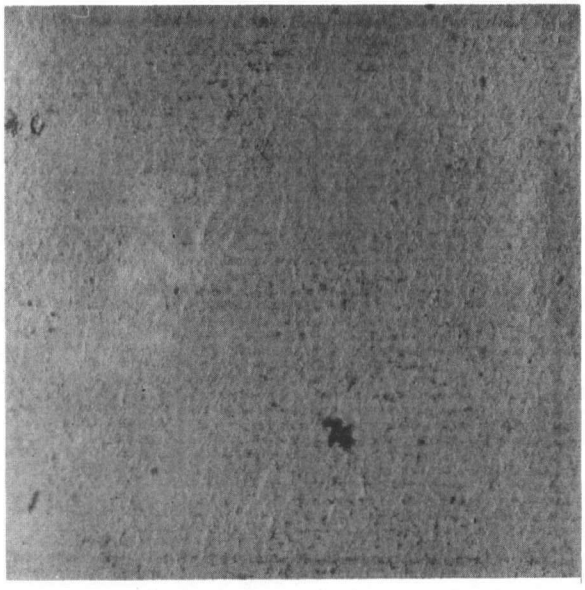

FIGURE 40 ELECTRON MICROGRAPH OF THE MIRROR REGION
(VYCOR GLASS X10,000)

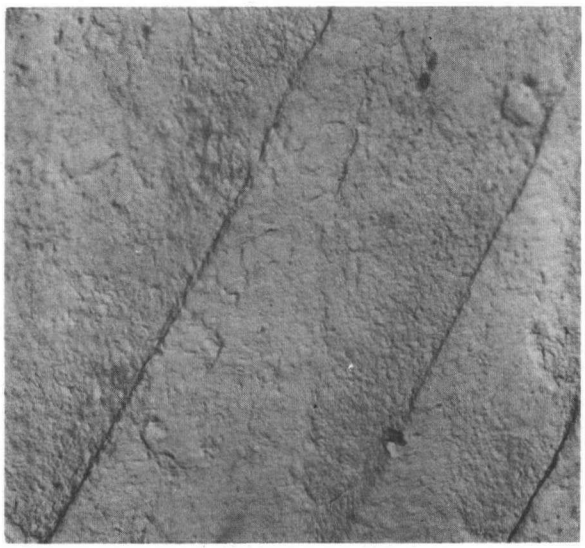

FIGURE 41 ELECTRON MICROGRAPH OF FINE HACKLE REGION (VYCOR GLASS X10,000)

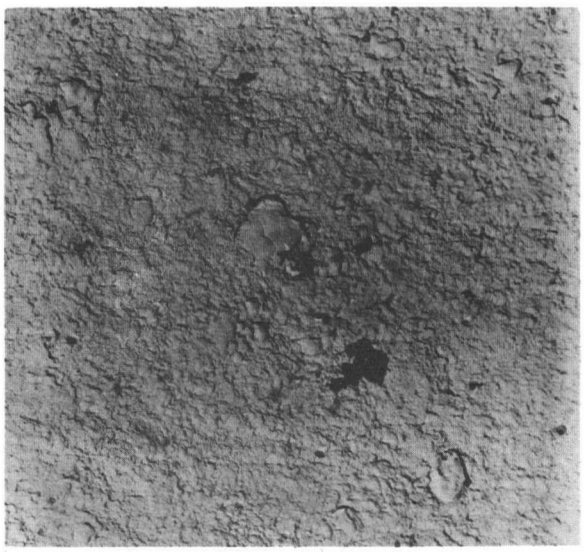

FIGURE 42 ELECTRON MICROGRAPH OF COARSE HACKLE ZONE (VYCOR GLASS X10,000)

(2) A fine hackle zone in which the velocity rises imperceptibly, usually at the edge of the mirror zone.

(3) A coarse hackle zone in which the crack is travelling at maximum velocity through the material.

The brittle solids studied exhibit these three zones, as illustrated in Figs. 38 and 39.

For glass specimens broken in vacuum the mirror zone is either non existent or very small. Thus the extent of crack growth at slow velocity is limited in the absence of environment. Therefore the function of the environment on the fracture process will be to control the initial crack propagation phenomenon. It seems logical to expect that a crack running at maximum velocity will not be affected by the presence of an active species.

Figs. 40 to 42 are electron micro-graphs of the fracture surface of the three regions. In the mirror zone the texture is extremely fine, (Fig. 41), becoming coarser as the crack velocity increases to the fine hackle zone, Fig. 42. In the coarse hackle zone the crack front is smashing through the glass at about one third of the velocity of sound in the material, tearing pieces of glass from the surface and forming large ripple steps, where the transverse pulses emanating from the crack tip interfere with the propagating crack front.

With the glass specimens it is significant that no differences could be detected between the size of the mirror formed in various environments. It might be expected

that the greater the weakening effect the greater the extent of the mirror zone. This may indeed be so, but a cleavage technique would have to be adopted to establish the fact. A fracture technique does not employ one specific surface crack, and fracture may develop from a host of correctly orientated flaws, resulting in the crack propagating from more than one surface. Thus the size of the mirror zone would not be indicative of the effect of the environment on crack growth.

Polymethyl-methacrylate shows a large mirror surface even when broken in vacuum at temperatures below 40°C. The extensive mirror region is associated with a large critical crack size. Thus the effects of environment might be expected to be more drastic in the case of the semi-brittle plastics than with the brittle glasses. Since the crack growth stage is very pronounced, any phenomenon resulting in an increase in crack velocity during this growth, will be manifested in a weakening and possible failure of the specimen.

5:9 Environmental Stress Cracking Mechanism

In many of the studies covered in the literature review the following explanation was given for the cause of environmental stress cracking. "Specific adsorption leads to a reduction in surface free energy of the solid, thereby decreasing the force necessary for fracture." This mechanism has been proposed for liquid metal embrittlement, weakening of rocks and glasses, and stress cracking of plastics. The explanation follows directly from the considerations of the Griffith criterion, since a decrease in γ must lead to a reduction in σ; $(\sigma \propto \gamma^{1/2})$.

This hypothesis is incomplete in that,

(i) It fails to explain the peculiar selectivity of the environment and the material.

(ii) Provides no account of the nature of the embrittling process on an atomic scale.

(iii) Experimental results show poor correlation when fitted to the equation. This lack of fit is often attributed to plastic flow in the vicinity of the crack tip.

(iv) Ductile metals fail spontaneously in a brittle fashion. The theory offers no explanation for the reduction of the plastic energy contribution (P).

Gilman (1959)[111], Stoloff and Johnston (1963)[112] and later Westwood and Kamdar (1964)[113], adopted an approach

whereby the cohesion forces of the atoms at the crack tip are considered. They concluded that the role of the adsorping species is to reduce, in some way, the bond strength, thereby causing the crack to propagate. Westwood's theory was based on the continued diffusion of the cracking species along the crack walls, to maintain propagation. Such a mechanism would limit the use of autophobic cracking agents, i.e. those which will not spread on their own monolayer, thereby offering a certain selectivity to the process. A constant supply of embrittling atoms at the crack tip is also necessary and it has indeed been shown that there must be a sufficient supply of liquid metal to maintain liquid metal embrittlement[114].

Nielsen[115] first demonstrated the deposition of corrosion products within cracks in an 18Cr-8Ni stainless steel. He suggested that these deposits might exert large hydrostatic pressures, thus introducing the wedging mechanism of corrosion products. Pickering et al[116] showed the wedging force to be sufficiently large to propagate the crack, but the effect is limited to only a few atomic diameters ahead of the crack tip. Brittle systems involving freely running cracks are not likely to involve such a mechanism.

In all mechanisms a tensile stress is essential to facilitate cracking. The stress need not be applied externally and may indeed be an integral property of the solid, causing spontaneous failure on introducing the environment, e.g. MgSn and H_2O[117].

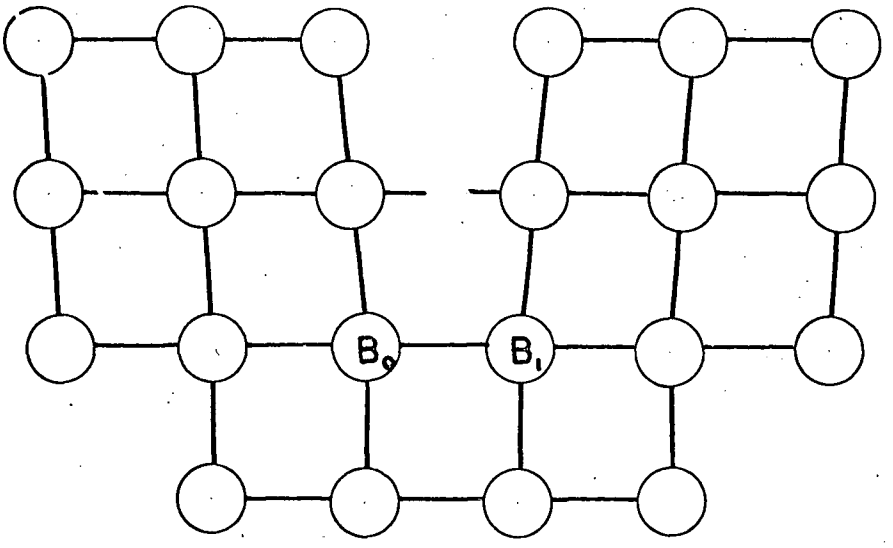

FIGURE 43 MODEL FOR THE IONIC RIGID SOLID

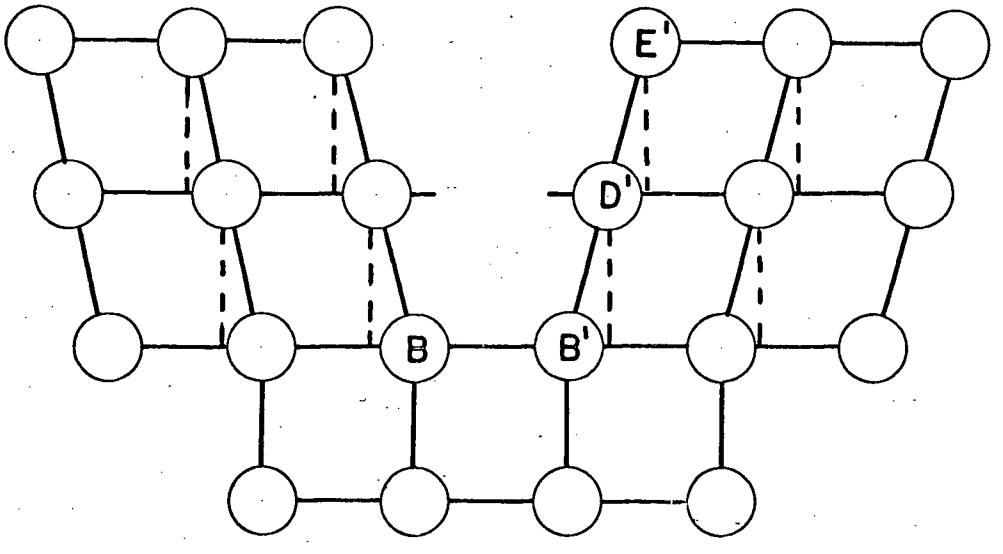

FIGURE 44 MODEL FOR THE COVALENT SEMI-BRITTLE SOLID

The existence of a 'threshold' stress below which cracking will not occur has been demonstrated for some metallic systems[118]. Theoretically for glass systems, which exhibit static fatigue, no such threshold exists and the glass will eventually fail, no matter how small the load.

The function of the tensile stress appears to be to increase chemical reactivity of the surface by three possible mechanisms.

(i) Increase of the spacial atomic arrangement, allowing penetration of the cracking species.

(ii) To contribute in some way to the surface reaction by supplying energy necessary for reaction.

(iii) By exposing fresh surface through a slip mechanism or by rupturing oxide films, the surface reaction may be accelerated, in the case of metallic systems.

Increase in the magnitude of the stress, above the threshold value, results in a more rapid failure, as does increase in temperature.

In comparing the results presented on two types of glass and on a brittle plastic a fairly complex mechanism suggests itself for the stress-sorption cracking of brittle materials. It is likely that a single mechanism will not suffice for all systems. Any adopted mechanism must explain, in the light of the data presented, the following:

(i) Glass is immediately weakened in the vapour phase whilst the plastic is not.

(ii) The reduction of strength for the glass is the same in concentrated vapour as in the liquid phase, whilst the plastic is considerably weaker in the liquid phase.

(iii) Glass has a high energy surface ($\simeq$ 500 dynes/cms^2), whilst the plastic is a low energy surface ($\simeq$ 30 dynes/cms^2). Thus from an adsorption point of view, the environment should have a greater effect on glass than on plastics. Glass does not fail catastrophically, whereas the plastic does.

(iv) The mechanism must explain the selectivity of the solid/environment system.

(v) The necessity for the liquid to wet the solid surface and spread is an inherent aspect of the process.

(vi) The process is tensile stress dependent.

(vii) The mechanism must include an explanation for the function of an embrittling species.

(viii) The variation of strength properties with surface condition, in the presence or absence of environment, must be explained.

(ix) The magnitude of the effect, in varying from a slight weakening in some systems, to catastrophic failure in others, must be included in the mechanism.

5:10 A Proposed Mechanism for Stress Sorption Cracking of Brittle Solids.

As a result of experiments such as those indicated in the section on the Joffé Effect, it appears obvious that

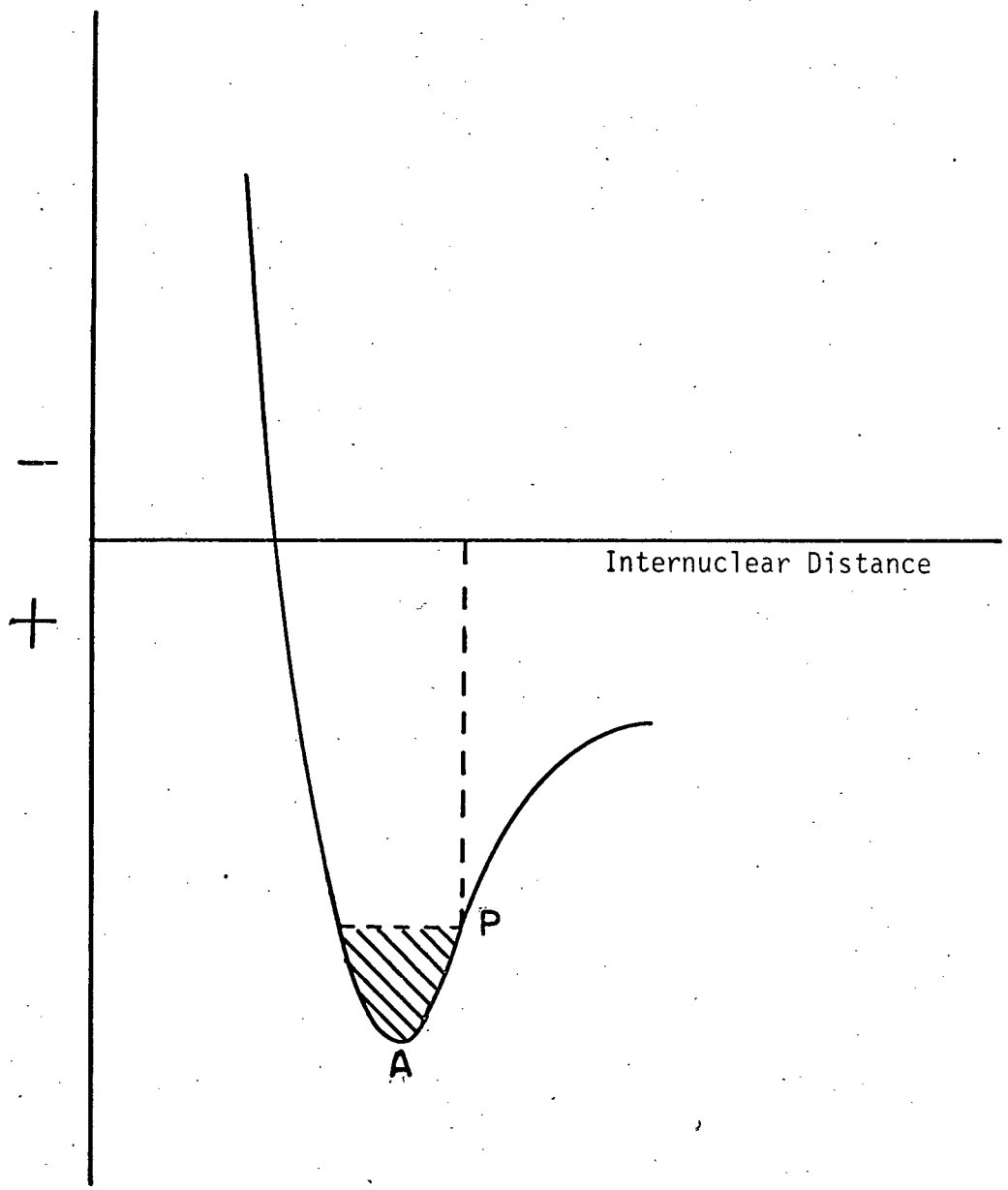

FIGURE 45 MORSE CURVE FOR THE IONIC SOLID

the existing surface cracks play the major role in determining the tensile fracture strength of the brittle materials. In the model of the solid surface, we therefore accept the presence of surface cracks or flaws, and regard the failure as a crack extension phenomenon, proceeding from the tip of flaws orientated in directions at right angles to the applied tensile load.

Therefore, we direct attention to the tip of an existing crack and adopt an atomic approach for determining a mechanism. For the crack to extend repeated breaking of bonds of the type B_0-B_1, B_2-B_3 etc. as shown in Fig. 43 would be necessary.

The cohesive or attractive strength of such bonds can be represented on a Morse diagram (Fig. 45) in the usual way. In the absence of environment the function of the tensile load will be to increase the bond lengths B_0-B_1, B_2-B_3, or to move up the potential energy curve in the direction of increasing separation distances. The slope of the Morse curve in this region is thus of prime importance in straining the solid. For an extremely rigid ionic solid the rate of change of potential with internuclear distance will be high, that is, deformation, or increase in bond length will only be achieved by the application of high loads. There is a point of secondary equilibrium P on the Morse curve to which the bond can be stretched without resulting in failure. Extension beyond this point is accompanied by parting of the

bond. (P is the point at which $d^2U/dr^2 = 0$).

For the rigid solid, extension to this point can only be achieved with the application of high loads, although the strain necessary to cause rupture might be very small. The curve is very steep in this region and small extensions will result in larger changes in attractive forces, and since the probability of the solid failing is based on the achievement of the potential barrier $E_{(a)}$, any extension will result in a higher probability of failure. This case for the rigid ionic solid e.g. glass, offers an adequate explanation for the static fatigue phenomenon, i.e. the application of a tensile stress will eventually cause failure according to the probability factor, $P \propto e^{\Delta E_a/1kT}$. The higher the load applied, the smaller ΔE, and hence the solid will fail in shorter times.

The bond is at all times oscillating about an equilibrium position. The greater the distorted internuclear distance the greater will be the frequency of oscillation. This frequency also contributes to the probability of achieving the potential barrier and of the solid failing.

In the presence of an environment the course of events would be as follows. Prior to the application of the load, physical adsorption of the active species results in a decrease in surface tension. This reduction in surface tension leads to a change in the surface stress, and the strains induced in the solid in vacuo are relieved. The

solid swells. The extent of the surface stress variation, on surface tension reduction, will be a function of the slope of the Morse curve in the region A-P. For glass, a rigid ionic solid of steep slope over AP, the term $\frac{\Delta\gamma}{\Delta E}$ will be large since ΔE must be small. Thus the change in surface stress will be very much different from the reflected change in the surface tension ($\Delta\gamma$). The slope of the curve and the terms $\frac{\Delta\gamma}{\Delta E}$ would therefore be a measure of the ability of the solid to withstand shear. It is this variation in surface stress resulting from large values of $\frac{\Delta\gamma}{\Delta E}$ which causes significant volume changes in rigid solids.

The effect of the increase in solid volume will be to increase the tensile force across the bond B_o-B_1, thereby extended the bond further than the equilibrium position, a, in the absence of adsorbate. On application of the load the internuclear distances will be increased still further. The adsorbate molecules, already attracted to the surface in the absence of the stress, will now have a greater affinity for the stressed region due to the lesser screening of the ion cores, resulting from the increased internuclear distance. The adsorbing species then screen the attractive cores to a larger degree and the bond extends still further. The load necessary to extend the bond beyond the breaking point is then assisted by the contributing factors above and the solid fails at a lower applied load.

However, since we are dealing with a rigid ionic

body, large amounts of energy are necessary to effect a small extension. The contribution from the adsorbing effects may be small, with the end result that the solid may not be considerably weakened. If the adsorption effects are capable of increasing the internuclear distance beyond point P, the solid will fail spontaneously in the absence of applied stress.

Since the effect of adsorption is a function of the screening power of the adsorbate, the greater the screening power, the greater the effect. The screening power may be measured by bond frequency shifts and volume changes of the solid. The strength of the adsorption bond will not necessarily relate to the strength of screening. If the molecular size of the adsorbate is large and blocks a large number of sites, whilst only attaching at one or two points, effective screening will not be achieved. Therefore a certain selectivity governs the cracking system.

Thus for rigid ionic solids the onset of catastrophic failure would be achieved with great difficulty, since a high tensile stress is necessary for increased internuclear distance leading to stress accelerated adsorption. The more rigid the solid the less susceptible it would be to stress sorption failure.

For the semi-brittle covalent acrylics the Morse curve would be as shown in Fig. 46. Extension of the solid can be achieved with relative ease. The ability of the solid to shear is included in the slow rate increase over the region

A'-P'. Lack of rigidity does not necessarily imply ductility. Rigidity is a measure of the elasticity of the solid whilst ductility is the ability of the material to swap bonds and flow.

The less rigid solid of equivalent strength will have a potential barrier of equal height to surmount, for failure in vacuo.

However, considerable extension can be achieved with only small changes in energy, viz, small applied loads would result in extensive strain. Due to the increased elasticity the slow crack growth stage of fracture will become more pronounced than in the former case for the rigid ionic solid. An additional force would come into play in this case which would not be effective in the former case.

Since low loads cause larger extension of the solid, the bonds of the type B'-D', D'-E' in Fig. 44, will become oblique to the tensile stress direction. The greater the extension the greater the contribution of these bonds through their component in the direction of the tensile stress. The end result is for the bond B-B' to extend still further, thus increasing the additive component, and the crack can propagate slowly under a very low load.

In the presence of an active environment the same situation will exist as for the rigid ionic solid except that the effect should be more pronounced if the adsorptive reaction were identical. However, the polymethyl metha-

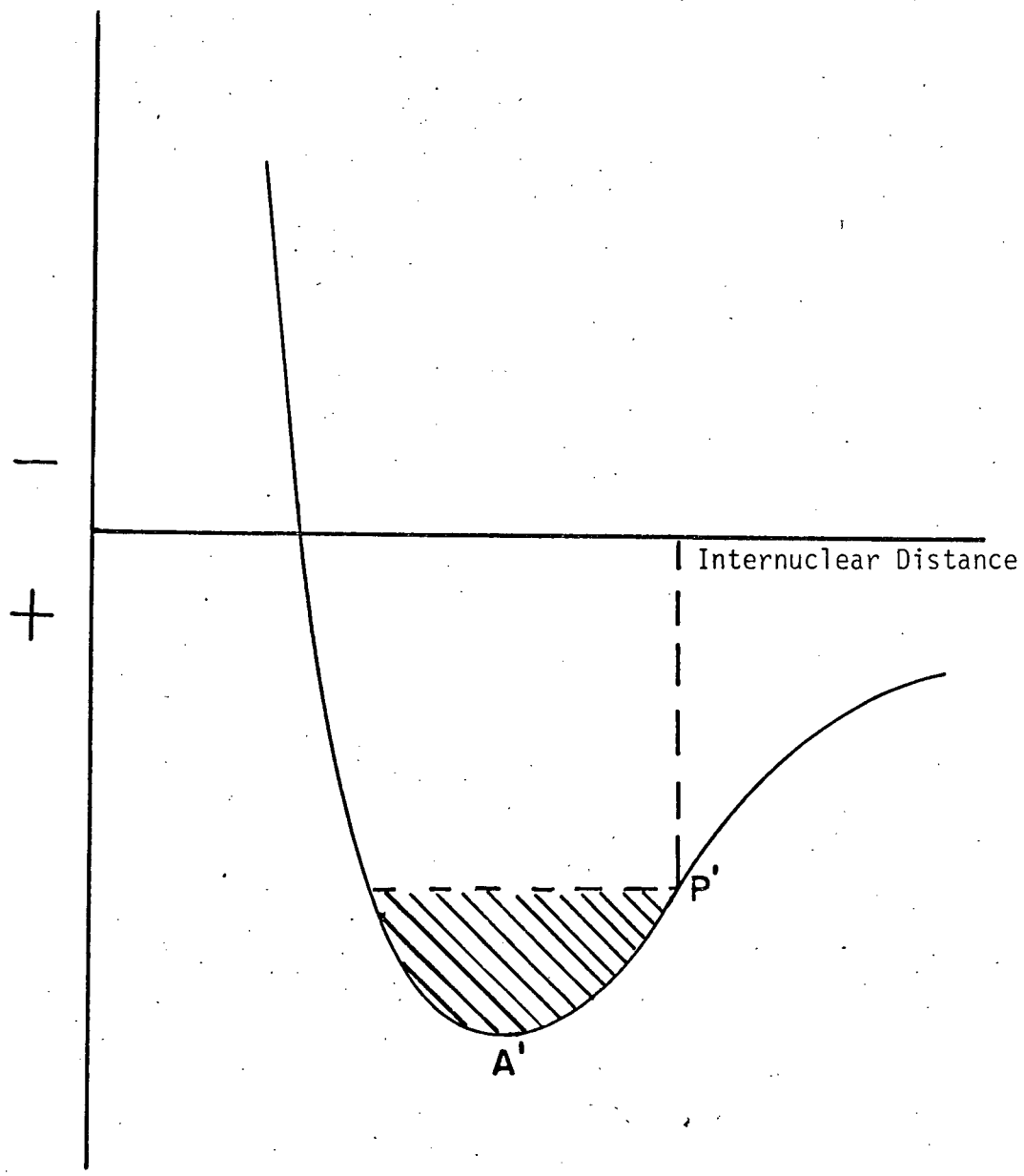

FIGURE 46 MORSE CURVE FOR THE COVALENT SOLID

crylate has a low energy surface and the $\Delta\gamma$ will not be large. Any change in γ will result in a change in the extension, but $\frac{\Delta\gamma}{\Delta E}$ will be small since $\Delta\gamma$ is small, and ΔE is large. Extending the case to the semi-liquid state $\frac{\Delta\gamma}{\Delta E}$ will almost vanish.

Thus the surface stress variation will be mainly reflected in changes in γ, which will be small, as the system could not be very adsorption sensitive, due to the low surface energy.

Also since the adsorbing forces on plastics with organic environments are largely non-specific and the polymers are non-ionic, effective screening would not accompany an adsorption reaction.

As we extend the bond B-B' towards its breaking point, the bond is oscillating at increasing frequencies. If the frequency of oscillation can be made to interact with the frequency of thermal vibration of the environment, strength reduction may be achieved by a sudden decrease in free energy of the surface. Catastrophic failure can ensue. Thus the probability of a system failing under these conditions would be greater, the closer the physical nature of the thermal vibrations of the solid and the environment. The liquid phase would be more conducive to cracking than the gas. The cracking of plastics in hydrocarbons and certain cases of liquid metal embrittlement could be explained in this manner.

That such a mechanism is operative may be demonstrated by the rate at which a gas is released from a super-saturated solution as a tool for studying adhesive forces[119]. Experiments with CO_2 from supersaturated aqueous solutions revealed that in a clean glass vessel a high supersaturation could be retained, because of the strong adhesive forces between the glass and water. However, supersaturation was rapidly released in contact with liquid paraffin. The liquid paraffin oil was not very effective unless it was smeared over a solid surface such as a glass plate. Thus the van der Waal's forces are modified if the adjacent phases are similar, so that they can adjust their thermal vibrations at the interface. There should be little difference between the surface energies of liquid and solid paraffin. During the thermal vibrations, the adhesive forces seem to fluctuate less at a water/liquid paraffin interface than at a water/solid paraffin interface. Liquid paraffin smeared as a thin film onto a glass surface has lost the ability to follow the thermal vibrations of the aqueous system.

Role of Ductility

Plastic deformation results in a loss of brittleness of the solid specimen. A certain amount of work must be expended in the production of plastic flow in the vicinity of the crack tip. The critical crack length in ductile materials would be several orders of magnitude larger than for brittle

solids, i.e. the stable crack propagating stage is accentuated. Excess ductility results in flow and the specimen will not crack since the work expended in plastic deformation is far greater than that needed to create fresh surface. However, a limited amount of plastic deformation would be beneficial to the brittle failure process. Plastic flow results in the creation of small areas of fresh surface, or preferential adsorption sites. Adsorption lowers the surface energy resulting in an imbalance of forces, and slip proceeds at a faster rate than in the absence of adsorbate. Thus the critical crack size is reached at an accelerated rate and the specimen fails. (In an ideally brittle material no such movement occurs, with the resulting strength decrease being only the decrease of initial surface free energy due to the environment.) The role of an embrittling species on a ductile solid would be to create, through a new surface compound, or adsorption dislocation locking, a limited amount of ductility thereby aiding brittle failure.

Therefore the role of plastic flow or slip dislocations in the stable crack propagation stage of brittle fracture in crystalline semi-brittle solids should not be underemphasized.

Since in all cases it is necessary for the environment to have an affinity for the solid and for the adsorbate effects to be felt in the existing flaws, wetting is a necessary aspect in stress-sorption failure.

It should be emphasized that not all adsorbing re-

actions will result in a weakening of the specimen. If the change in surface stress on adsorption is compressive, strengthening effects will result. This change will be a function of the solid surface and of the adsorbing species, indicating a selectivity in the stress cracking system.

The proposed variation in the slope of the Morse curve in the expansion regions of the rigid and semi-brittle solids can be emphasized by considering the energy released per unit area of crack surface. The Irwin[61] relationship for the critical energy released at the onset of unstable fracture propagation was given as

$$G_{CR} = \pi \sigma_{CR}^2 \, c_{CR}/E$$

σ_{CR} = Critical Stress for Failure
c_{CR} = Critical Crack Length
G_{CR} = Energy Released/Unit Crack Area

The value of G_{CR} has been found to be 0.08 in-lbs./sq. inch[120] for glass at 2% relative humidity, and 4.0 in-lbs./sq. inch for polymethyl methacrylate[120]. Since the breaking loads are of the same order of magnitude for the two solids, the difference arises from differences in critical crack size.

Therefore for very rigid solids (glass), under a steadily increasing load, the crack has only to extend very slightly to reach the critical size. It may be assumed therefore that, under these tensile test conditions, fracture initiation and strength failure occur almost simultaneously. For the semi-brittle material, on the other hand, a period of stable crack propagation occurs during which strength failure mechanisms due to environment can become operative.

Thus for the rigid ionic solid the environment essentially affects the fracture initiation process. For the semi-brittle covalent solid the environment operates in both the fracture initiation and stable crack propagation stages.

CHAPTER SIX

SUMMARY AND CONCLUSIONS

A study of stress-environmental cracking of two types of silica glasses and an acrylic plastic has been conducted in a unique high (10^{-6} mm Hg) vacuum apparatus. Adsorption isotherms for a number of gases and vapours constituting the environment of silica glasses were determined and correlated with fracture data obtained under corresponding conditions. The results have led to the following major conclusions:

(a) Glass

(1) Glass does not fail catastrophically in contact with an aqueous environment that may give "corrosion" -like reactions. Due to the rigid ionic structure, failure and fracture initiation occur almost simultaneously, any adsorption effects primarily affect the initial stage of the failure.

(2) In comparison with the clean, vacuum fractured specimens, all environments tested resulted in a decrease in the tensile fracture strength. Water vapour is the critical adsorbate, even at coverages of approximately 1/3 of a condensed monolayer, the strength then falling gradually with increase in vapour concentration.

(3) Contrary to the findings of others, the tensile strength is not a linear function of surface tension of the wetting liquid, in fact, they are unrelated. Again, moisture contamination affects the results drastically.

(4) Any dissolution process at existing surface flaws acts to increase the strength by blunting the crack tip. The effect is most prevalent in the acid and alkaline regions (pH < 5 and pH > 9).

(5) The measured "fracture isotherms" do not coincide with those calculated from adsorption data. This does not invalidate the Griffith equation, since the adsorption data refer to bulk measurements and Griffith equation to a localized stress-sensitive site on the surface of the sample.

(6) The magnitude of the surface bond (between the adsorbate and the site) is not the decisive parameter, but steric effects also play an important role, e.g., acetone is bonded more strongly than water (Δv Acetone=360 cms.$^{-1}$; Δv Water=280 cms.$^{-1}$) but the effect of water on fracture is greater.

(7) Dry gases, N_2 and CO_2, do not affect the tensile strength of Vycor glass.

(b) Polymethyl Methacrylate

(1) Stress-environmental fracture does not occur in the vapour phase. Stressing in a liquid organic

solvent that is wetting the plastic surface causes a drastic reduction in tensile strength

(2) Those dissolution processes which occur faster than the crack propagation act as a healing mechanism and increase the solid's strength.

(3) A non-wetting liquid, water, has no effect on the tensile fracture strength of the plastic.

(4) The existence of a large stable crack growth region and a large critical crack size of the covalently bonded semi-brittle material results in a catastrophic failure in organic solutions at very low applied loads.

(c) Quartzitic Rock

(1) Fracture of siliceous material is not facilitated by adsorption from aqueous solution. Rock in its normal weathered condition will already be in a lower energy state compared to the clean, adsorption-free condition. This does not exclude the possible effects of adsorption from a less active solution, or the possibility of separation of mineral particles along their boundaries with silica.

The main outcome of the study was to extend the previously conceived ideas for the stress-sorption cracking of brittle solids; a modified mechanism for stress-environmental cracking is proposed by taking into account the nature of the solid surface and the specific action of active adsorbing species on the surface (under the described testing conditions).

Changes in surface tension with adsorption may not be a sufficient condition for cracking to occur. Resulting surface stress variation can counteract the decrease in γ, thereby cancelling the weakening effect. Increase in surface tensional stress assists the surface tension reduction effect to cause failure at lower applied tensile loads. The strength of the bonding of the solid substrate surface can indicate the extent of stress environmental weakening, in an adsorption system.

BIBLIOGRAPHY

1. Penn, S.H., Trans. Soc. Min. Eng. 238, (1967), 72.

2. Dupre, A., "Constitution of Glass", Weyl and Marboe, J. Wiley, N.Y., p. 1012. 1968.

3. Griffith, A.A., Phil. Trans. Roy. Soc. (London), A 221, (1920-1), 163.

4. Benkendorff, G.W. and Hardie, G.P., Fracture Proc. 1st Tewksbury Symp., Melbourne, 1965.

5. Berry, J.P. and Beuche, A.M., Proc. of Symp. Adhesion and Cohesion, Elsevier, Amsterdam, 1962, p. 24.

6. Hahn, G.T. et al, Proc. Int. Conf. Fracture (Mass), (1959) J. Wiley, N.Y.

7. Rehbinder, P.A., Schreiner, L.A. and Zhiguch, K.F., Hardness Reducers in Drilling, Academy of Science, Moscow 1944.

8. von Szantho, E., Der EnfluB von oberflackenaktiven Stoffen bei der Feinzerkleinerung Z fur Ergbergbau und Metallhuttenwesen, 2(1949), 353/392.

9. Gotte and Ziegler, VDI-Z, 98 (1956), p. 373.

10. Von Engelhardt, W., Nachr Acad. Wiss. Gottingen Math-Phys. Klasse 1942 No. 2, Oel u Kohle 39 (1943), p. 707.

11. Moorthy, V.K. and Tooley, F.V., J. Amer. Ceram. Soc., 39 [6] 215-17 (1956).

12. Sato, M., Proc. Japan Acad. 30, 193, (1954).
    Proc. Japan Acad. 30, 369, (1954).

13. Frangiskos, A.Z., and Smith, H.G., Effect of Surface Active Agents on Comminution, Trans. Inst. Min. Dressing Congress, Stockholm 1957, p. 67-84.

14. Ghosh, S.K., Harris, C.C. and Jowett, A., Beneficial Effects of Reagents in Solution on Wet Crushing of Rock, Nature, 188 (1960), p. 1182.

15. Hammond, M.L. and Ravitz, S.F., J. Amer. Ceram. Soc., 46 No. 7, p. 329 (1963).

16. Siebel, J. and Zeisel, H.G., Verhaven zur Verbesserung der technisher Zerkleinerung von Erzen, Mineralien und Kohla mit Hilfe von chemischen Zusatzmitteln., Deutsches Patent 1, 071, 455, (1959).

17. Alberti, R., Verhaven zur Kornverfeinerung von Erzen, Deutsches Patent No. 904, 019 (1954).

18. Gilbert, L.A. and Hughes, T.H., Symp. Zerk Verlag Chemie (1962), p. 170-193.

19. Price, N.J., The Compression Strength of Coal Measure Rocks, Colliery Engineering, July 1900, p. 283-292.

20. Colback, P.S.B. and Wiid, B.L., Proc. of Rock Mechs. Symp. (1965), Dept. Min. Tech. Surveys, Ottawa, p. 65.

21. Dunn, J.R., C. and E.N., Feb. 21, 1966, p. 102.

22. Roesler, F.C., Proc. Phys. Soc. 69, [442B], 981-92 (1956).

23. Rehbinder, P. and Aslanova, M.S., Doklady Akad. Nauk, S.S.S.R., 1954 96, p. 299-302.

24. Benedicks, Pittsburgh Int. Conference on Surface Reactions, 1948, p. 196.

25. Benedicks, K. and Harden, Arkiv Fysik 3, 407-40, 1951-52 [4-5].

26. Dollimore, D., and Gregg, S.J., Research 11, (1958), 183.

27. Desai, N. and Gregg, S.J., Inst. of Fuel, A56, (1958).

28. Flood, E.A., Canad. J. Chem 33, (1955), 979
_____ and Lachampal, M.L., Second Int. Congress of Surface Activity (1957), II, p. 131.

29. Dinsdale, A., Moulson, A.J. and Wilkinson, W.T., Trans. Brit. Ceramics Soc. 61, (1962), 259.

30. Wiederhorn, S.M., Materials Science Research, Vol. 3, Plenum Press, N.Y. 1966, p. 503.

31. Hoek, E. and Bieniawski, Z.T., Int. J. Fracture Mechs. 1, (3), (1965), 139.

32. Charles, R.J., Proc. Int. Conf. Fracture, (Massachusetts), J. Wiley, N.Y., (1959), p. 225.

33. Jones, R. and Kaplan, M.F., Mag. Concrete Res. 26, (1957), 89.

34. Schardin, H., Proc. Int. Conf. Fracture (Mass.), (1959), p. 297.

35. Roesler, F.C., Proc. Phys. Soc. 69, [442B], (1956), 981.

36. Berenbaum, R. and Brodie, I., Brit. J. Appl. Phys. 10, [6], (1959), 281.

37. Hertz, H., "Miscellaneous Papers", (London) 1896, MacMillan.

38. Timoshenko, T. and Goodier, J. , "The Theory of Elasticity", McGraw-Hill, 1951.

39. Frocht, M.M., "Photoelasticity", J. Wiley, N.Y. (1946).

40. Carniero, F., Reunion des Laboratories d'Essai de Materiaux (1947).

41. Peltier, R., "Theoretical Investigation of the Brazilian Test", Union of Testing and Research Laboratories for Materials and Structures, No. 19, (1954).

42. Rudnick, A., Hunter, A.R. and Holden, F.C., "An analysis of the diametrical compression test", Materials Research and Stds., April 1963.

43. Yang-Shyang Yu, "The Physical Props. of Sigma Porphyry", M.Sc. Thesis, McGill, 1964.

44. Zachariason, W.H., J. Amer. Chem. Soc. 54, (1932), 3841.

45. Sun, K.H., J. Amer. Ceram. Soc. 30, (1947), 279.

46. Warren, B.E., J. Appl. Phys. 8, (1937), 654.

47. Dzisko, V.A., Vishnevskaya, A.A. and Chesalova, V.S., Zhur. Fiz. Khim. 24, (1950), 1416.

48. Bungenberg de Jong, "Colloid Science", Elsevier Publishing Co., N.Y., (1949), II, p. 310.

49. Bartell, F.E. and Dobay, D.G., J. Amer. Chem. Soc. 72, (1950), 4388.

50. Yates, D.J.C., Advances in Catalysis, Academic Press, (1957), IX, p. 481.

51. Culf, C.J., J. Soc. Glass Tech. 41, (1957), 157.

52. Beuche, F., J. Appl. Phys. 28, (1957), 784.

53. Richards, R.B., Trans. Far. Soc. 42, (1946), 10.

54. Howard, J.B., J. Soc. Plastics Eng. 15, (1959), 397.

55. Hittmair, R. and Ullman, R.J., J. Appl. Polymer Science 6, (1962), 1.

56. Spohn, W.W. and Frey, H.J., A.I.E.E. Winter Meeting, N.Y., (1957).

57. Lander, L.L., J. Soc. Plastics Eng. 16, (1960), 1329.

58. Wolcock, I., Kies, J.A. and Newman, S.B., Proc. Int. Conf. on Fracture (Mass.), 1959, p. 250.

59. Poncelet, E.F., Fracture of Metals, Amer. Soc. Metals, Cleveland (1948), p. 201.

60. Orowan, E., Repts. Prog. Phys. 12 (1949), 185.

61. Irwin, G.R., "Structural Mechanics", (Goodier & Hoff), Permagon Press (1960), p. 557.

62. Mott, N.F., Fracture of Metals Eng. 165, (1948), 15.

63. Roberts, D.K. and Wells, A.A., Engineering 178, (1954), 820.

64. Schardin, H. and Struth, W., Glastech, Ber., Vol. 16, (1958), 219.

65. Bieniawski, Z.T., Rept. S.A.C.S.I.R., M.E.G. 493, Oct. (1966).

66. Elliott, H.A., J. Appl. Phys. 29 (1958), 224.

67. Charles, R.J., J. Appl. Phys. 29 (1958), 1554.

68. Poncelet, E.F., A.I.M.E., T.P. (1944), 1684.

69. Gordon, J.E., Marsh, D.M. and Parratt, M.E.M.L., Proc. Roy. Soc. (London), A249, (1959), 65.

70. Elliott, H.A., Proc. Phys. Soc. (London), B59, (1947) 208.

71. Shand, E.B., J. Amer. Ceramics Soc. 37, (1954), 559.

72. Andrade, E. and Tsien, L.C., Proc. Roy. Soc. (London), A159, (1937), 346.

73. Bieniawski, Z.T., Rept. S.A., C.S.I.R., M.E.G. 459, (1966).

74. Gurney, C. and Pearson, S., "Ceramics and Glass", Research Rpt. No. 10.

75. Orowan, E., Nature, 154, (1944), 341.

76. Gibbs, J.W., "The Collected Works of Gibbs", Longmans-Green, N.Y., (1931), 1, 219.

77. Shuttleworth, R., Proc. Phys. Soc. (London), A63, (1950), 444.

78. Nicolson, M.M., Proc. Roy. Soc. (London), A228, (1955), 507.

79. Bangham, D.H. and Razouk, R.I., Proc. Roy. Soc., A166, (1938), 571.

80. Maggs, F.A.P., Trans. Far. Soc. 42B, (1946), 284.

81. Sato, M., Proc. Japan. Acad. 30, (1954), 445.

82. Yates, D.J.C., Proc. Roy. Soc. A224, (1954), 526.

83. Amberg, C.H. and McIntosh, R., Can. J. Chem. 30, (1952), 1012.

84. Yates, D.J.C., Advances in Catalysis, XII, (1960), 298.

85. Kiselev, A., Koklady Acad. Sci. (U.S.S.R.), 106, (1956), 1046.

86. Belyakova, Dzhigit, and Kiselev, A., Zhurn. Fiz. Khim. 31, (1957).

87. Kiselev, A., "Surface Chemical Compounds and Their Role in Adsorption Phenomena", Moscow Univ. 1957.

88. Kiselev, A., Second Int. Congress of Surface Activity II, p. 179.

89. Folman, M. and Yates, D., Proc. Roy. Soc. A246, (1958), 32.

90. McDonald, R.S., J. Amer. Chem. Soc. 79, 850, (1957).

91. Siderov, A.M., J. Phys. Chem. (U.S.S.R.) 30, (1956), 995.

92. Hering, C., "Structure and Prop. Solid Surfaces", Univ. of Chicago Press, 1953.

93. Folman, M. and Yates, D., Trans. Far. Soc. 54, (1958), 1684.

94. Brunauer, S., Deming, L.S., Deming, W.E., and Teller, E., J. Amer. Chem. Soc. 62, (1940), 1723.

95. Bangham, D.H., Trans. Far. Soc. 33, 805, (1937).

96. Berry, J.P., Proc. Int. Cont. Fracture (Mass.), 1959, p. 263.

97. Maxwell, B. and Rahm, Ind. Eng. Chem. 41, (1949), 1988.

98. Joffe, A.F., "The Physics of Crystals", McGraw-Hill, N.Y., (1928).

99. Dienert, F. and Wandenbulcke, F., Compt. Rend. 176, 146, (1923), 1478.

100. Alexander, G.B., Heston, W. and Iler, R.K., J. Phys. Chem. 58, 453, (1931).

101. Inglis, C.E., Trans. Inst. Naval Architects 55, p. 219, (1913).

102. Young, T., Phil. Trans. Roy. Soc. London 95, 65 (1805).

103. Dupre, A., Theorie Mechanique de la Chaleur, Gauthier-Villars, Paris, 1869.

104. Weyl, W.A., Marboe, E.C., Sonders, L.R., J. Appl. Phys. 20, 1011, (1949).

105. Deryagin, V., Research, London 8, 70, (1955).

106. Fowkes, F.M., J. Phys. Chem. 66, 1863, (1962); Ind. Eng. Chem. 56 (12), 40, (1964).

107. Stuart, D.A. and Anderson, O.L., J. Amer. Ceram. Soc. 32, (1953), 416.

108. Charles, R.J., Prog. in Ceramics Sci. I, Permagon Press, N.Y., 1961, p. 1.

109. Culf, C.J., J. Soc. Glass Tech. 41, (1957), 157.

110. Poncelet, E.F., Trans. Soc. Glass. Tech. 17, (1958), 279.

111. Gilman, J.J., Fracture, 1959, Wiley and Sons, N.Y., p. 163.

112. Stoloff, N.S. and Johnston, T.L., Acta. Met. 11, (1963), 251.

113. Westwood, A.R.C. and Kamdas, M.H., Phil. Mag. 8, (1963), 787.

114. Rostoker, W., McCaughey, J.M. and Markus, H., Embrittlement by liquid metals, (1960), Reinhold, N.Y.

115. Nielsen, N.A., "Phys. Met. of Stress Corrosion Fracture", Rhodin, T.N. ed., Wiley, N.Y., (1956).

116. Pickering, H.W., Beck, F.H. and Fontana, M.G., Corrosion 18, (1962), 230.

117. Robertson, W. and Uhlig, H., J. Appl. Phys. 19, (1948), 814.

118. Morris, A., Trans. A.I.M.E. 89, (1930), 256.

119. Jones, G.O., J. Soc. Glass Tech. 33, (1949), 120.

120. Marboe, E.C. and Weyl, W.A., J. Soc. Glass Tech. 32, (1948), 281.

121. Herbert, T.C. and Ford, Int. Science and Technology, March 1963.

122. Petch, N.J. and Sables, P., Nature 169 (1952), 842.

123. Uhlig, H., "Phys. Met. Stress Corrosion Fracture", Pittsburgh 1959, p. 1.

124. Uhlig, H. and Sava, J., Trans. Am. Soc. Metals 56, (1963), 361.

Additional pertinent references

"Tensile Strength of Brittle Materials," by R. Sedlacek, Stanford Research Institute, Technical Report AFML-TR-65-129, August 1965.

"Studies of the Brittle Behavior of Ceramic Materials," Technical Documentary Report No. ASD-TR-61-628, Part II, April 1963.

"Method for Tensile Testing of Brittle Materials," Rudolf Sedlacek and Frank A. Halden, Review of Scientific Instruments, Vol. 33, No. 3, pp. 298-300, March 1962.

"Surfaces, Stress-Dependent Surface Reactions and Strength," by W.B. Hillig and R.J. Charles, Chapter 17 in HIGH STRENGTH MATERIALS, ed. V.F. Zackay, John Wiley & Sons, Inc., New York 1964, p. 682.

Appendix A

Description of Apparatus Components

(i) Load Measuring System

(a) Load Cell - Baldwin, Lima Hamilton Corp. (B.L.H.) SR-4, Model CXX, Capacity 50,000 lbs.

(b) Strain Indicator - Budd, Model P-350.

(ii) High Vacuum Pumping System

(a) Rotary Vacuum Pump - Welch Duo Seal Model 1397 B, 2 stage 425 litres/min full air displacement with vented exhaust.

(b) Rotary Pump Oil - Welch Duo Seal Oil.

(c) Oil Diffusion Pump - Consolidated Vacuum Corp. Model PAS-61 C
6 inch - 3 stage fractionating type
300 litres/min pumping speed.

(d) Diffusion Pump Oil - Silicone DC-705 S.G., 1.095 Flash Pt., 470°F, B.P. 245°C at .5 torr.

(e) Cooling coil safety switch - Ranco Pressure Control Type "010", low and high pressure cut-in.

(f) Cold Trap - C.V.C. Multicoolant Baffle, Type BCN Coolant-Liquid Nitrogen.

(g) High Vacuum Valves - C.V.C. right angle vacuum valves type VRA.

Gate Valve - Type VCS 61B.

(h) Gaskets, O rings - Buna-N and Neoprene gaskets and O-rings.

(i) Vacuum Gauges - C.V.C. Model GIC - 200 hot filament gauge. Range $1x10^{-3}$ - $2x10^{-12}$ mm Hg. C.V.C. Thermocouple gauge Model GTC - 004. Range 2.0 mm. $1x10^{-3}$ mm Hg. C.V.C. GIC - 017.2 ion tube.

(j) Bellofram Rolling Diaphragm - 'Impervon' Elastomer.

Appendix B

Calibration of Load Cell

The B.L.H. SR-4 load cell was calibrated against a Baldwin Testing Machine by loading in increments of 2,000 lbs., then unloading in decrements of 5,000 lbs. A calibration curve of load, in lbs., versus strain, in μ-strains, gave a linear plot of slope 12.5 lbs/μ-strain.

FIGURE 47 LOAD CELL CALIBRATION

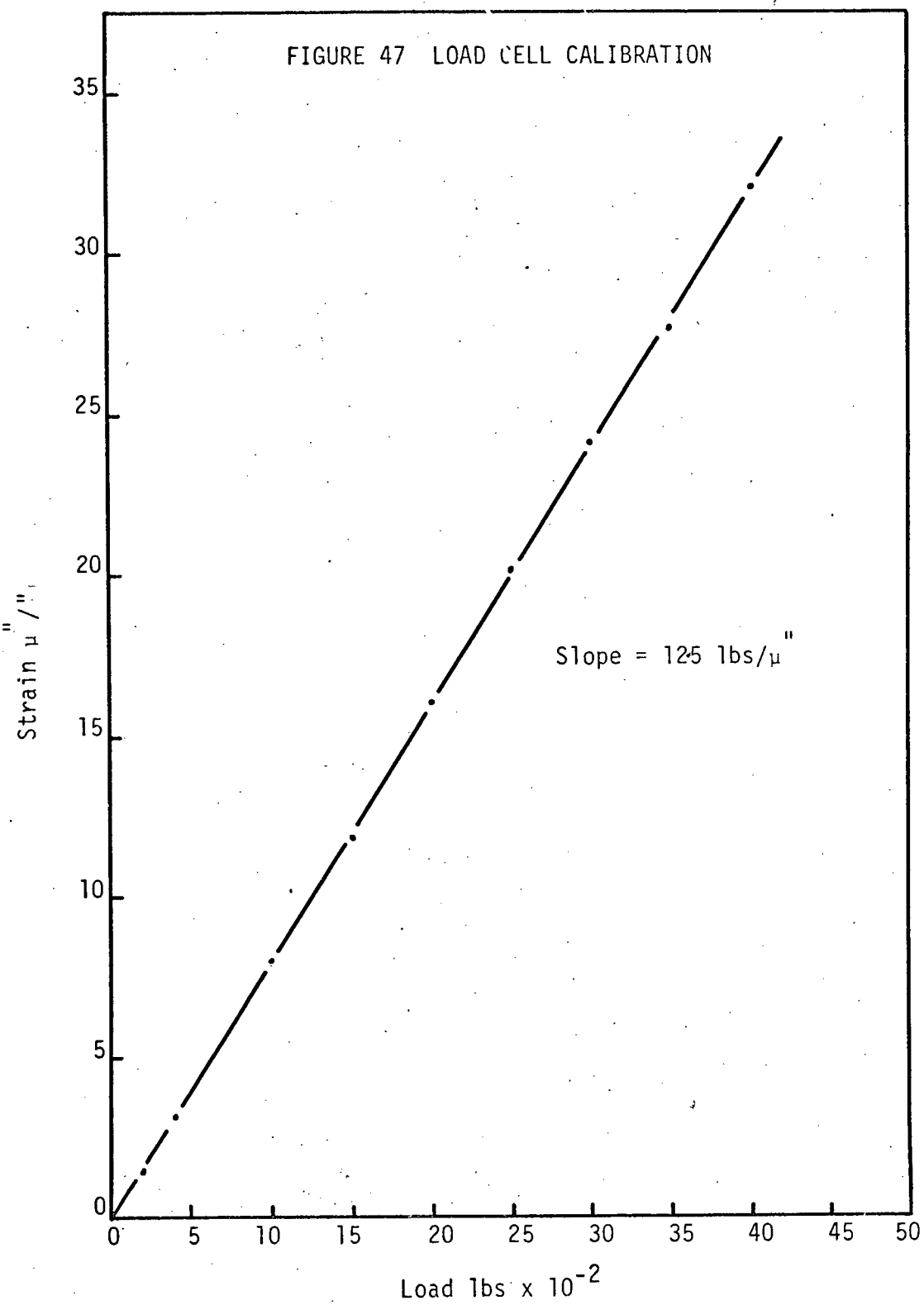

Appendix C

B.E.T. Calibrations

(i) Gas Burrettes

The volume of each bulb was determined by weighing amounts of water run from the inverted burrettes between the etch marks. For water calibration the burrettes are inverted to simulate the mercury meniscus. During the calibration the bulbs were thermostated at 30°C. Results are given in Table 16.

(ii) Free Volume (Va)

The free volume of the apparatus is the volume from the zero etch marks on the gas burrettes, including the manometers with the mercury raised to the constant volume marks, to the sample vessel stopcocks, i.e. the internal apparatus volume excluding the volumes of the sample vessels. The free volume may be calculated by admitting a dose of He to the apparatus with the sample vessels closed, and measuring the pressure, with all mercury levels adjusted to the constant volume marks. By raising the mercury in the gas burrettes one bulb at a time a series of pressure readings are obtained. If V is the volume of the empty bulbs, and knowing the volumes of the bulbs, we have,

$$P(V+Va) = K \qquad \text{T is constant}$$

$$PV+PVa = K$$

$$PV = K-PVa$$

TABLE 16

Bulb Calibrations

Burrette No. 1

Temp. 30.2°C

Density of H_2O=.99561

Bulb No.	Ave. Wt. H_2O	Vol(ccs)
1	98.9319	98.49
2	29.5515	29.42
3	20.0473	19.96
4	10.3928	10.35

Burrette No. 2

Bulb No.	Ave. Wt. H_2O	Vol(ccs)
1	145.2499	144.60
2	98.8351	98.39
3	30.0427	29.91
4	9.7848	9.74

A plot of PV versus P has slope-Va.

(iii) Dead Space Vd

The dead space is the unoccupied volume of the sample vessel. This includes the internal volume of the specimen and should therefore be determined before each run. The method is the same as for the free volume calibration but with the sample vessel open to the system. The difference between the total volume obtained and the free volume yields the dead space.

Typical results are given in Table 17 and plotted in Fig. 48.

TABLE 17

Volume Calibration

		P cms	V ccs	P x V	
(a)	Free Vol.	7.823	440.841	3448.699	V = Vol of empty bulbs
		10.813	296.245	3203.297	Temp = 32.6°C
		14.548	197.756	2876.983	
		22.376	99.368	2223.458	
		26.764	69.949	1872.115	
		33.217	40.041	1330.041	
(b)	Dead Space	7.573	440.841	3338.488	
		10.284	296.245	3046.583	
	(1)	13.655	197.758	2700.385	
		20.220	99.368	2009.220	
		23.667	69.949	1655.982	
		13.666	197.758	2702.560	
	(2)	7.313	440.841	3223.870	
		9.949	296.245	2947.341	
		13.194	197.758	2609.219	
		19.641	99.368	1951.686	
		22.933	69.949	1604.140	
		13.220	197.758	2614.360	
	(3)	7.104	440.841	3131.293	
		9.652	293.245]	2859.356	
		12.739	197.758	2512.239	
		19.141	99.368	1902.002	
		22.443	69.949	1569.865	
		9.779	296.245	2896.979	

Volume Calibration Calculations

(a) Free Vol.

Slope of curve = $\frac{800}{95}$ = 84.1 ccs

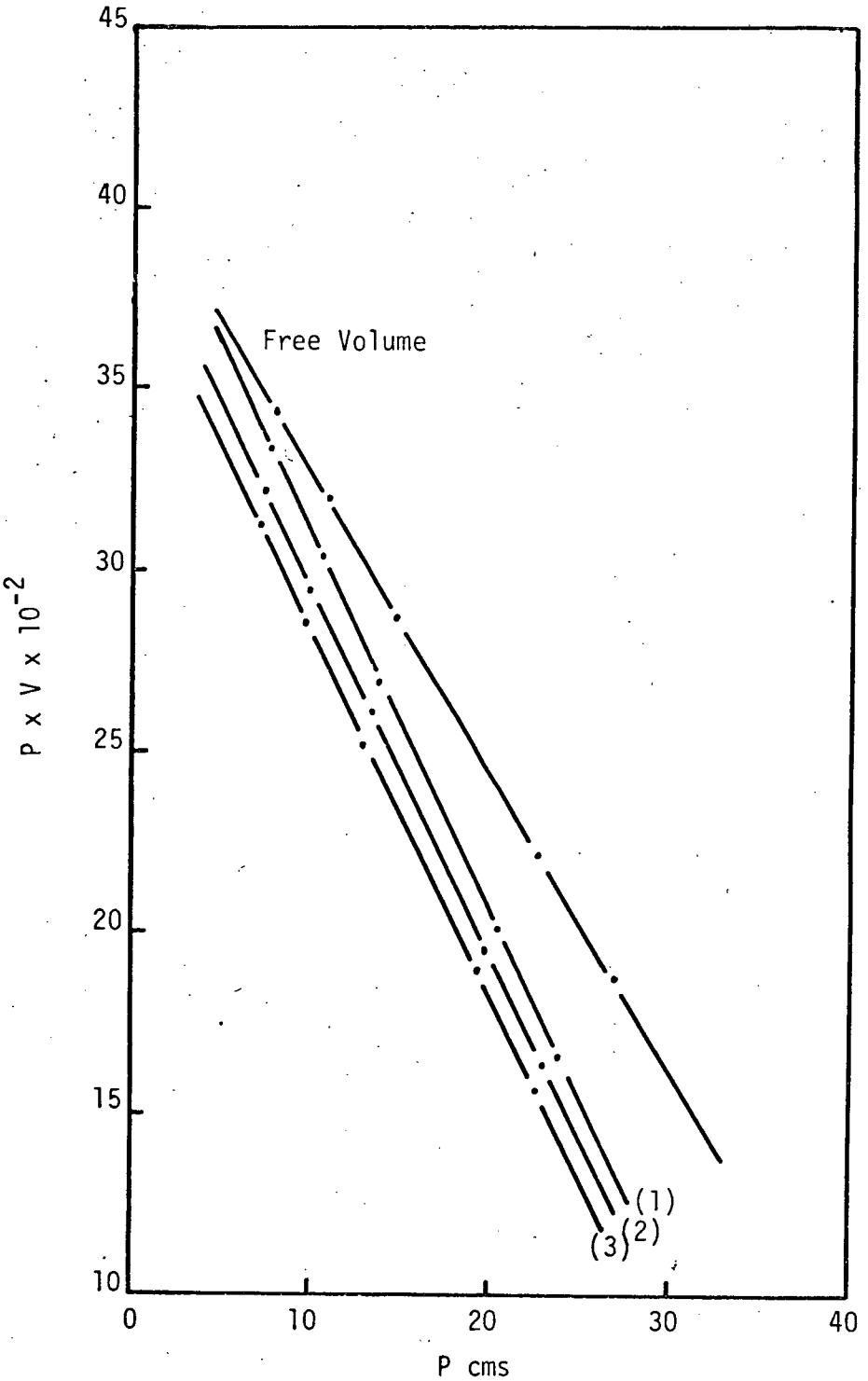

FIGURE 48 ADSORPTION APPARATUS CALIBRATION

TABLE 17 (Cont'd)

(b) Dead Space

Sample Vessel 1 Slope = $\frac{10.45}{10} \times 100 = 104.5$ ccs

Vol 1 = 20.4 ccs

Sample Vessel 2 Slope = $\frac{1022}{10} = 102.2$ ccs

Vol 2 = 18.1 ccs

Sample Vessel 3 Slope = $\frac{1028}{10} = 102.8$ ccs

Vol 3 = 18.7 ccs

Appendix D

B.E.T. Isotherm Calculations

(a) Isotherm

A plot of Relative Pressure versus Volume adsorbed in ccs/gms at STP is called the adsorption isotherm.

If P_1 is the initial pressure occupying the free volume Va and P_2 is the pressure after admission to the sample vessel, then the amount of gas adsorbed is the initial volume less the final volume at the temperature of the experiment T.

In ccs/gms at STP the volume adsorbed is,

$$V = \frac{P_1 x Va - P_2(Va+Vd)}{760} \times \frac{273}{(273+T)} \times \frac{1}{m}$$

where m is the specimen weight. For each additional dose since an amount at P_2 and Vd was already enclosed in the sample vessel the amount adsorbed will be given by,

$$V = \frac{P_3 x Va + P_2 Vd - P_4(Va+Vd)}{760}$$

$$\times \frac{273}{273 x T} \times \frac{1}{m} \qquad \text{ccs/gm S.T.P.}$$

The volume of gas adsorbed at the equilibrium pressure P_4 is then the sum of the amounts adsorbed for the first and second doses.

The example for H_2O is given in Table 18.

(b) B.E.T. Linear Plot

The B.E.T. equation is written in the form

$$\frac{P}{V(P_o-O)} = \frac{1}{VmC} + \frac{C-1}{VmC} \cdot P/P_o$$

A plot of $\frac{P}{V(P_o-P)}$ versus P/P_o will give a straight line of slope $\frac{C-1}{VmC}$ and intercept $\frac{1}{VmC}$.

Vm is given by,

$$Vm = \frac{1}{\text{Slope} + \text{Intercept}}$$

Table 18 and 19 give details of the data from which Fig. 22 is constructed. Table 20 lists the monolayer volumes for the four systems measured.

(c) Specific Surface Area Calculations

In order to determine the surface area of the adsorbant it is necessary to know the cross-section of the gas molecule. This area is given by

$$A = 4(0.866) \left(\frac{M}{4\sqrt{2ND}}\right)^{2/3}$$

where M is the Molecular weight of the gas, d its density and N Avogadro's No. For nitrogen at liquid N_2 temperatures A is equal to 16.2 A°.

Knowing Vm per gms. the specific surface area may be calculated as follows

TABLE 18

Adsorption Isotherm Data on Vycor Glass

Vycor Glass Area = 225 m^2/gms

Temperature Constant at 25.2°C

Water Vapour	
P/P_o	Vads (ccs/gm STP)
0.021	17.9
0.033	35.0
0.088	62.4
0.10	70.4
0.19	95.0
0.24	104.8
0.31	116.7
0.43	130.2
0.625	155.0
0.69	199.0

TABLE 19

B.E.T. Linear Plots

	P mms	P/P_o	Vads ccs/gm	P_o-P	$V(P_o-P)$	$\frac{P}{V(P_o-P)}$
H_2O	2.11	.088	62.4	21.89	1365.9	.00154
	2.40	.1	70.4	21.60	1520.6	.00158
	5.76	.24	104.8	18.24	1911.5	.00301
	7.44	.31	116.7	16.56	1932.5	.00385

TABLE 20

Monolayer Volumes from B.E.T. Linear Plots

	Slope	Intercept	Slope+Intercept	$Vm=\frac{1}{S+I}$
H_2O	.010	.001	.011	90.9
n-Butylamine	.046	-.0015	.0445	22.5
Acetone	.026	.0015	.0275	36.4
Benzene	.054	.005	.059	17.0

$$\text{Surface Area} = \frac{Vm \times 6.023 \times 10^{23} \times 16.2}{22.4 \times 10^{3} \times 10^{20}}$$

square metres/gram.

The surface coverage θ at a volume of gas V, is given by $\theta = \frac{V}{Vm}$.

(d) Surface Free Energy Changes on Adsorption

If γ_o is the free energy required to create 1 cms^2 of new surface in vacuo, and this is reduced to γ in the presence of an adsorbable gas, then the decrease in surface free energy is $= \gamma_o - \gamma$.

$\pi_e = \gamma_o - \gamma$ is also called the spreading pressure. The Gibb's adsorption equation gives,

$-d\gamma = RT\ N\ d\ln P$ where N is the number of moles adsorbed per cms^2 at pressure p.

Integrating

$$\gamma_o - \gamma = RT \int N\, d\ln P$$

$$= \frac{RT}{MS} \int x\, d\ln P$$

$$= \frac{2.303\ RT}{MS} \int_{o}^{P/P_o} x\, d \log P/P_o.$$

X is the number of gms. adsorbed per gm. of solid and S is the surface area.

Thus by plotting X versus log P/P_o and integrating graphically the decrease in surface free energy an adsorption may be determined.

The method is normally applicable to reversible processes, i.e. where adsorption and desorption are equal. However in this application we are only interested in the surface free energy decrease on adsorption and the hysteresis on desorption is not taken into account.

$$\pi_e = \Delta\gamma = \frac{2.308\ RT}{MS} \int_0^{P/P_o} x\ d \log P/P_o$$

x = gms/gms adsorbed

M = Mol. Wt.

S = Surface Area

$$\pi = \frac{2.303 \times 1.98 \times 2.98}{225 \times 10^4} \times 10^{-3} \quad \frac{\text{Area}}{M}$$

$$= \frac{A}{M}\ 6.03 \times 10^{-7}\ \text{cals/cms}^2$$

$$= \frac{\text{Area}}{M} \times 6.03 \times 4.184\ \text{ergs/cms}^2$$

$$= \frac{\text{Area}}{M} \times 25.2\ \text{ergs/cms}^2$$

Units $$= \frac{\text{cals}}{\text{degree}} \times \frac{\text{mole}}{} \times \frac{\text{degrees}}{\text{moles}} \times \frac{\text{gms}}{\text{gms}} \times \frac{1}{\text{cms}^2}$$

$$= \frac{\text{cals.}}{\text{cms}^2} \rightarrow = \frac{\text{ergs.}}{\text{cms}^2} \rightarrow$$

TABLE 21

Surface Energy Plots

$$\pi = \frac{RT}{MS} \int_{o}^{P/P_o} \underset{gm/gm}{Vads} \; d\ln P/P_o$$

H_2O

P/P_o	$-\log P/P_o$	Vads mgms/gms
.021	+ 1.6778	14.4
.033	+ 1.4815	28.3
.088	1.0555	50.5
.10	1.0000	57.0
.19	.7212	76.9
.24	.6198	84.8
.31	.5086	94.5
.43	.3665	105.4
.625	.2041	125.5
.69	.1612	161.1

Appendix E

Tensile Fracture Strength Calculations

1 microstrain ≡ 12.5 lbs load.

From Brazilian Test the tensile strength is given as

$$\delta_x = -\frac{2P}{\pi Dt}$$

where P is the load in lbs

D is the specimen diameter = .5"

t is the specimen thickness = .5"

$$\delta_x = -2.55 \overrightarrow{P}$$

An example for H_2O on Kimble glass is given in Table 23.

TABLE 22

Surface Tension Reductions on Adsorption

(Vycor Glass)

	Area	Area/M	$-\log P/P_o$	P/P_o	$\Delta\gamma$	$\Delta\gamma^{1/2}$
H_2O	8	.44	1.5	0.032	11.08	3.33
	29	1.61	1.0	0.100	40.57	6.37
	49	2.72	0.7	0.200	68.54	8.28
	66	3.66	0.5	0.316	92.23	9.60
	99	5.50	0.2	0.631	138.60	11.77
	144	8.00	0	1.0	201.60	14.20

TABLE 23

Fracture Isotherms - H_2O on Kimble Glass

P_o = 24 mms Hg

μ"/"	Load	Tensile Strength P.S.I.	P mms	P/P_o
292	3650	9297	VAC	0
205	2563	6527	.62	.026
151	1890	4822	1.2	.048
141	1758	4484	1.8	.071
145	1810	4616	2.5	.106
157	1962	5003	2.6	.108
156	1954	4982	3.7	.153
163	2039	5200	5.8	.24
150	1869	4765	7.0	.29
146	1820	464]	9.1	.38
151	1890	4822	11.3	.47
144	1800	4584	14.2	.59
148	1847	4711	18.2	.76
141	1856	4222	20.4	.85
151	1890	4822	21.4	.89
135	1685	4298	22.8	.95